Theoretical and Experimental Investigation of the Material Removal Rate, Surface Roughness, and Tool Wear Ratio in Electrical Discharge Machining

Hamed Hosseingholi Pourasl

Submitted to the
Institute of Graduate Studies and Research
in partial fulfillment of the requirements for the degree of

Doctor of Philosophy
in
Mechanical Engineering

Eastern Mediterranean University
January 2019
Gazimağusa, North Cyprus

Approval of the Institute of Graduate Studies and Research

Assoc. Prof. Dr. Ali Hakan Ulusoy
Acting Director

I certify that this thesis satisfies all the requirements as a thesis for the degree of Doctor of Philosophy in Mechanical Engineering.

Assoc. Prof. Dr. Hasan Hacışevki
Chair, Department of Mechanical Engineering

We certify that we have read this thesis and that in our opinion it is fully adequate in scope and quality as a thesis for the degree of Doctor of Philosophy in Mechanical Engineering.

Asst. Prof. Dr. Mohammed Bsher A. Asmael
Co-Supervisor

Assoc. Prof. Dr. Neriman Özada
Supervisor

Examining Committee

1. Prof. Dr. Ali Oral
2. Prof. Dr. Ibrahim Etem Saklakoğlu
3. Assoc. Prof. Dr. Hasan Hacışevki
4. Assoc. Prof. Dr. Neriman Özada
5. Assoc. Prof. Dr. Qasim Zeeshan
6. Asst. Prof. Dr. Tülin Akçaoglu
7. Asst. Prof. Dr. Mohammed Bsher A. Asmael

ABSTRACT

Material removal rate (MRR), tool wear ratio (TWR) and surface roughness (Ra) is major parameters that affect the quality of electro discharging machining (EDM). Recently many research works have done to optimize these important factors. A significant number of techniques such as: Fuzzy logic, Artificial neural networks (ANN), Response surface method (RSM), Grey relational analysis (GRA) and Taguchi method have been applied to optimize the mentioned parameters. As an instance some researches have used ANN and Taguchi method to predict and optimize the Ra, TWR and MRR in electro discharge machining of Titanium alloy, AISI 2312 and AISI 1040 tool steel. The AISI-D6 steel is extensively used as a dies and molds material.

In this current study, the Electric Discharge Machining (EDM) of the said material is carried out following a test plan composed of 32 runs. The effects of some important operating parameters, namely pulse on-time (Ton), pulse current (I) and voltage (V), on the performance measures of EDM process such as Material Removal Rate (MRR), Tool Wear Ratio (TWR), and Average Surface Roughness (Ra) are quantified. Also in this investigation, response surface method (RSM) was used to predict and optimize the material removal rate, tool wear ratio and surface roughness during electrical discharge machining of AISI D6 tool steel. Pulse on time, pulse current, and voltage were considered as input process parameters. Furthermore, the analysis of variance was employed for checking the developed model results. The results revealed that higher values of pulse on time resulted in higher values of material removal rate and lower amounts of tool wear ratio. In addition, increasing

the pulse current caused to higher amounts of both material removal rate and tool wear ratio. Moreover, the higher the input voltage, the lower the both material removal rate and tool wear ratio. The optimal condition to obtain a maximum of material removal rate and a minimum of tool wear rate was 40 μs, 14 A and 150 V, respectively for the pulse on time, pulse current and input voltage. Also, the pulse on time was the most effective parameter influencing the roughness. It was found that the higher values of pulse on time and pulse current and lower values of input voltage caused to in higher amounts of surface roughness. The optimal condition to obtain a minimum of surface roughness was 10.22 μs, 8.02 A and 174.74 V, respectively for the pulse on time, pulse current and input voltage.

Even though the prior investigators explored mathematical models in the case of some alloys, a research into the establishing mathematical relationships between the input parameters and output responses during EDM of AISI D6 tool steel is lacking. Therefore, the aim of this study was to apply RSM in conjunction with full factorial design, to establish the functional relationships for EDM of parameters i.e. pulse on time, pulse current and voltage, and responses of AISI D6 tool steel i.e. material removal rate, tool wear ratio and surface roughness. In order to guide the process users, process maps (i.e., parameter-effect correlations) are generated. It is found that the parametric effects are quite contradictory in nature. Further, to obtain a trade-off among various performance measures, it is proposed to choose intermediate values of parameters as given in the manuscript. Outcomes of the performed research demonstrated that the mathematical model can be developed for different work piece and electrode materials for EDM processes, also there is a need of microscopic

studies to clarify the variation in parameters that may affect the microstructure of the work-piece.

Keywords: Electrical discharge machining, AISI D6 tool steel, Material removal rate, tool wear ratio, surface roughness

ÖZ

Malzeme kaldırma oranı, takım aşınma oranı ve yüzey pürüzlülüğü, elektro deşarj işleminin (EDM) kalitesini etkileyen ana parametrelerdir. Son zamanlarda bu önemli faktörleri optimize etmek için birçok araştırma yapılmıştır. Söz konusu parametreleri optimize etmek için Fuzzy Logic, Artificial neural networks, Response surface method, Grey relational analysis ve Taguchi yöntemi gibi önemli sayıda teknikler uygulanmıştır. Örnek olarak, bazı araştırmalar Titanyum alaşımı, AISI 2312 ve AISI 1040 çeliklerini elektro deşarj işleminde Ra, TWR ve MRR'yi tahmin etmek ve optimize etmek için ANN ve Taguchi yöntemlerinde kullandı. AISI-D6 çeliği yaygın bir kalıp ve kalıp malzemesi olarak kullanılır.

Bu çalışmada, söz konusu malzemenin Elektrik Deşarj Makinesi (EDM) tarafından 32 örnekle oluşan bir test planının ardından gerçekleştirilmiştir. Bazı önemli çalışma parametreleri, darbe süresi (Ton), darbe akımı(I) ve voltaj(V) etkileri EDM işleminin Malzeme Kaldırma (MRR), Takım Aşınma Oranı (TWR), ve Ortalama Yüzey Pürüzlülüğü (Ra) gibi ölçüm performasları nicelleştirilmiştir. Ayrıca bu araştırmada, AISI D6 çeliğinin elektriksel deşarj işlemi sırasında malzeme kaldırma oranını, takım aşınma oranını ve yüzey pürüzlülüğünü tahmin etmek ve optimize etmek için yanıt yüzey yöntemi kullanılmıştır. Darbe zamanı, darbe akımı ve gerilim giriş işlemi parametreleri olarak kabul edildi. Ayrıca, geliştirilen model sonuçlarını kontrol etmek için varyans analizi kullanılmıştır. Sonuçlar, zaman içindeki daha yüksek darbe değerlerinin, daha yüksek malzeme kaldırma oranı değerleri ve daha düşük miktarda takım aşınma oranı ile sonuçlandığını ortaya koydu. Ek olarak, darbe akımının arttırılması hem malzeme uzaklaştırma oranı hem de takım aşınma oranının

daha yüksek miktarlarda olmasına neden olmuştur. Ayrıca, giriş voltajı ne kadar yüksek olursa, hem malzeme kaldırma oranı hem de takım aşınma oranı o kadar düşük olur. Maksimum malzeme kaldırma oranı ve minimum takım aşınma hızı elde etmek için en uygun koşul, darbe süresi, darbe akımı ve giriş voltajı için sırasıyla 40 μs, 14 A ve 150 V idi. Ayrıca, darbe süresi pürüzlülüğü etkileyen en etkili parametre idi.

Önceki araştırmacılar bazı alaşımların matematiksel modellerini araştırsalar da, AISI D6 çeliğinin EDM sırasındaki girdi parametreleri ile çıktı yanıtları arasında matematiksel ilişkiler kurma araştırması eksiktir. Bu nedenle, bu çalışmanın amacı, tam etkenli tasarımı ile birlikte RSM'yi uygulamak, darbe süresi, darbe akımı ve gerilimi ve AISI D6 çeliğinin yani malzeme kaldırma oranı, takımın yanıtları gibi parametrelerin EDM'si için aşınma oranı ve yüzey pürüzlülüğü fonksiyonel ilişkileri kurmaktı. İşlem kullanıcılarına rehberlik etmek için işlem haritaları (yani parametre-etki korelasyonları) üretilir. Parametrik etkilerin doğada oldukça çelişkili olduğu bulundu. Ayrıca, çeşitli performans ölçütleri arasında bir denge elde etmek için, metinde verilen parametrelerin ara değerlerinin seçilmesi önerilir. Yapılan araştırmanın sonuçları, matematiksel modelin EDM prosesleri için farklı iş parçası ve elektrot malzemeleri için geliştirilebileceğini, ayrıca iş parçasının mikro yapısını etkileyebilecek parametrelerdeki değişimi açıklığa kavuşturmak için bir mikroskobik çalışmaya ihtiyaç duyulduğunu göstermiştir.

Anahtar Kelimeler: Elektriksel deşarj işlemesi, AISI D6 takım çeliği, Malzeme kaldırma oranı, takım aşınma oranı, yüzey pürüzlülüğü

DEDICATION

TO MY FAMILY

ACKNOWLEDGMENTS

I would like to express the deepest appreciation to my supervisor Assoc. Prof. Dr. Neriman Özada who has the attitude and the substance of a genius: He continually and convincingly conveyed a spirit of adventure in regards to research, and an excitement to teaching. Without his guidance and persistent help, this thesis would not have been possible.

Foremost, I would like to express my sincere gratitude to my Co-Supervisor Asst. Prof. Dr. Mohammed Bsher A. Asmael for the continuous support of my Ph.D study and research, for his patience, motivation, enthusiasm, and immense knowledge. His guidance helped me in all the time of research and writing of this thesis. I could not have imagined having a better advisor and mentor for my Ph.D study.

TABLE OF CONTENTS

LIST OF TABLES

LIST OF FIGURS

Chapter 1

INTRODUCTION

1.1 Overview

The difficulties in processing of hard-to-cut materials have led to the advent of several advanced machining methods such as Electric Discharge Machining, Electrochemical Machining, Water Jet Machining, Electron Beam Machining and Laser Machining. These methods, generally called as non-traditional machining processes, make use of energy to remove excess material from the stock to produce the desired component. Of these processes, Electric Discharge Machining (EDM) has attracted a great attention from aerospace, automobile and nuclear sectors [1-3] bearing the fact that the other processes either suffer from the drawback of high equipment cost (e.g. water jet, laser and electron beam machining) or hazardous sludge (e.g. electrochemical machining).The shaping tool, which is called electrode and whose geometry is an inverse of the cut geometry, in this process is made of a conductive material. The extra material is cut by a series of sparks between the tool and work-piece in the presence of a dielectric fluid which acts as an insulator to prevent the deposition of removed material onto the tool surface. The EDM process has found several applications such as manufacturing of molds/dies and cutting of holes in a variety of materials including metals and composites [4-9] with large depth to diameter ratio.

Electrical discharge machine (EDM) is a unique method of manufacturing, introduced in the late 1940s and which has been widely adopted as a standard processing phase in manufacturing of forming tools to output plastics moldings, die castings, forging dies and etc. Among the used electrodes is the tool-electrode, or simply the “tool” or “electrode”, and the pieceworker-electrode, or “work-piece”. Electrical discharge machining (EDM) is a process which utilizes the removal phenomenon of electrical-discharge in dielectric [10].

An electrical discharge machining (EDM) is founded on the erosive effect of an electric spark on both the electrodes utilized. Electrical Discharge Machine (EDM) evolved to be one of the most important technologies in the manufacturing industries since many complex 3D shapes can be machined by means of a simple shaped tool electrode. EDM is utilized mainly to machine otherwise complex materials and high strength temperature resistant alloys. Conventional machining technique is usually based on material removal using tool material harder than the work material, but such technique proved weak machining results. Work piece to be machined by EDM has to be electrically conductive. Updated advancement in the area of material science has resulted in newer engineering metallic materials, composite materials, and high tech ceramics, having quality mechanical properties and thermal characteristics as well as sufficient electrical conductivity so that they can readily be machined by spark erosion. EDM can also be used to machine complex geometries for few units or even for dense manufacturing needs. Thus, the input parameters

contribute an essential part, which affects the material rate of removal (MRR) and the tool wear rate (TWR) [11]. Material is eroded by the work-piece through several instantaneously repetitive current discharges between two electrodes, separated by a dielectric liquid and subject to an electric voltage.

1.2 Problem Statement

In electrical discharge machine (EDM), unsuitable choice of input process parameters, such as pulse on time, pulse current, and voltage, may cause weak machining rate or performance. In order to increase machining effectiveness, erosion of the work piece is elevated to the most possible extent and the electrode reduced in EDM process. This is due to material removal rate (MRR) characteristic. Thus, researching electrode wear and relative important factors would work more to improve the machining results and process dependencies [12].

Another possible effect of the poor parameter choice is the lowered accuracy of the product due to the influence of electrode wear ratio (EWR). Less material removal rate (MRR) requires longer machining process, thus it wastes valuable production time. Low precision of the products may be caused by high electrode wear ratio (EWR), or by an unsuitable material removal rate (MRR). Furthermore, electrode wear requires replacement which can be costly for manufacturers. Therefore, studying the electrode wear and relative wear contributing factors can prove effective in the enhance of machining productivity and process reliability [13].

The suggested methodology of this thesis comprises of sections termed as problem identification, research & development and Results & Comparison (Figure 1.1).

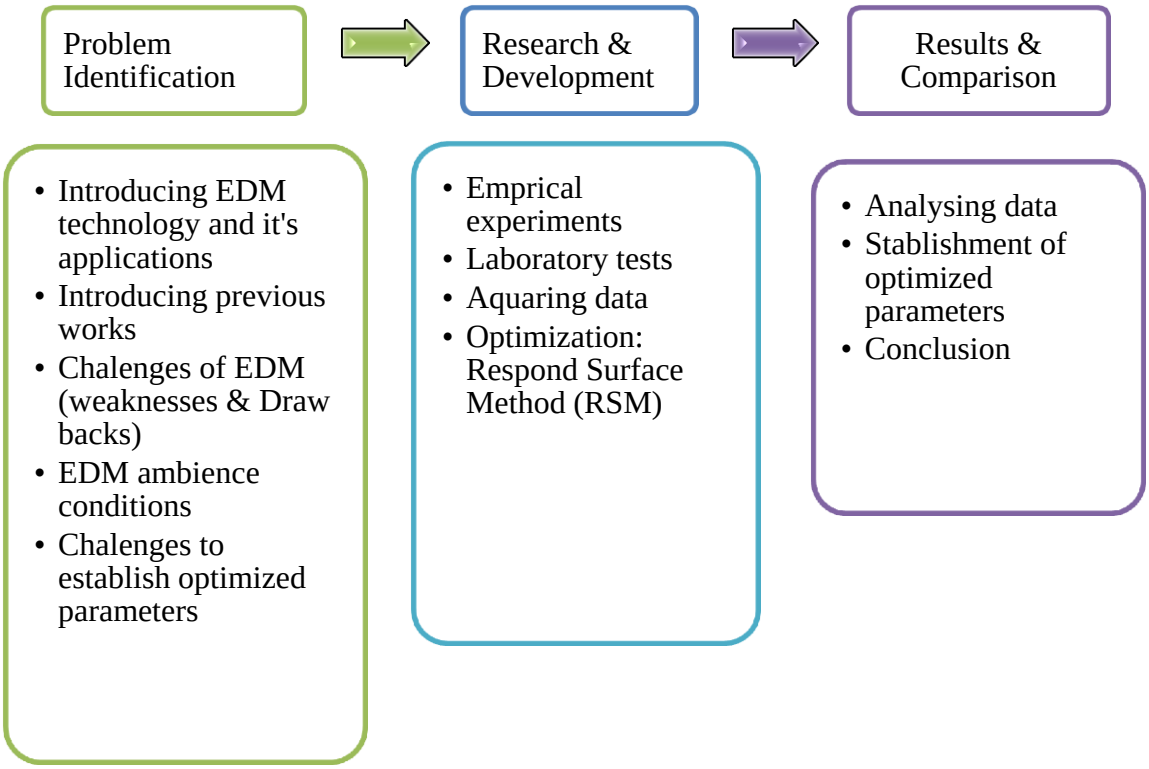

Figure 1.1: Proposed Methodology.

Surface damage due to EDM processes causes adverse effect on the reliability and the performance of components. In current practice the damaged layers of EDMed surfaces are removed either by finishing passes or by chemical milling, which is an added cost to the machining cost. Knowledge of extent of surface damage is essential for the subsequent finishing operations. Due to large number of variables and stochastic nature of the process, even a highly skilled operator is rarely able to achieve the optimal performance. Most of the EDM equipment are probably performing at lower efficiency level. An effective way to solve this problem is to

determine the relationship between the performance of the process and its controllable input parameters (i.e. model the process through suitable mathematical techniques).

A quantitative characterization of the surface taking into account the randomness of its generation and reflecting the peculiarities arising from the electrical discharge is needed so that factor level combination can be obtained at which the desired surface finish can be achieved. The execution of this exercise will need understanding of the limits i.e. best possible surface, process robustness against the perturbations on the process parameters, achieving targets by getting the data at what combination of parameters the EDM surface would achieve specific roughness and understanding the interaction between the parameters. The experimental design approach to this problem may give the insight of the process robustness issues. The design of experiment will consider several factors and interaction effects among them pertaining to the process and response measured will be surface roughness. The objective of this research is to develop mathematical models for surface roughness in die-sink electro-discharge machining by response surface methodology in order to optimize the surface finish of the machined surface. The optimum machining condition is obtained by constructing contours of constant surface roughness and used for determining the optimum cutting condition for required surface roughness.

1.3 Research Contribution and Objectives

The main contribution by this research is to find the feasibility of machining AISI D6 tool steel using circle shaped copper electrode and internal flushing. Also, the machining parameters selected for discharge current, pulse on time, and voltage using response surface methodology. The design approach is based on analysis of MRR, TWR, and Ra responses. To achieve this, machining characteristics must be determine as higher material removal rate (MRR) and less tool wear ratio (TWR) which will lead to better performance and cost effective manufacturing.

The main aim this thesis is as follows:

- To evaluate the effect of pulse on time, pulse current and voltage condition on material removal rate (MRR).
- To evaluate the effect of pulse on time, pulse current and voltage condition on Tool Wear Ratio (TWR) and surface roughness (Ra).
- To investigate the predicting and modeling the optimal set of EDM parameters using Response Surface Methodology (RSM).

1.4 Structure of This Thesis

The main aim of this thesis is to showcase a complete content of electrical discharge machine, advances and applications in industries for EDM.

The remainder of this research is organized as following:

Chapter 2 is the literature review of the research which also postulates the objective and contribution to science.

Chapter 3 broadens the methods used in the research which comprises of buildup of the empirical experiment in alignment with introduction of base materials, tool selection, and EDM parameters as well as the processes for conducting the material removal rate, surface roughness, and tool wear ratio.

Chapter 4 shows the outputs of the EDM process as well as the outputs of mechanical experiments and metallographic studies. However, in this chapter the analysis and the outputs expatiate on the correlation between them.

Chapter 5 refers to the optimization methods utilized in EDM, with response surface method and also presents examples of optimization for EDM process parameters.

Conclusively, the last chapter is concentrated on finalization and future works, which are all conversed in Chapter 6.

The research of this thesis is published in two journals as bellow:

1) Electrical discharge machining of the AISI D6 tool steel: Prediction and modeling of the material removal rate and tool wear ratio. *Precision Engineering, 45*, 435-444. *WOS:000376212000043*
2) Elucidating the effect of electrical discharge machining parameters on the surface roughness of AISI D6 tool steel using response surface method. *Indian Journal of Engineering & Materials Sciences, 24*, 83-90. *WOS:000410464500011*

Chapter 2

LITERATURE REVIEW

Abstract: Literature review is one of the areas of studies. It will provide insight into electrical discharge machine (EDM) process and the techniques implemented to perform experiments. From the previous stage of the project, several literature researches have been executed. Research journals, books, printed or online conference article provided the materials used in the project guides. It works as a guide to execute this analysis. Literature review sections works as a reference, to provide in-depth information and guidance based on journals and other academic sources. This section will contain operations such as the test, history, machining properties and results. History of the electrical discharge machine (EDM) will be the main topic depicted in this section.

2.1 Background of Electric Discharge Machine (EDM)

The beginning of electrical discharge machining (EDM) goes back to the 1770's when the English scientist Joseph Priestly found the erosive effect of electrical discharges. In the 1930s, trials were conducted for the first time to machine diamonds and metals with electrical discharges. Erosion was instigated through sudden arc discharges happening in air between the tool electrode and work piece attached to a DC power supply. The processes were not effective due to machine

sections overheating, thus it can be labeled as “arc machining” Instead of “spark machining” [14].

Initial implementations of electrical discharge machining took place in the 1943 during World War II by two Russian scientists, B.R. and N.I. Lazarenko at the Moscow University [14]. The erosive effect of electrical discharge was a utilized through a controlled process to machine materials. The RC (resistance–capacitance) relaxation circuit was brought in 1950s, which made the first stable trustworthy control of pulse times and also a simple servo control circuit to instantly locate and retain a given distance between the electrode (tool) and the work piece. The RC circuit was widely used in the 1950s and after which served as the model basis for continuous advancements in EDM technology. There have been similar statements of ownership made at around that time when three American employees said that they were using electrical discharges to remove broken taps and drills from hydraulic valves.

These activities evolved to be the foundations for vacuum tube EDM machine along with an electrical circuit for a servo system which lead to appropriate electrode-to-workpiece spacing (spark gap) for sparking, without the electrode contacting the workpiece [14, 15].

In 1980s, with the introduction of Computer Numerical Control (CNC) its utilization in EDM brought about numerous advancements in efficiency enhancement of the Machining activities. As a result of such developments, EDM machines have turn into a more stable alternative that these can be operated by all day long monitored by an adaptive 3 control system. This process makes it possible to machine any material with electrical conductance characteristic regardless of its hardness, shape or strength [14]. The recompenses brought by EDM have been effectively pursued by the manufacturing sector which brought economic advantages and induced research interests.

2.2 Introduction of Electric Discharge Machine (EDM)

EDM has been continually utilized for a long time in machining pieces in the aeronautical industry which included engine parts and landing gear components, thus, the non-conventional machining techniques for example electrochemical machining, ultrasonic machining, electrical discharging machine (EDM) etc. are introduced to perform complex machining. However, such materials are hard to machine through local machining techniques. In retrospect, EDM is able to produce a fine, precise, corrosion and wear resistant outer layer.

Electrical discharge machining (EDM) is an unconventional machining process founded on a thermo-electrical material deletion mechanism, but its surface durability, and consequently the reliability, of the machined parts have been doubted for long time as a result of the thermal form of this machining process. With EDM

process, alloy steel, conductive ceramics and aerospace materials can be machined regardless of their toughness and hardness. Following the advancement of mechanical industry, the need for alloy materials having high hardness, toughness and effective resistance are accelerating [16].

2.3 Principle of EDM

In die-sinking EDM, the electrode is formed and out puts its negative form into the workpiece. In the EDM process a voltage difference is introduced between the electrically conductive tool electrode and a workpiece material at a particular distance between the tool and electrode. The basic idea of EDM is particularly same for both die-sinking EDM and wire- EDM with the variations in the buildup. This process is repeated severally in the machining process. The degree and amount of the current, which can be gotten by the open gap voltage and the resistance, results in the energy of the spark and therefore the spark gap area. The removed metal hardens into small spheres spread in the dielectric, which is removed by 5 dielectric in the pulse interval [17].

The die- sinking EDM is more widely utilized for machining parts with complicated 3D shapes, often with little or odd shaped angles. The volume of material flushed per discharge is usually in the limit of 10-6–10-4 mm3 [18] depending on its usage. Additionally, it is necessary to watch the gap conditions (voltage and current) and synchronously maneuver the various axes to machine the reflected image of the tool into the work piece. Since the shaped electrode shows the area in

which the spark erosion will happen, the correctness of the part outputted after EDM is fairly high. Die-sinking EDM also referred to as sinker EDM, volume EDM or cavity type EDM is one of the two most common types of EDM. This single spark (which is 6000-12000°C relies on the machining state [19]), which occurs within a small gap between the electrode and the work piece known as the spark gap, vaporizes and melts the material within this spark gap, forming a crater in the process. Due to the heat of the spark, the electromagnetic flux is disintegrated and thus the disintegrate, going back to the first state again.

Simultaneously, the dielectric fluid reduces the temperature of the spark gap area and the electrode stays away from the work piece. As the tool electrode goes towards the workpiece in the view of a dielectric fluid (usually de ionized water or hydrocarbon oil, which acts as an insulator and coolant), a column of high electromagnetic flux is created on getting close to the metal work piece. As the insulating effect of the dielectric fluid disintegrates under high electric field, it leads to a single spark to be ejected between the tool electrode and the workpiece. Electrical Discharge Machining (EDM) process removes electrically conductive materials by means of rapid repetitive spark discharges in the presence of dielectric liquid, while a voltage difference is applied between the electrode and workpiece. The duration at which the current is turned on and off is referred to as the pulse period (T_{on}) and pulse limits (T_{off}) time and helps in allowing the spark gap area to reproduce the states important for sparking again [17].

Figure 2.1 shows the schematic diagram of the fundamental principle of EDM [17, 20]. Conclusively, the crater is created by the internal burst of the vapor bubble. The die-sinking EDM is a reproductive shaping process which the form of the electrode is reflected in the workpiece. The wear has to be very low, in order to keep the electrode's initial shape unchanged in the whole machining process. The electrical field has the greatest strength (energy density of 1011 - 1014 W/m2) at the instance where the distance between the electrode and workpiece is smallest [18]. Figure 2.2 shows the fundamental schematic diagram of the die-sinking EDM [21].

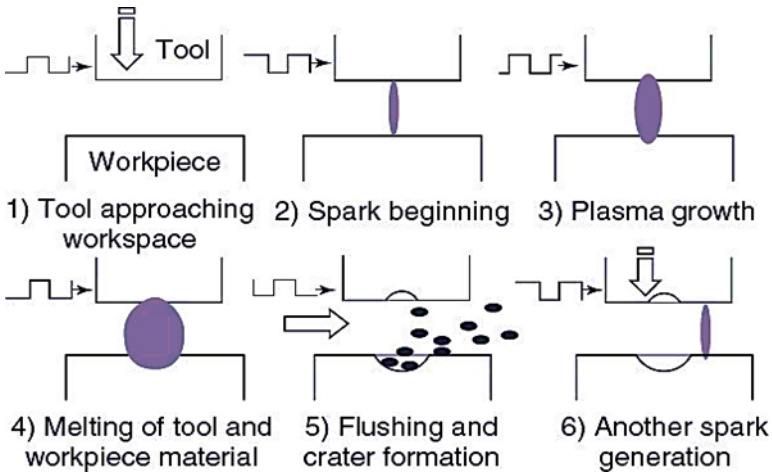

Figure 2.1: Schematic representation of the basic principles of EDM [17, 19].

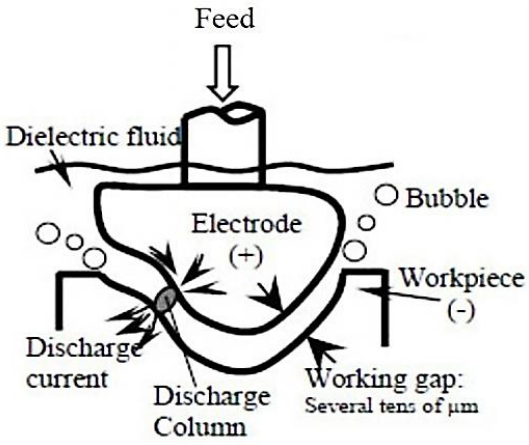

Figure2.2: Schematic showing the principle of die-sinking EDM [21].

2.4 Types of EDM

There are several types of EDM present which is briefly elaborated below. It is also utilized for coinage die forming, metal disintegration machining, etc. EDM process is among the most generally used processes by mold-making tool and die industries. It is transforming into a widely used technique of producing prototype and manufacturing parts, particularly in the aerospace, auto-mobile and electronics industries in which manufacturing volumes are specifically less [22].

2.4.1 Sinking EDM

In this process, copper or graphite is widely utilized as electrode material. The numerical control checks the gap states (voltage and current), synchronously controls the different axes and the pulse producer. When the pulsating direct current supply is switched off, the plasma channel disintegrates. In such procedure electrical energy metamorphose into thermal energy by means of a series of discrete electrical discharges taking place between the electrode and work piece immersed in a dielectric fluid [22, 23]. In sinking EDM process, mirror image of tool shape takes

place on the outer layer of work piece. The thermal energy produces a ray of plasma contained within the cathode and anode sides. The dielectric liquid is filtrated to eliminate residual particles and decomposition outputs. This leads to an abrupt minimization in the temperature permitting the circulating dielectric fluid to make use of the plasma channel and remove the molten material from the work piece outer layer [24]. Figure 2.3 shows the schematic diagram of the sinking EDM.

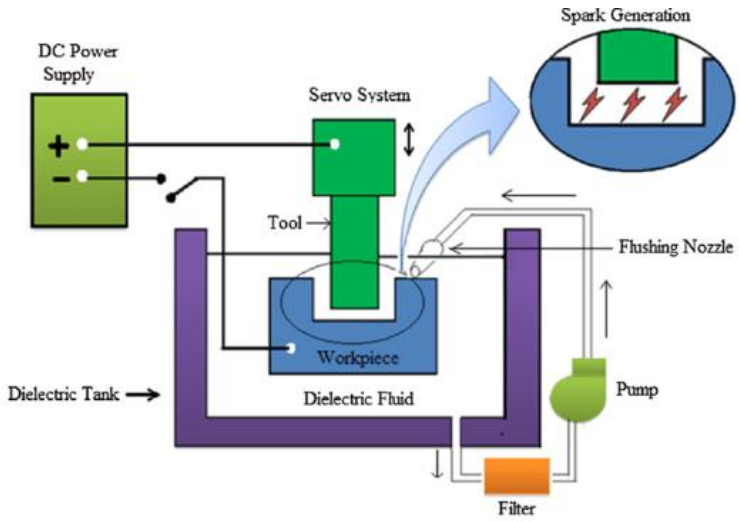

Figure 2.3: Schematic diagram of the sinking EDM [25]

2.4.2 Wire EDM

Wire EDM process is generally not limited to tool and die-making industry, it is also employed in electronics, medicine, and the automotive industry fields [22]. It utilizes a small continuously moving wire feeding through the work piece by a micro-processor removing the requirement for reshaped electrodes, which are needed in the EDM. EDM Wire-cut EDM (WEDM) is among the most likable variants due to its capability to machine conductive, exotic and high strength and temperature resistive (HSTR) materials with the aim of producing intricate forms and profiles [22]. The

process of wire-cut EDM employs a slim copper wire of 0.1–0.3 mm diameter as the electrode, and the work piece is placed on a movable worktable, permitting sophisticated two-dimensional shapes which can be sliced on the work piece with the help of numerically controlled movements over X–Y worktable [26]. Figure 2.4 shows the fundamental schematic diagram of the wire – EDM.

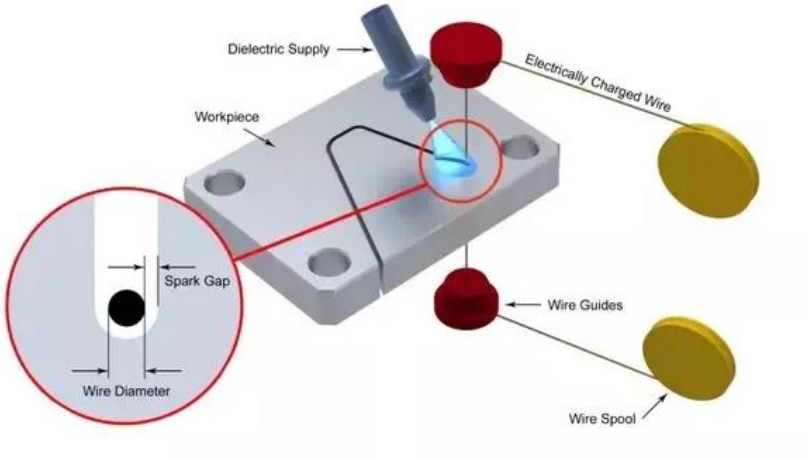

Figure 2.4: Fundamental schematic diagram of the wire - EDM

2.4.3 Micro EDM

In micro-wire EDM, a wire with 0.02 mm diameter minimum is utilized to cut through a work piece. Micro-EDM is has the abilities including but not limited to, micro-holes and micro-shafts as little as 5 mm in diameter. It can also machine sophisticated three-dimensional (3D) micro cavities as well [22]. Indie-sinking micro-EDM, an electrode is utilized having micro-features to cut its mirror image in the work piece. In micro EDM drilling, micro-electrodes with a minimal diameter of 5–10 mm are utilized to create micro-holes in the work piece. Micro EDM process is fundamental of four kinds: micro-wire EDM, die-sinking micro-EDM, micro EDM

drilling and micro-EDM milling. In Micro-EDM milling, micro-electrodes (of diameters down to 5–10 _m) are used to output 3D cavities by using a motion technique which looks like that in conventional milling [24]. Figure 2.5 shows the fundamental schematic diagram of the micro EDM. The recent in vogue pattern of minimizing the dimension of products has provided micro-EDM an important level of research focus.

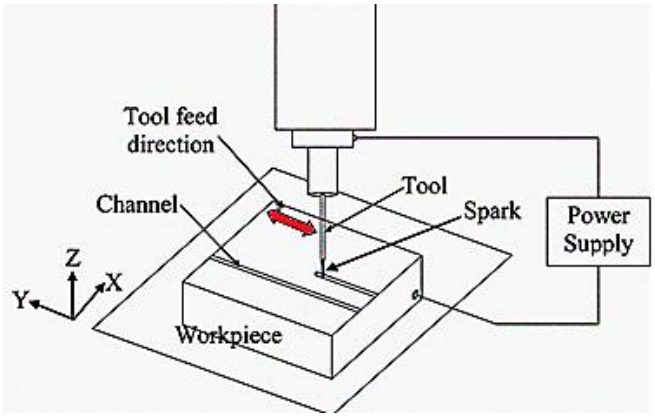

Figure 2.5: Fundamental schematic diagram of the micro EDM [28]

2.4.4 Powder Mixed EDM (PMEDM)

The mechanism of PMEDM is holistically dissimilar than the normal EDM [22]. When a better voltage is imputed, the spark gap filled up with additive particles and the gap length setup between tool and the work piece jumped up from 25–50 to50–150 mm [22]. These excited particles are sped up by the electric field and behaves as conductors. A better material in the particulate nature is joined into the dielectric fluid of EDM. The powder particles get excited and act in a zigzag fashion Figure 2.6. The chain formation contributes in bridging the gap between both the electrodes, which causes the early explosion. Quicker sparking within discharge takes place

leads to quicker removal from the work piece outer layer. The powder particles sort themselves under the sparking area and come together in clusters.

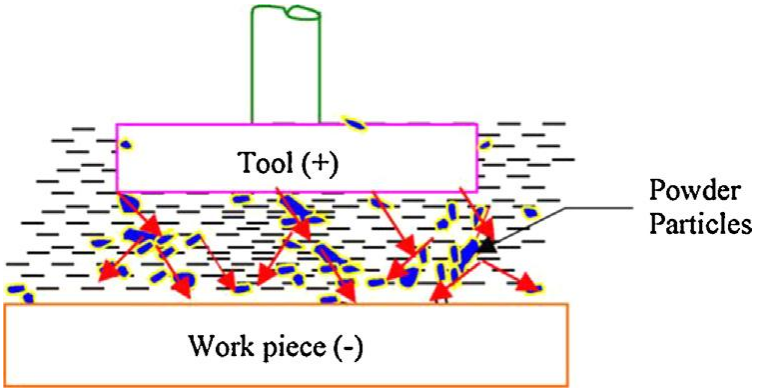

Figure 2.6: Principle of powder mixed EDM [22]

2.4.5 Dry EDM

In this procedure a slim walled pipe is utilized as tool electrode by which high-pressure gas or air is provided. The work of the gas is to prevent the eroded particles from entering the electrode, and also to cool its inner wall. The procedure was made to reduce the pollution caused by liquid dielectric which generates vapors during the machining process, and the amount needed to control the waste [24]. Figure 2.7 shows the fundamental schematic diagram of the dry EDM machine.

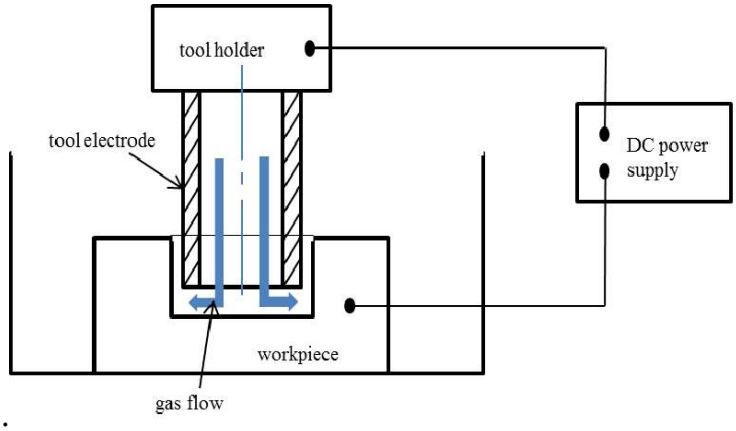

Figure 2.7: Principle of dry EDM machine [29]

2.5 Important Input Parameters of EDM

2.5.1 Spark On-Time (Pulse Time or T_{on})

Material elimination is equally proportional to the quantity of energy put in during this on-time. This energy is actually controlled by the peak current and the length of the on-time. The amount of time (μs) the current is permitted to flow per cycle [30].

2.5.2 Spark off-Time (Pause Time or T_{off})

Thus, if the off-time is too small, it will lead the sparks to be unbalanced. The amount of time (μs) between the sparks, on-time, controls the quickness and the balance of the cut. This time permits the molten material to harden and to be cleansed out of the arc gap [17, 30].

2.5.3 Arc Gap (or Gap)

It can be referred to as spark gap. Spark gap can be controlled by servo system (Figure 2.3). The Arc gap is length between the electrode and work piece when in the process of EDM [17, 30].

2.5.4 Discharge Current (Current Ip)

Discharge current is directly proportional to the Material elimination rate. Current is quantified in amp permitted to per cycle [30].

2.5.5 Duty Cycle (τ)

It is the duration of on-time with respect to the total cycle time. The parameter is obtained by dividing the on-time by the total cycle time (on-time pulse off time) [17, 30].

$$\text{Duty cycle (\%)} = T_{on} / (T_{on} + T_{off})$$

2.5.6 Voltage (V)

It is a potential difference that can be quantified by volt, it also has a contribution to the material elimination rate and permitted to per cycle [30].

2.6 Performance Output Parameters of Die-Sinking EDM

2.6.1 Material Removal Rate (MRR)

The MRR is a show of machining quickness when in EDM. The material removal rate (MRR) can be expressed as the quantity of material eliminated over a unit period of time. The MRR can be gotten by calculating the quantity of material from the machined characteristic geometry or from the weight difference of the work piece before and after machining. The MRR is more generally defined by the unit [mm3/min]. Additionally, to these electrical parameters, other non-electrical parameters and material properties have great effect on MRR. The more the MRR, the quicker the machining speed. A larger value of discharging voltage, peak current,

pulse duration, duty cycle and smaller values of pulse range can lead to a larger MRR [17].

2.6.2 Tool Wear Ratio (TWR)

The tool wear ratio also relies on electrode polarity and the electrode materials properties. The tool wear ratio (TWR) or electrode wear ratio (EWR) or relative electrode wear (REW) is expressed as the ratio of volume of materials eliminated from the tool electrode to that of work piece. However in some cases, frontal electrode wear or corner wear is quantified (in mm or micron) to show the electrode wear, the most precise way of showing electrode wear is the TWR.

As it is known that the electrode wear is to be smaller than the material eliminated from the work piece, the TWR in actually identifies the volumetric wear of electrode in comparison to the work piece. The TWR is fantastic reliant on the operating parameters. This is a show of the electrode wear in EDM, and is identified by percentage (%). The larger numbers of gap voltage, capacitance, peak current and pulse time maximizes the tool wear ratio. The volumetric wear ratio of the electrode becomes little for the electrode material with large boiling point, large melting point, and large thermal conductivity [17, 31]. This is due to the fact that when in the EDM, the electrode wears out from both sides of the electrode instead of one direction. Smaller numbers of TWR is always expected as it shows a more balanced and economic machining during EDM.

2.6.3 Surface Roughness (Ra)

The surface roughness shows a little minimizing pattern with increasing dielectric removal pressure. Larger discharge energy leads to thicker recast layer [32]. The surface roughness also relies on non-electrical parameters. The surface roughness is a much significant parameter to take into consideration in die-sinking EDM. In short, the surface roughness maximizes with the increase of discharge energy. The surface roughness is identified by the 'mean surface roughness (Ra)', which is quantified in micron [μm]. In most of the die-sinking activities, segregate roughing and finishing operation are performed to finalize the end output. Conclusively, the surface roughness can change due to the electrode materials also [33].

The surface roughness maximizes with the increase of gap voltage, capacitance, peak current and pulse time. The degree of level of recast layer is affected by resistance and capacitance for RC type pulse generator, and by gap voltage, peak current and pulse duration for transistor type pulse generator, as these parameters influences the discharge energy. At larger settings of discharge energy, the crater sizes become coarser, which leads to a larger number of surface roughness [33]. The peak-to-valley surface roughness or maximum roughness (Rmax) is one other way of identifying the roughness of the machined surface [17].

In some cases, the surface quality is defined by additional definitive term which is the 'surface integrity' which has surface topography, crater characteristics, and recast layer thickness, surface defects etc. One does a mixture of the machining parameters

to find the best performance for any work. On the other hand, for better finishing of the machined surface the value of surface roughness parameter should be smaller. The effect of die-sinking EDM can be found by the above mentioned performance parameters. For cost management of the electrodes, the electrode wear should be small. Due to this, greater performance can be identified by a larger MRR, smaller Relative wear Ratio (RWR), and small value of Ra. The needs of machining parameters for higher performance are outlined in table 2.1 [17, 34]. Normally larger MRR can make the machining quicker.

Table 2.1: Summary of the effect of machining parameters on EDM performance

Machining parameters	To increase MRR (mm^3/min)	To lower the value of RWR (%)	To lower the value of R_a (μm)
Electrode polarity	Negative	Negative	Negative
Open circuit voltage	Low	Low	Low
Peak current	High	Moderate	Low
Pulse duration	High/moderate	Low	Low
Pulse interval	Low	Moderate	Moderate
Duty cycle	High	Low	Low
Pulse frequency	High	Low/moderate	Low
Flushing pressure	Low	Moderate	Moderate

2.7 Dielectric fluid

The significant properties of dielectric that should be taken into consideration when choosing are chemical compositions, viscosity, dielectric strengths, and cooling rates. The dielectric material acts as insulator, which only disintegrates when the input of

voltage permitting controlled sparking to eliminate the materials from work piece. In the die-sinking EDM, the machined area is totally placed in the dielectric liquid. As can noted that both electrode and work piece are electrically conductive in EDM, upon imputing the voltage there would be a production of uncontrollable sparking without the effect of dielectric. Thus, the choosing of dielectric fluid is a significant activity in the die-sinking EDM activity. The dielectric liquid not only acts as controlled sparking, but also acts as coolant and helps to remove the residues out of the machined area. For a greater EDM performance, the following points should betaken into consideration when choosing the dielectric fluid [17]:

- Flash point: The larger flash point temperature is favorable for safety reasons.
- Dielectric strength: Large dielectric strength can help in a smother amount of control.
- Viscosity: The smaller the viscosity of the dielectric fluid, the better the accuracy and finishing as it is much simpler to remove little spark gaps with less dense and thinner oil.
- Specific gravity: Lower specific gravity is favorable for greater performance.
- Color: Dielectric fluid color should be as clear as it n be.

Both water and oil has some benefits and dis-benefits, which need to be taken in to account for choosing the right dielectric for EDM activities. The most often utilized

dielectric fluids in the die-sinking EDM are mineral, hydrocarbon or EDM oil, kerosene and di-ionized water. A relative research on the performance of water and oil as dielectric fluid is showcased in table 2.2 as a help for choosing process [17]:

Table 2.2: Comparison of the performances of oil and water as dielectric for die-sinking EDM

Oil as a dielectric fluid	**Water as a dielectric fluid**
1. Do not lead to any electrolytic destruction 2. Become more prone to thermal destruction and micro-cracking 3. Can make the EDMed outer layer more harder and thus more brittle 4. Constrained cutting speed 5. Enhanced outer layer completed can be gotten 6. More frequently electrodes are used as positive polarity if oil is used as dielectric 7. Less electrode wear 8. Lower operating and maintenance costs	1. Electrolysis occur which may cause electrolytic damage 2. May cause corrosion and rust due to electrolysis 3. After machining the surface is not so hard and brittle 4. Cutting speed may be high using water as a dielectric fluid 5. Surface becomes rougher after EDM 6. In water as dielectric fluid, normally electrodes are used as negative polarity 7. Electrode wear is severe 8. High operating and maintenance costs

2.8 Dielectric Circulation and Flushing System

The parts of this system are tank or reservoir, dielectric pump, filter, pipe and nozzle. In EDM, the greater the flushing state, the less the off-time needed for machining and consequentially the larger the effectiveness of the whole EDM activity. The pump is utilized to bring in dielectric fluid into the work tank and the filter is utilized to trap and collect the residual particles dielectric and to ensure re-circulation of

newer dielectric to the machining area. The dielectric revolving and removal system is in charge of flushing out removed materials and bringing in new dielectric to the machining area. The major work of the dielectric circulation and flushing unit are [17]:

- To spread the dielectric flow by means of the spark gap to eliminate gaseous and solid residues produced when in the EDM.
- To bring in newer and clean dielectric fluid to the cut.
- To flush away the chips or metal particles produced in the spark gap.
- To control and balance the dielectric temperature well below its flash point.
- To serve as a temperature controller for cooling the electrode and work piece.

However, in modern die-sinking EDM there are particularly three kinds of flushing. In majority of the die-sinking EDM activities, both the electrode and work piece stay immersed into the dielectric and the flushing takes place due to the jump action of the electrode towards the work piece. During the jump movement, turbulence is formed in the liquid in between the electrode and work piece to eliminate the residual particles from the spark gap. The type of flushing should be chosen from the need of the work to be performed and its usage [17, 35].

The kinds of flushing are:

- Pressure flushing or injection flushing
- Suction flushing
- Jet or side flushing

The flushing pressure is a significant parameter to take into account in die-sinking EDM. Alternatively, too much flushing pressure can speed up electrode wear as well as form turbulence in the cavity. If the flushing pressure is too low, it is hard to eliminate the gaseous and solid residues. The effect of flushing pressure on the machining characteristics, as summarized from the literature, are listed in table 2.3 [17].

Table 2.3: Effect of flushing pressure on the machining performance during EDM

Machining characteristics parameter	**Effect of flushing pressure**
Material removal rate (MRR)	The MRR slightly decreases with higher flushing pressure
Relative wear ratio (RWR)	RWR first decreases and then increases again on the increase of flushing pressure. An optimal flushing pressure can be found for each operation
Surface roughness (R_a)	Surface roughness tends to reduce first then again increase with the increase of flushing pressure.

Generally kerosene and deionised water is utilized as dielectric fluid in EDM. Dielectric base is generally flushed around the spark area. It is also put inside through the tool to get efficient elimination of molten material. Tap water cannot be made use of as it ionises too quickly and thus breakdown as a result of the effect of salts as impurities takes place.

2.9 Tool Material

Electrode material is to be chosen based on wear resilience when exposed to positive ions. Therefore, the localized increase in temperature has to be lowered by guiding or adequately selecting its properties, so even when temperature maximizes there would be lower melting. Further, the tool should provide ease when applied to intricate shaped geometric characteristics are machined in EDM [17]. Therefore, the fundamental characteristics of electrode materials are:

• High electrical conductivity – electrons emitted whilst keeping cooler temperature as there is less bulk electrical heating

• Larger thermal conductivity – for the similar heat load, the electrode temperature increase would be less as a result of quicker heat controlled to the larger part of the tool and thus less tool wear

• Larger density – for similar heat load and similar tool wear by weight there would be less volume elimination or tool wear and thus less dimensional loss or non-precision

• High melting point – high melting point leads to less tool wear due to less tool material melting for the same heat load

• Easy manufacturability

• Cost – cheap

The followings are the different electrode materials which are used commonly in the industry:

• Graphite

• Electrolytic oxygen free copper

• Tellurium copper – 99% Cu + 0.5% tellurium

• Brass

2.10 Application of EDM

2.10.1 Prototype Production

The EDM process is most generally utilized by the mold creation tool and die industries, but it is evolving to become a wide spread technique of production parts and prototypes, particularly in the industrial fields of automobile, aerospace, and electronics for which production volumes are relatively low. In sinker EDM, a copper tungsten, graphite, or pure copper electrode is machined into the needed (negative) shape and attached into the workspace over the end of the vertical ram [35].

2.10.2 Coinage Die Preparation

Figure 2.8 shows the Coinage die process. For the forming of dies for manufacturing jewelry and badges, or blanking and piercing (through use of a pancake die) by the coinage (stamping) technique, the positive master may be made from sterling silver,

since (with appropriate machine settings) the master is significantly removed and is utilized only once. Relatively weaker materials like silver may be engraved by hand as refinement. For badges these flats may be additionally shaped to a curved outer layer by another die. The final object may be additionally refined by hard (glass) or soft (paint) enameling and/or electro plated with pure gold or nickel. The output negative die is then solidified and utilized in a drop hammer to make stamped flats from cutout sheet blanks of bronze, silver, or low proof gold alloy [35]. This type of EDM is normally carried out immersed in an oil-based dielectric.

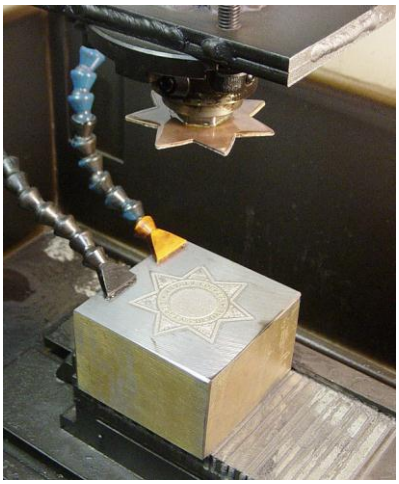

Figure 2.8: Coinage die preparation [35]

2.10.3 Small Hole Drilling

Small hole drilling EDM is utilized in various forms of usage. The high-temperature, very hard, one crystal alloys used in these blades makes normal machining of these holes with high aspect ratio really hard, if not impossible. Small hole EDM is also utilized to form microscopic orifices for fuel system components, spinnerets for synthetic fibers such as rayon, and other usage. On wire-cut EDM machines, small

hole drilling EDM is utilized to make a bypass hole in a work piece by which to thread the wire for the wire-cut EDM activity. Gas move by these small holes which permits the engines to use a larger temperature than necessarily possible. A different EDM head particularly for small hole drilling is placed on a wire-cut machine and permits huge hardened plates to possess completed parts removed from them as required and without pre-drilling. Leading and trailing edges of turbine blades utilized in jet engines. Figure 2.9 and 2.10 respectively shows the Small hole drilling EDM machines and a turbine blade with internal cooling as applied in the high-pressure turbine.

The electrode tubes function similar to the wire in wire-cut EDM machines, which has a spark gap and wear rate. There exists stand-alone small hole drilling EDM machines with an x–y axis referred to as a super drill or hole popper and they can machine blind or through holes. Holes of 0.3 mm to 6.1 mm can be achieved in this drilling activity. EDM drills drill holes with a long brass or copper tube electrode that revolves in a chuck with a stable movement of distilled or deionized water moving through the electrode as a flushing agent and dielectric. Some small-hole drilling EDMs are able to drill through 100 mm of soft or through hardened steel in below 10 seconds, having an average of 50% to 80% wear rate. Brass electrodes are much more simpler to machine but are not advised for wire-cut activities due to eroded brass particles that causes “brass on brass” wire breakage, thus, copper is suggested [35].

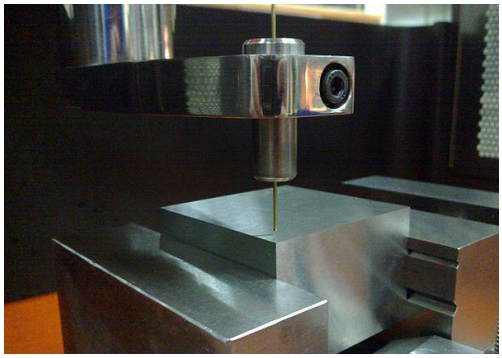

Figure 2.9: Small hole drilling EDM machines [35].

Figure 2.10: A turbine blade with internal cooling as applied in the high-pressure turbine [35]

2.10.4 Metal Disintegration Machining

In this usage, the process is called “metal disintegration machining” or MDM. The metal disintegration process eliminates only the center out of the tap, bolt or stud leaving the hole untouched and permitting a part to be recovered. Numerous manufacturers produce MDM machines for the particular reason of eliminating disintegrated tools (drill bits, taps, bolts and studs) from work pieces.

2.10.5 Closed Loop Manufacturing

Closed loop manufacturing can enhance the precision and minimize the tool costs

2.11 Advantages of EDM

Benefits of EDM include machining of [35]:

- Sophisticated geometries that would otherwise be hard to manufacture with normal cutting tools.
- Very hard material to very close tolerances.
- Very small work pieces where normal cutting tools may destroy the part from too much cutting tool pressure.
- There is no direct contact between tool and work piece. Thus delicate sections and weak materials can be machined without any change.
- A nice outer layer finish can be achieved.
- Very fine holes can be drilled.

2.12 Disadvantages of EDM

Dis benefits of EDM include [35]:

- The slow rate of material elimination.
- Possible fire hazard connected with use of combustible oil based dielectrics.
- The added time and cost used for forming electrodes for ram/sinker EDM.
- Remaking sharp corners on the work piece is hard as a result of electrode wear.
- Particular power consumption is very high.
- Power consumption is high.
- "Overcut" is created.
- Too much tool wear occurs during machining.

- Electrically non-conductive materials can be machined only with particular set-up of the process.

2.13 Recent Research on the EDM Machine Performance

Craig Smith and Philip Koshy (2013) [36] studied on the Applications of acoustic mapping in electrical discharge machining, The discharges distribution of a wide spread in electrical discharge machining (EDM) is composed of important process information, which is not precisely perceived from electrical signals that are utilized extensively for process monitoring and control. Specifically, the work is in regards to the realistic process conditions, in which AE from successive discharges can lead to repeated signal interference, which is unfavorable for reliable time lag estimation. The use of this capability for the relative identification process of workpiece height and electrode length in fast-hole EDM and wire EDM are presented. This research study hence explored the utilization of acoustic emission (AE) to map the discharges, in consideration of the acoustic time lag.

Alexander Goodlet and Philip Koshy (2015) [37] analyzed the Real-time analysis of gap flushing in electrical discharge machining. This permitting technology is readily adapted for the in-process monitoring, quantification, and optimization of flushing, and this built the foundation for flushing-related adaptive control of EDM. In This paper reports on acoustic emission (AE) from electrical discharge machining (EDM) in the context of gap flushing, and showcases its sensitivity to gap contamination from both metallic residues and gas bubbles. AE is further presented to be connected

to the local medium (liquid or gas bubble) by which which individual discharges occur, and thus comprise special and valuable process information on the effectiveness with which material is erased at the scale of a single discharge.

Shabgard et al. [38] researched on the ascertainment of white layer thickness, heat affected areas, and outer layer roughness by 3D-FEA inEDM process. Other ways to identify recast layer is to classify it with the other surface integrity parameters such as micro-hardness, residual stress and micro cracks as postulated by Rajurkar [39]. Pandit and Rajurkar [39] came up with a stochastic approach with the aid of Data Dependent Systems (DDS) to thermal modeling of EDM. A viable cohesion was found between experimental and the numerical outcomes. In this way, a melting isothermal curve defining equation was expatiated from the profiles of actual machined outer layers.

Guojun Zhang et al.[40] researched on the machining process of nano-electrical discharge machining based on put together atomistic-continuum modeling method. Nano-electrical discharge machining (nano-EDM) is an alluring measure to manufacture parts with nanoscale accuracy; however, as a result of the incompleteness of its theories, the advance making of more advanced nano-EDM technology is hampered. The melting process is critically looked into. Before the material that its temperature has been raised gets melted, thermal compressive stress higher than 3 GPa is induced. In Addition, a computational simulation model bringing together the molecular dynamics simulation model and the two-temperature

model for one discharge process in nano-EDM is made to study the machining mechanism of nano-EDM from the thermal perspective.

They observed that in the time of the cooling process of the melted material, tensile stress more than 3 GPa comes, causing the dismembering of material. The formation of the white layer is connected to the homogeneous solidification.

Sabouni and Daneshmand [41] conducted a research on EDM process parameter for NiTi SMA using graphite tool. For experimentation L18 Taguchi's DOE is being used. To improve the accuracy of experiments and to prevent the effect of oil-based dielectrics in reacting with the workpiece surface de-ionized oil water with an EC of less than 1 ms (micro Siemens) has been implemented along with the constant spray type of flushing. In this research study voltage is kept at 2 levels and pulse on, pulse off, gap current is at 3 levels.

Y. Zhao et al.[42] investigated on the Experimental investigations into EDM behaviors of single crystal silicon carbide. The present study aims to investigate the fundamental electrical discharge machining (EDM) characteristics of silicon carbide (SiC) single crystal material. The EDM machining performances of SiC are experimentally studied and compared to that of steel. Die-sinking EDM of SiC by utilizing copper foil electrodes was proposed and investigated. It was found that EDM characteristics of SiC have a big difference from those of steel. The EDM

speed of SiC is higher and the tool wear ratio is lower compared to that of steel material, although SiC has a higher thermal conductivity and melting point.

Thermal crack caused by the thermal shock of electrical discharges was found as another main factor contributing to the removal of the material in EDM of SiC material. Also it is concluded that the new foil EDM method for slicing SiC ingot has potential for slicing SiC wafers in the future.

In this study, the fundamental EDM behaviours of SiC are investigated and compared with those of metal materials (cool tool steel SKD11). Furthermore, the possibility of slicing SiC by utilizing foil EDM method is discussed.

Min Zhang et al. [43] investigated on the Effects of some process parameters on the impulse force in single pulsed EDM. This study aims to have a systematic research on the effects of the other machining parameters, including dielectric medium, polarity, tool geometry, gap width, and immersion depth, on the impulse force.

Except peak current, the effects of other machining parameters have been studied. Klocke et al. have found that the impulse force of planar electrode was larger than that of sphere electrode [44]. Zhang et al. indicated that there was no impulse force when the dielectric medium was gas [45]. However, little systematic research on the effects of other machining parameters has been carried out. The impulse force causes deformations and vibrations of tools and workpieces, which can lead to a change of

gap width and short circuit [46]. To completely understand the impulse force is helpful for the machining of highly precise or high aspect ratio geometries [47].

Saravanan M et al. [48] paid more attention on optimization of process parameters at the time of wire electrical discharge machining of Ti gr 2 for enhancing corner precision. In this experimental work, an trial has been executed to conclude on the optimized parameters whuch includes diameter of wire, on/off pulse time, current, tension in wire for reducing surface roughness (SR) & for maximizing MRR (metal removal rate) during machining by wire electrical discharge (WEDM) process of Titanium Grade 2 (Ti Gr 2) alloys. Ti Gr 2 alloys are widely used in fabrication of a variety of aerospace components because of their low weight ratio, high strength and superior resistance to corrosion. This paper discusses extensively about optimizing process parameters of WEDM which includes SR and MRR related with the corner machining mechanism employing Taguchi technique.

From various literature reviews [49–57] related with the experiments focusing on the characteristic features of WEDM, it can be known comprehensively that the parameters like speed of wire, tension in the wire, voltage and current discharge, frequency of pulse, fluid (dielectric) pressure etc are found to play key role in determining the performance characters like kerf width, cutting speed, surface finish etc.

G. Anand et al.[58] Did work on optimization of process parameters in edm with magnetic field utilizing grey relational analysis with taguchi method. this technique is used to get the optimal selection of machining parameters such as peak current (I), pulse duration (Ton), voltage (V), Servo reference voltage (Sv) in Electrical Discharge Machining (EDM) process to identify the differnces in two performance characteristics of the work material HCHCr i.e. DIN 17350-1.2080 using copper electrode. Thus machining parameters for EDM were optimized to geta mixed performance characteristics objectives of greater metal removal rate and lower surface roughness value with EDM in magnetic effect and standard EDM on work piece during machining process. The metal removal rate and surface finish is enhanced with aid of magnetic field.

Manish Gangil and M. K. Pradhan [59] worked on Optimization the machining parameters by using VIKOR (VIšekriterijumsko KOmpromisno Rangiranje) Techique during EDM process of Titanium alloy. In this research thirty experiments were carried out on Ti-6Al-4V (Titanium alloy) work piece with copper tool using Central Composite Design (CCD).The optimal Condition of experiment were formed utilizing the Pi value gotten from VIKOR technique, a multi criteria decision making technique which decides the raking list based on the particular measure of closeness to ideal solution. From the analysis it is deduced that the Ip = 12A, Ton=100μsec, Tau=18%, V=30V gives greates Pi values.so found to better best equilibrium.

L. Selvarajan et al.[60] researched on experimental investigation of edm parameters on machining si3n4-tin conductive ceramic composite using hallow tube electrode for enhancing geometrical precision. This research showcases the result gotten by the experimental studies that are executed to carry out an investigation on the effect of electrical discharge machining processes (EDM) input parameters on the characteristics of output process parameters.

2.13.1 Recent Research on Material Removal Rate (MRR)

Yakup Yildiz (2016) [39] investigated prediction of material removal rate in electrical discharge machining and the thickness of the white layer through thermal analyses. On the other hand, material removal rate (MRR) can be slow and its approximation is hard in that process. Thus, precise estimation of this result is crucial for EDM activities. In this study recast or white layer formation is either not needed or inevitable result of EDM processes.

Errors of mean results are 1.98% and 3.34% by FEA in estimation of white layer thickness and material removal rate. Numerical outcomes of the models have been comparatively analyzed with outcomes of an experimental study. In this research, white layer thickness and material removal rate were estimated through theory supported thermal model and 3D finite element (FE) model. When compared to theoretical model, finite element analysis (FEA) proved supportive to the results achieved through experimentations. This investigation combines and cross checks

the discharge current with the white layer thickness and material removal percentages in the EDM processes.

N. saha et al investigated the electrical and non- electrical parameters of sintered the silicon carbide (SiC) of 5- 20 wt% in zirconium diboride composites. They kept the parameters of input as fixed and studied machining performance as well as Metal removal rate (MRR) and as they concluded, when the SiC weight percentage is more MRR become less due to the increase in composite resistivity [61].

A.Muttamara et al. [62] investigated on the Effect of electrode material on electrical discharge machining of alumina.Graphite was used as electrode material in EDM. As for EDM-C3, MRRwas increased by 80% under the same condition. The value of MRR was found to increase by 60% for EDM-3 with positive electrode polarity. It is expected that carbon from graphite electrode implant and generate a conductive layer. The electrical discharge machining of 95% pure alumina shows that the EDM-C3 performs very well, giving significantly higher material removal rate (MRR) and lower electrode wear ratio than the EDM-3 and copper electrodes. When the results were investigated with energy dispersive spectroscopy (EDS), no element of copper was observed on the conductive layer with both EDM-3 and EDM-C3.

The formation mechanism of the electrical conductive layer on the EDMed surface is much different as compared to other ceramics. Surface roughness was improved to 25µm with positive polarity of EDM-C3. In addition to this, the electrically

conductive layers are not formed sufficiently to adhere to the EDMed work piece surface and keep a stable and continuous discharge generation on the ceramics. However, surface resistivity of a conductive layer created with EDM-C3 is less than with EDM-3. Copper, graphite (Poco EDM-3) and copper-infiltrated-graphite (Poco EDM-C3) electrodes were used to compare the effects of generation of a conductive layer on alumina corresponding to EDM properties. In this research during the machining of Al2O3 ceramics, inferior machining properties have been obtained.

Vaibhav Gaikwad and Vijay Kumar S. Jatti [63] investigated on the Optimization of material removal rate during electrical discharge machining of cryo-treated NiTi alloys using Taguchi's method. In this study they focused on optimization of electric discharge machining process parameter for maximization of material removal rate while machining of NiTi alloy. The current, pulse on time, pulse off time, work piece electrical conductivity, and tool conductivity were considered as process variables. Experiments were carried out as per Taguchi's L36 orthogonal array. Based on the analysis it was found that work electrical conductivity, gap current and pulse on time are the significant parameters that affect the material removal rate. The optimized material removal rate obtained was 7.0806 mm3/min based on optimal setting of input parameter.

Prihandana et al. [64] investigated the effect of vibration on electric discharge machine. Material used for conducting these experiments is stainless steel (SS-304) with a low frequency vibration. This research study shows that use of a low

frequency vibration improves the material removal rate and diminishes tool wear rate and surface finish.

Manjaiah et al. [65] investigated machining of NiTi alloy on wire electric discharge machine. In this research experiments were conducted as per L27 orthogonal array. During this research anal- ysis of variance and analysis of means were performed to optimize the processes. From this research it was concluded MRR is affected significantly by pulse on time.

Rajmohan T et al. [66] conducted a research study on Optimization of Machining Parameters in Electrical Discharge Machining (EDM) of 304 Stainless Steel. in this investigation, the effect of electrical discharge machining (EDM) parameters such as pulse-on time (TON), pulse-off time (T_{OFF}), Voltage (V) and Current (I) on material removal rate (MRR) in 304 Stainless steel was studied. The experiments are carried out as per design of experiments approach using L. orthogonal array.

The results were analyzed using analysis of variance and response graphs. From this study, it is found that different combinations of EDM process parameters are required to achieve higher MRR for 304 Stainless steel. Signal to noise ratio (S/N) and analysis of variance (ANOVA) is used to analyze the effect of the parameters on MRR and also to identify the optimum cutting parameters. The contribution of each cutting parameters towards the MRR is also identified. The results from this study

will be useful for manufacturing engineers to select appropriate EDM process parameters to machine Stainless steel 304.

Anand Prakash Dwivedi and Sounak Kumar Choudhury [67] worked on increasing the performance of EDM process using tool rotation methodology for machining AISI D3 steel. In this study the adoption of tool rotation methodology increases the material removal rate by increasing the spark efficiency and effective debris clearing. The experiments have been performed on AISI-D3 Steel. Results show that the tool rotation phenomenon significantly improves the average MRR and surface finish by 41% and 12% respectively. Moreover, the final surface is more uniform in structure with less number of micro cracks and thinner recast layer as compared to the stationary tool EDM.

Nuclear, automotive and aeronautical industries are among the leading users of very hard alloys for machining purposes. EDM is used to machine such alloys easily with a high level of accuracy. The discharge current is the most influential parameter which affects the material removal rate (MRR), whereas the pulse on-time highly affects the electrode wear rate [68, 69].

Krishnakant and Akshay Dvivedi [70] perticipated on Experimental Research on Near-dry EDM using Glycerin-Air Mixture as Dielectric Medium. In this study, face centered central composite design (CCD) had utilized to plan the experiments. Response surface methodology (RSM) was used for bringing forth the mathematical

model. The mathematical model was proposed to evaluate the important effect of input parameters on response characteristic. In this investigation, input parameters used for experimentations were current, duty factor flushing pressure and lift. The response characteristic was taken through measurement in terms of material removal rate (MRR). Analysis of the outcome showed that, all the input parameters were significant for MRR. It was noticed that glycerin-air dielectric medium produced higher MRR than water-air dielectric medium at same parametric setting.

Shahadev B. Ubale and Sudhir D. Deshmukh [71] researched on Experimental Investigation and Modelling of Wire Electrical Discharge Machining Process on W-Cu Metal Matrix Composite. This overview sheds more light on the experimental explantiation on the wire electrical discharge machining (WEDM) of WCu metal matrix composite on material removal rate (MRR). Experiments are carried out in line with central composite design (CCD). Furthermore, response surface methodology (RSM) has been used for modelling and investigating the outcome of process parameters: Pulse on time (Ton), Pulse off time (Toff), Peak current (IP), Wire tension WT) and Spark gap voltage (SV) on MRR. Subsequently, analysis of machining of W-Cu MMC in WEDM is made as a result of the developed model. Furthermore, the model has been verified and checked for its adequacy.

Lin et al. [72] tested Grey Taguchi technique to optimize the micromilling EDM process parameters in Inconel 718 alloy to achieve different performance characteristics like low working, low electrode wear and high MRR. The influence as

a result of spark gap, peak current, pulse on time and pulse off time on MRR, working gap (WG) and electrode wear were checked.

Chandramouli S and Eswaraiah K [73] studied the Experimental investigation of EDM Process parameters in Machining of 17-4 PH Steel using Taguchi Method. In this research ANOVA method was used with the help of MINITAB 17 software to analysis the influence of input process parameters on output response. The process parameters were optimized in order to obtain maximum material removal rate and minimum surface roughness by considering the inter action effects of process parameters and the experimental results were validated by confirmation tests.

The result of ANOVA reveals that pulse on time has highest percentage contribution for MRR (58.3%) and for SR (76.7%). The confirmation experiments were conducted to verify the optimal machining parameters and there is a significant improvement in MRR and SR from initial machining parameter to the optimal machining parameters is about 8.63% and 70.4% respectively.

Aditya Kumar et al. [74] performed the parametric analysis of wire EDM parameters by taguchi method and developed a mathematical model for simultaneous optimization by hybrid genetic algorithm.

Arshad Noor Siddiquee et al. [75] focused on optimizing deep drilling parameters of CNC lathe machine using solid carbide cutting tool on material AISI 321 austenitic stainless steel based on Taguchi method for minimizing surface roughness.

Srinivasa Rao et al. [76] studied hybrid method combining grey, fuzzy and Taguchi approaches was implemented for submerged arc welding. S. Assarzadeh et al. [77] modeled and optimized process parameters in EDM of tungsten carbide-cobalt composite using cylindrical copper tool electrodes in planned machining based on statistical technique Response surface methodology has been used to plan and analyze the experiments.

Rajesh Choudhary and Gagandeep Singh [78] studied the Effects of process parameters on the performance of electrical discharge machining of AISI M42 high speed tool steel alloy. In this report effect of current, pulse on time, voltage, and tool polarity on material removal rate of AISI M42 alloy is concluded. Taguchi's L18 orthogonal array is used for design of experiments. ANOVA analysis was carried out to study the experiments results.

Following conclusions were drawn from the study:

- Among all the selected parameters tool polarity influences MRR most followed by the current during the Electrical discharge machining of AISI M42 tool steel alloy.

- Material removal rate was found to increase with increase in gap current and pulse on-time.
- Maximum material removal rate was observed at negative tool polarity (0.191 g/min) ,
- 12 amperes, 150μs pulse on time and 55 volts' gap voltage.

Nur Sheril et al. [79] worked on the prediction of material removal rate in die-sinking electrical discharge machining. This study proposes a semi-empirical model to predict material removal rate in die-sinking electrical discharging machining (EDM). Four different workpiece materials -- high strength steel, high strength low alloy steel, brass, and aluminum -- are utilized in the study. Full factorial experiments using peak current, on-time at two levels are selected for each workpiece material while keeping other parameters the same. The removed volumes are calculated by measuring sectional area of an EDM'ed hole and its dimensions. The developed MRR model includes the EDM cumulative electrical charge for each cycle and melting temperature of workpiece material; it predicts two orders of magnitude closer to experimental data compared to a published model that is based on melting temperature and peak current alone.

Goswami and Kumar [80] wire-EDM'ed Ninomic alloy. The authors varied on-time, off-time, gap voltage, peak current, wire feed and wire tension in their experiments

and concluded that MRR depended not only on the on-time T_{on} and off-time T_{off}, but also the products ($T_{on} \times T_{off}$) and ($T_{on} \times Ip$).

A.Pramanik et al. [81] studied the Electrical discharge machining of 6061 aluminium alloy. In this study the wire electrical discharge machining (EDM) of 6061 aluminium alloy in terms of material removal rate, kerf/slit width, surface finish and wear of electrode wire for different pulse on time and wire tension was studied. Result show that the longer pulse on time induces higher wear in the wire electrode. On the other hand, higher tension in the wire electrode reduces the wear by providing steady machining.

Dave et al. [82] also used Taguchi methodology to study microholes generated on 1100 aluminum alloy using micro-electro-discharge machining. Gap voltage, capacitance, pulse on time, electrode thickness and electrode rotation were input parameters, and top radius, bottom radius, taper angle and electrode depletion were output parameters.

Selvakumar et al. [83] investigated wire electrical discharge machining (WEDM) of 5083 aluminum alloy using Taguchi experimental design (L9 orthogonal array) method, where pulse on time, pulse off time, peak current and wire tension were input parameters and the surface roughness and cutting speed were output parameters.

S. Singh [84] used the designs of experiments and grey relational analysis (GRA) approach to optimize parameters for electrical discharge machining process of 6061Al/Al2O3p/20P aluminium metal matrix composites. The results of ANOVA indicated that aspect ratio and pulse current were the most significant process parameters affecting the multiple performance measures followed by tool electrode lift time and pulse on time [84, 85].

2.13.2 Recent Research on Tool Wear Ratio (TWR)

Marafona and Chousal [86] developed a thermal-electrical finite element model based on Joule heating effect for EDM. Put together resources was been utilized to simulate the evolution of the recast layer generation process. Achieved outcomes were through comparisons with experimental measurements, and it shows a viable similarity between predictions and experimental data.

In that model, a cylindrical shape discharge pathway is formed between anode and cathode materials as an electrical conductor and heat dissipation element. FEA outcomes of tool wear ratio, material removal rate and surface roughness were comparatively analyzed with the experimental outcomes of other related research in literature and reasonable agreement was documented. The radius of the conductor is a function of discharge current and pulse time.

Muttamara et al (2009) had studied the " Effect of electrode material on electrical discharge machining of Alumina" lots of industrial filed are demanded to machine the insulating ceramic materials but Si3N4, SiC, and Zro2- are machined in

Electrical discharge machining EDM successfully. EDM-C3 very good result in machine 95% pure alumina by EDM and gives High MRR and less TWR over the EDM-3 and copper electrode. Positive polarity of EDM-C3 improve surface roughness 25μm [87, 88].

Electrode like Copper, graphite (Poco EDM-3) and copper-infiltrated-graphite (Poco EDM-C3) machine alumina. A. They concluded that the element of copper is not observed on with EDM-3 and EDM–C3 conductive layer and surface resistivity of conductive layer is less in EDM-3 over the EDM-C3. Also while machining the Al2O3 ceramics indeterminate discharge is occurs and obtain the low quality machining properties. They found that 60% in EDM-3 and 80% in EDM-C3 is increase with the positive polarity in MRR.

S.Suresh kumar et al (2014) investigated the parameters like Pulse on time, pulse duty factor, pulse current and voltage by machining of EDM against the composite of Al (6351) - 5 wt% silicon carbide (SiC) 5 wt% boron carbide (B4C).They summarized that increases the pulse current the tool electric spark energy discharge is also increased and make TWR to increase. Their practical outcome response was good ability by pulse current with contribution of TWR- 33.08%, SR-76.65% and 48.08% of PC. And while increase pulse current and pulse duty can less the power consumed [89].

Singh et al. [90] studied the effect of continuous and discontinuous vibration on work piece. In this study experiments were carried out using Taguchi's L18 orthogonal array. For experimentation high chromium high carbon steel is being used as work piece and copper is being used as tool material. On the basis of experiment they concluded that discontinuous vibrations give more MRR and TWR. Also the intensity of development of cracks is more in case of discontinuous vibration as compared with continuous vibration.

M.Dastagiri and A.Hemantha kumar [91] focused on experimental investigation of EDM parameters on stainless steel&en41b. In this paper Metal removal mechanism in Electrical Discharge Machining (EDM) is mainly a thermal phenomenon where thermal energy is produced in plasma channel, and is dissipated though work piece, tool and dielectric. The process is mostly used in situations where machining of very hard materials, intricate parts, complex shapes. The aim of this work is to pursue the influence of four design factors current (I), voltage (V), pulse on (Ton), and duty factor (η) which are the most connected parameters to be controlled by the EDM process over machining specifications such as material removal rate (MRR) and tool wear rate (TWR) and characteristics of surface integrity such as average surface roughness (Ra) and the hardness (HR) and also to quantify them. In this paper the experiments have been conducted by using full factorial design 23 with three central point in the DOE techniques and developed a mathematical model to predict material removal rate, average surface roughness and hardness using input parameters such as

current, voltage, pulse on, and duty factor. The predicted results are very close to experimental values. Hence this mathematical model could be used to predict the responses such as material removal rate, and average surface roughness effectively within the input parameters studied.

Misbah Niamat et al.[92] studid the effect of different dielectrics on material removal rate, electrode wear rate and microstructures in EDM. In this study Dielectrics and electrical parameters were considered as the main factors for EDM performance. In this paper, the effects of pulse-on-time (μs) and current (ampere) were analyzed for measures using kerosene and water as dielectrics. A comparative analysis was done for both dielectrics in lieu of material removal rate (mm3/min), electrode wear rate (mm3/min), and microstructures. Aluminum 6061 T6 alloy was utilized as material for this study as a result of its wide spread utilization in aerospace and automotive industries. Experiments were formed and created utilizing Taguchi L9 orthogonal array (OA). Time series graphs were plotted to comparatively analyze material removal rate and electrode wear rate. Microstructures were taken by scanning electron microscope to study the surface produced in terms of cracks, globules and micro-holes. Higher material removal rate and lower electrode wear were gotten with kerosene dielectric. The importance of this research work, apart from its real application, is that Aluminum 6061 T6 alloy is utilized as work material to comparatively analyze the performance of dielectrics (kerosene and distilled water).

This study work objective is to study the effects of kerosene and distilled water on an aluminum alloy 6061 T6 by varying levels of current and Pulse-on-Time (Pon). These two electrical parameters have been used due to its important effect on EDM performance which is also showcased by Gostimirovic et al [93] and Sarosh et al [94]. Material Removal Rate (MRR), Electrode Wear Rate (EWR) and microstructures were studied in this research. Dielectrics role is significant in EDM as they made the removal mechanism possible by aiding the discharge phenomena. Surface characteristics and cost of the machined part is reliant on the kind of dielectric used [95].

In EDM, dielectrics usually play four functions; insulation, ionization, debris removal from the working tank, and cool down the heat of a spark. Hydrocarbon oils, water base and gaseous are three main categories of dielectrics commonly used for EDM [96].

Zhang et al [97] researched the different dielectrics with same experimental condition which showed craters of different shapes and sizes and discovered that liquid dielectrics have higher removal efficiency and water/oil emulsion stand pressure for longer time. Wang et al [98] performed comparative experiments in distilled water, compound dielectric and kerosene on titanium alloy to evaluate MRR, EWR and surface roughness. Compound dielectric showed better results as compared to other dielectrics. As water content increases in water/oil emulsion, it reduces the MRR and EWR which results in low cost of process [99,100]. Valaki and

and Rathod [101] experimentally assessed the feasibility of using waste vegetable oil as an alternative dielectric in EDM for performance measures (MRR and EWR). Shen et al [102] experimentally evaluated EWR and found enhancement in EWR with the increase in current and Pon for dry EDM. Liquid dielectrics are preferred over dry EDM, since they offer stable discharging [103].

Guo Yongfeng et al. [104] research on experimental investigation of EDM parameters for zrb2-sic ceramics machining. In this study, the process parameters including polarity of electrode, peak current, pulse-on time and pulse-off time are selected to study the influence on material removal rate, side gap, and surface roughness. Machined surfaces are analyzed using scanning

electron microscopy (SEM), polygonal material layer and flat area are found on the machined surface. The forming of polygonal material layer is due to different thermal physical properties in the process of resolidification of ZrB2, SiC and pyrolytic carbon. The flat area is the central point of larger energy discharge channel. Tiny craters with few microns caused by removal of SiC grains are found on the machined surface, the number of them increases with increase of discharge energy.

At present, researches on EDM machining for ZrB2 based ceramics are concentrated in two aspects: one aspect is ZrB2 based ceramics used as electrode, the high melting point property of the material will reduce the electrode wear [104]; the other aspect is

EDM machining for ZrB2 based ceramics, the machined workpiece will used for high temperature property application [105-107].

Gurpreet Singh et al. [108] worked on Experimental studies on material removal rate, tool wear rate and surface properties of machined surface by powder mixed electric discharge machining. In this study, effects of various parameters such as workpiece material, dielectric fluids, powder and other machining parameters have been studied. Material removal rate increased with increasing the current input and powder combination in electric and tool wear rate has been acomplished significantly with powder combination. X-ray diffraction has excuted to analize the placement of powder on surface after machining. Surface characteristics analyzed by SEM for cracks on the surfaces.

P Prasanna et al. [109] researched on Optimizing The Process Parameters Of Electrical Discharge Machining On AA7075 - SiC Alloys. In this study it has decided to analyze the performance of conventionally used copper electrode using kerosene as die-electric fluid in an Electrical discharge machining of AA7075 SiC Metal matrix composites. Experiments were

Carried out under different values of process input parameters such as current, pulse on time, pulse of time and coating thickness. The Material removal rate (MRR), Tool wear rate (TWR) ,Relative wear ratio (RWR) and surface roughness (Ra) at different input parameters are measured. The relative outcome values are then optimized with

the use of Principal Component Analysis. Further Sensitivity was also carried out to identify the most influencing factors.

Chandramouli. S et al. [110] worked on optimisation of EDM process parameters using Taguchi technique and he saw the best optimal process parameters on machining the RENE80 nickel super alloy material with aluminium as electrode material where what he acertained that current is the most influence parameter for the responses MRR, TWR and SR.

Abhijeet singh V Makwana et al. [111] investigated on AISI16 SS material with copper electrode material having different shapes (circular, rectangular and triangular) utilizing Taguchi method L9 array where input variables are current, pulse on time, pulse off time and output responses are MRR, EWR and Ra. Conclusively, outcomes expressed that current and pulse on time is the most overpowering parameters of MRR, EWR and Ra.

Binoy Kumar Baroi et al. [112] worked on electric discharge machining of titanium grade 2 alloy and its parametric study. The present study concentrates on the electric discharge machining (EDM) of Titanium Grade 2 alloy. The differences in material removal rate (MRR), tool wear rate (TWR), and surface roughness (SR) with the differences of process parameters, for example, current and pulse on time is studied in this research. Experiments have been executed as per the Taguchi L16 orthogonal array design of experiments (DOE). All the experiments have been excuted out

utilizing electrolytic copper as tool electrode and hydrocarbon oil as a dielectric fluid. The best state for each response has been assesed by analyzing the influence of input parameters on the average of the responses. Analysis of difference (ANOVA) has been performed to study the percentage addition of each input parameter on the output responses. Highest MRR of 0.0053367 g/min, lowest TWR of 0.0000067 g/min and SR of 2.960 μm has been accomplished.

The efficiency of EDM particularly relies on MRR which reflects the active usage speed of production. MRR can be stated in terms of weight or volume of the material removed from the workpiece over the machining time [113,114]. Surface quality contributes to usage and salability of a product [115].

Wang et al. [116] machined titanium alloy (TC4) in three various kinds of dielectric fluid such as a compound dielectric fluid, distilled water and kerosene. They noticed that compound dielectric fluid has greater superior MRR, lesser TWR, and higher surface finish than kerosene.

Shabgard and Khosrozadeh [117] studied the machining characteristics of Ti-6Al-4V by mixing CNT powders in the dielectric fluid. They found that MRR reduced initially, but with a high pulse on time and lower current combinations, the MRR increased. TWR decreased for the low pulse on time values. For stable machining conditions, surface roughness in CNT mixed EDM is lower than the conventional EDM and vice versa.

Torres et al. [118] studied the machining of TiB2 using copper electrode in EDM. They observed that current was the main contributing factor for MRR and surface roughness, but for TWR pulse on time was the most important factor.

Shukry H. Aghdeab and Amani I. Ahmed. [119] worked on the Effect of Pulse on Time and Pulse off Time on Material Removal Rate and Electrode Wear Ratio of Stainless Steel AISI 316L in EDM. This study focuses on the study of machining responses such as material removal rate (MRR) and electrode wear ratio (EWR) under the effect of different machining conditions in EDM process. The process parameters are pulse on time (Ton), pulse off time (Toff) and electrical current (Ip). The main purpose of this work is to achieve best MRR and least EWR using copper electrode with fixed diameter (10 mm) for the machining of stainless steel AISI 316L with a constant thickness (0.8 mm).

2.13.3 Resent Research on Surface Roughness (Ra)

B. Izquierdo et al. [120] researched on Numerical prediction of heat affected layer in the EDM of aeronautical alloy. In a former publication an actual model of the EDM process was showcased and was utilized to estimate material removal rate and surface finish for the EDM of steel. In this particular article the potential of that modelling tool was used to illustrate discharge properties and to predict recast layer spread when performing EDM over an aeronautical alloy used as work piece.

Manjaiah et al. [121] investigated wire electric discharge machining of Ti50Ni50_xCux shape memory alloy. Performance measures considered during the

machining were surface roughness, material removal rate, surface topography and metallographic changes. It was noted during the experimentation that with brass and zinc coated wire servo voltage, pulse off time and pulse on time were significant parameters which affect the MRR and surface roughness.

S. Vinoth Kumar andM. Pradeep Kumar [122] worked on the Machining process parameter and surface integrity in conventional EDM and cryogenic EDM of Al–SiCp MMC. In this investigations were carried out on the machining of Al–MMC with 10% SiCp reinforcement, and conven-tional electrical discharge machining (CEDM) and a cryogenic cooled electrode in the electrical discharge machining process (CCEDM). The machining parameters included discharge current, pulse on time and gap voltage. The output responses comprised electrode wear ratio, material removal rate, surface rough-ness, electrode temperature, work piece temperature, microstructure, micro hardness, SEM and EDX analysis. Discharge current, pulse on time, and gap voltage were found to have the most significant effect on electrode wear, while pulse on time with discharge current having the most significant effect on surface roughness.

The electrode wear was reduced to 18% by cryogenic cooling. Surface roughness was also improved while machining with cryogenic electrode cooling. The scanning electron microscope (SEM) analysis was carried out to study the surface characteristics of the machined surface.

Kumar K.M and Hariharan P [123] studied Experimental Determination of Machining Responses in Machining Austempered Ductile Iron (ADI). This work investigates the machining characteristics of Austempered Ductile Iron (ADI) using Electrical Discharge Machining (EDM) process with copper as an electrode. Experiments have been carried out to analyze the effect of each parameter on the machining characteristics, and to predict the optimal choice for each EDM parameters such as peak current, pulse on time, and pulse off time and tool geometry.

Three different specimens were austenised at 900° C for 90 min and then austempered in a salt bath at 360° C, 380° C, and 400° C for 120 min. Experiments have been designed as per taguchi s L_{18} orthogonal array. Analysis of variance (ANOVA) is used to find the level of significance of machining parameters. Machining responses such as the metal

Removal rate (MRR), Tool wear rate (TWR), surface roughness (SR) and taper angle (DVEE) for entrance exit of the tool was studied while machining the Austempered Ductile Iron (ADI) with copper as an electrode. Discharge current, Pulse on time and Austempering temperature are found most influential parameters on each performance measure. Tool geometry is found the least influential parameters.

Md. Ashikur Rahman Khan et al. [124] studied on the neural network modeling and analysis for surface characteristics in electrical discharge machining. In this research the problem appeared owing to selection of parameters increases the deficiency of

electrical discharge machining (EDM) process. Modelling can facilitate the acquisition of a better understanding of such complex process, save the machining time and make the process economic. Thus, the present work emphasizes the development of an artificial neural network (ANN) model for predicting surface roughness (*Ra*).

The surface topography of the machined part was analyzed by scanning electronic microscopy. The result shows that the ANN model can predict the surface roughness effectively. Low discharge energy level results in smaller craters and micro-cracks producing a suitable structure of the surface. This approach helps in economic EDM machining.

M Manohar et al. [125] worked on the Experimental study to assess the effect of Electrode bottom profiles while machining Inconel 718 through EDM Process. In this study to understand the effect of the electrode bottom profile and also its extent of influence on machining Inconel alloy, experimental study was carried out through EDM. Electrodes of different bottom profiles were used and the machined surfaces were analysed in terms of recast layer, surface topology, form tolerance and MRR. Electrodes having Convex, Concave and Flat profile at their bottom surface were chosen for the experimental study; electrodes were made of copper rod of 12 mm diameter with convex or concave profile at their bottom with three different radii of curvature namely, 6,8 or10 mm. The surface roughness of the machined surface was measured and the nature of recast layer formed was evaluated and characterized

using scanning electron microscope (SEM). The observations and results of the above experimental study are discussed and analyzed in this paper. Nature of the machined surface obtained using the above mentioned electrodes are compared and discussed. It is concluded that the adverse effects caused due to the erosion of flat profile electrodes on the machined surfaces could be overcome by employing convex profile electrodes; concave profile electrodes almost simulate the condition of eroded flat-profile electrode; convex profile electrodes produce machined surfaces of better quality in terms of higher surface finish, thinner recast-layer and closer geometry, in addition to higher MRR compared to flat profile or concave profile electrodes.

In this study, influence of process parameters and effect of three different bottom surface profiles of the electrode on the machined surface including topology, recast layer, formability and the MRR were studied,

M.A. Razak et al. [126] worked on electrical discharge machining on biodegradable AZ31 magnesium alloy using taguchi method. In this study Nine EDM experiments with three levels and four parameters were conducted using Taguchi method on AZ31 magnesium alloy to explore the optimum machining parameters. It was found that pulse on-time was the most significant parameter affecting the surface roughness (Ra) of the machined surface. The optimum EDM condition obtained was 47 A peak current, 80 V voltage, 16 μs pulse on-time and 512 μs pulse off-time. A confirmation test was conducted and the result shows 95.5% similarity with the predicted Ra. However, the formation of cracks and craters were found on the machined surface

area. It is proposed to solve this problem by applying powder mixed EDM method in future research work.

Anand Prakash Dwivedi and Sounak Kumar Choudhury [127] investigated improvement in the surface integrity of AISI D3 tool steel using rotary tool electric discharge machining process. In this research work focusses on the surface integrity improvement of the AISI D3 Tool Steel using the tool rotation during the EDM process. Surface Roughness (Ra), Micro-Cracks and Recast Layers have been examined and studied as the output parameters. The results show that the machined workpiece has a finer surface, fewer micro-cracks and thinner recast layers as compared to the stationary tool EDM process.

Vikas Gohil and Y. M. Puri [128] researched on the enhancement of electrical discharge turning process utilizing taguchi-grey connecting approach. Electrical discharge turning (EDT) is a unique type of electrical discharge machining (EDM) process, which is being especially made to produce cylindrical forms and helical profiles on hard to machine materials at both macro and micro levels. This researched showcased an experimental investigation of electrical discharge turning of titanium Ti-6Al-4V alloy. The aim was to investigate the effects of machining parameters also having peak current, pulse-on time, gap voltage, spindle speed and flushing pressure on performance characteristics at reverse polarity. Taguchi-grey relational technique which is reliant on multi objective optimization has been utilized to optimize material removal and surface roughness simultaneously.

Nakka Nagaraju et al. [129] worked on Optimization of Process Parameters of EDM Procedure Using Fuzzy Logic and Taguchi Methods for Improving Material Removal Rate and Surface Finish. The main aim of this work is to optimization of multiple responses of Electric discharge machining (EDM) using Fuzzy method cobined together with Taguchi is attempted. The work piece material was AISI 304 Stainless Steel and a cylindrical copper electrode with side impulse flushing was utilized. The effect of machining parameters, i.e., discharge current ,pulse on time , discharge voltage and Inter Electrode Gap (IEG) on the Material Removal Rate (MRR), Tool Wear Rate and Surface Roughness (Ra) in EDM are analyzed.

Optimization of process parameters has been execute and have been identified as to bring about the best combination of process variables like Discharge current=10A, Pulse-on-Time=500μs, Voltage=45V, and Inter Electrode Gap=150μm. Also the performance characteristics such as MRR, Ra and TWR were enhanced by utilizing the current analysis.

Neelesh Singh et al. [130] concentrated on Study of machining characteristics of Inconel 601in EDM using RSM. In this study the effect on material removal rate (MRR) and surface roughness (SR, Ra) with varienty of input variables which are gap voltage (Vg), peak current (Ip) and pulse on time (Ton) at the time EDM of Inconel 601 utilizing electrolytic copper. Experimental work is carried out utilizing Box-Behnken Design (BBD) along with variety of a mixture of process parameters.

Response Surface Methodology and ANOVA are utilized for comparing the process parameters with the responses and to analyses the significant of the derived model.

Rahul et al. [131] assed the machining performance of Inconel 625, 718, 601 and 825 at the time of EDM utilizing 5-factor 4-level L16 orthogonal array by replacing duty factor, flushing pressure, pulse on time, peak current and gap voltage for checking the change in tool wear rate, material removal rate, surface crack density and surface roughness. For Inconel 601 most desirable machining condition is gap voltage=80V, peak current=7A, flushing pressure=0.3 bar, duty factor=80% and pulse on time=500μs.

K. Buschaiah et al. [132] researched on the Investigation on the effect of EDM parameters on machining characteristics for AISI 304. The current work is geared towards characterising the electric discharge machining of AISI304 steel on EDM with the copper electrode. Twenty-seven experiments are carried out by diffrentiating EDM parameters such as current, pulse-on time, and electrode diameter. Each test was carried out for 20 min and ED30 was utilized as a die-electric fluid. The performance measures surface roughness (SR) evaluated. Deduction of experimental layout was carried out with the use Taguchi technique to analyse the influence of each parameter on the machining characteristics, and to determine the optimal decision for each EDM parameter such as peak current, pulse duration and electrode diameter. It is seen that these parameters have a great effect on machining characteristic such that surface roughness (SR). The analysis of the Taguchi

technique showed that peak current significantly affects the SR and experimental outcomes are given to prove this approach.

Sengottuvel P et al. [133] reported the four parameters and four levels L16 OA for machining the Inconel 718 utilizing Cu electrode material with output parameters as MRR, TWR and SR on EDM and came to a conclusion that current is important among these parameters.

Vishnu P et al. [134] worked on performance determination of electric discharge machining of inconel-718 using artificial neural network. Inconel-718 is a nickel founded on alloy which show case very great output, tensile and creep rupture properties at temperatures of up to 978 K. This alloy has much use in jet engines, high speed air frame parts, power plant turbine components, automobile engine components and high temperature fasteners. This study concerns itself with a non-traditional approach of machining Inconel-718 utilizing Electric Discharge Machining (EDM). Experiments were formed and carried out in line with Taguchi's L18 orthogonal array. Experiments were executed under variety of cutting conditions of polarity, pulse on time, pulse off time and peak current. Electrolytic copper was utlized as tool electrodes. This model is important in optimizing the process parameters, depending on the needs such as MRR or surface roughness. Thus, this is taken as as an optimization tool also.

Nimo Singh Khundrakpam et al. [135] researched on the grey-taguchi optimization of near dry edm process parameters on the surface roughness. Near Dry Electrical Discharge Machining (ND-EDM) utilized a lowest quantity lubrication (MQL) system to give a little quantity of controlled two phase dielectric fluid droplets between the gap of workpiece and electrode. In current study, Grey- Taguchi approach with L27 orthogonal array was taken to research and optimize the process parameters of ND-EDM viz. Pulse On Time, Pulse Off Time, Discharge Current, Gap Voltage and Tool Rotating Speed on the responses of surface roughness viz. Ra (Average (arithmetical mean) surface roughness (μm)), Rt (Maximum surface roughness depth (μm)), Rsm (Root Mean Square average surface roughness (μm)), Rsk (Skewness surface roughness (dimensionless)) and Rku (Kurtosis surface roughness (dimensionless)) utilizing the combination of deionized water and air as the dielectric fluid for EN-8 material.

Rashed Mustafa Mazarbhuiya et al. [136] researched on an experimental study on parametric optimization for material removal rate and surface roughness on edm by utilizing taguchi technique. The aim of this research study is to find out about the best process parameters of EDM(Electric Discharge Machining) on Aluminium work piece with Copper as a tool electrode. The influence of different process parameters on machining performance is researched in this study. The input parameters considered are Discharge Current, Pulse ON time, Flushing Pressure and Polarity. ANOVA techniques is utilized to check the influence of process parameters on the

machining characteristics and get the best process parameters of EDM.S/N ratio calculations and Average performance graphs are plotted for the optimal setting of the controlling parameters.

Aharwal K R et al. [137] studied the optimization of material removal rate and surface roughness in edm machining of metal matrix composite using genetic algorithm. The present work has been carried out to optimize the machining parameters on Electric Discharge Machine (EDM) using AlSiC as work piece and pure copper as electrode. Machining parameters which are investigated in this work are Material Removal Rate (MRR) and surface

roughness. Control parameters used are discharge voltage (v), discharge current (Ip), Pulse duty factor (Tau), Pulse on time (Ton). Taguchi technique (L16b orthogonal array) was used for design of experiments and genetic algorithm for optimization. The analysis of material removal rate yields optimum values when current is high and voltage is low whereas surface roughness is best when both are low. A relative research on the optimization technique is showcased in table 2.4 as a help for choosing process:

Table 2.4: in the chronological order from 2010 onwards which the use of suitable optimization technique was adopted for the EDM process and its versions.

Year/ author(s)	Process version	Work material	Import input variables	Objective (s)	Technique used	Remars
2010/Kumar et al.[138]	Abrasive mixed EDM	EN-24 tool steel	Concentration of abrasive powder in dielectric fluid	MRR SR	GRA	Effect of abrasive particles was very significant in comparison to other variables.
2010/Jung and Kwon [139]	EDM	6061Al/Al_2O 3p/20P Al, MMC	Input V, Capacitance, Resistance, Feed rate, Spindle speed	EW	GRA	GRA is utilized to estimate the optimal machining parameters, among which the input voltage and the capacitance are known to be The most significant.
2010/Reza etal.[140]	EDM	SS 304	Polarity, Ton Ip,V, depth diameter Dielectric pressure	MRR EWR SR	GRA	The enhancement in grey relational grade after optimization of EDM control parameters is0.1639.
2010/Chen et al.[141]	WED M	Pure tungsten	Ton, Pulse-off-time, Arc of time, Servo V, Wire feed rate, Wire tension, Water pressure	SR, Cutting velocity, MRR	ANN integrated with SA	Pulse-on time was shown as the most important factor. From the outcome and conformation experiments.

2010/Pradhan and Biswas [142]	Die sinking EDM	AISI D2	Ip, Pulse duration, Duty cycle, V	MRR TWR	ANN Neuro-fuzzy	Discharge current was the most important factor affecting the MRR and radial overcut.
2010/Somashekhar etal.[143]	Micro -EDM	Aluminium	Gap V, Capacitance, Feed rate,	MRR	ANN GA	More variation in MRR was noticed due to capacitance in comparison to others.
2011/Joshi and Pande [144]	Die-sinking EDM	AISI P20 Mold steel	Ip, Discharge V, Duty cycle, Break down V, Discharge Duration	Crater size MRR TWR	FEM ANN GA	Mathematical models in terms of input-output variable were not showcased.
2011/Majhi and Pratihar[145],	Die- sinking EDM	Mild steel	Ip, Ton, Pulse duty factor	MRR SR	GA NN	Pareto-optimal front of solutions was gotten.
2011/Amini et al.[146]	WED M	TiB_2 nano-Compositeite ceramic	Ton, Pulse-of-time, Servo V, Wire feed rate	MRR SR	ANN GA	Shown that the achieved optimization result in good agreement with the experimental outcomes.
2012/yang et al.[147]	WED M	Tungsten	Ton Toff, Arc-off time, Servo V, Wire feed rate, Wire tension, Water pressure	MRR Av. Ra Corner deviation	RSM ANN SA	Optimized outcomes were executed in a production line of industry making the semiconductor components.

2012/Somashekh ar et al.[148]	Micro-WEDM	Aluminium	Gap V, Feed rate, Capacitane	MRR Overcut SR	SA algorithm	Capacitance was shown as the most effective variable affecting the performance.
2012/Bharti et al.[149]	Die-Sinking EDM	Nickel-based Inconal78 alloy	Shape factor, Ton, Ip, Duty cycle, Gap V, Flushing pressure	MRR SR	ANN GA	Mathematical models in terms of input-output variable were not presented.
2012/Kumar and Agrawal [150]	WEDM	High Speed, steel (M2,SKH9)	Pulse-Ip, Ton, Pulse- off-time, Wire feed, Wire tension	MRR SR	Tag uchi NSGA	Pareto optimal solution was presented.
2012/Shrivastava and Dubey [151],	EDD G	Cu-iron-Gr MMC	Ip, Ton	MRR TWR	ANN GA GRA	Improved the MRR by about 76% and wheel wear rate by about 31%.
2012/baraskar et al.[152]	Die sinking EDM	EN-8 carbon steel	Ton, Toff, Ip, Ip, Pulse-on-duration	MRR SR	RSM NSGA-II	Results were gotten directly using optimization tool box.
012/Shahali et al.[153]	WEDM	DIN 1.4542	Ton, Toff, V, Number of finish passes	SR WLT	Micro-GA	Ra and WLT were minimized by 52 and 67% respectively
2012/Reza Atef et al.[154]	EDM	Hot work, steel, DIN1.2344	Pulse Ip, Pulse V, Ton, Pulse-off-time,	SR	ANN	A hybrid model is constructed to minimize the error In optimization of complex.

2012/Rajesh and Anand [155]	EDM	Al Alloy with Grade HE9	Working Ip, Working V, Oil pressure, Spark gap, Ton, Toff	MRR Surface finish	RSM GA GRA	Empirical models for MRR and SR are developed by carrying out a designed experiment.
2012/Moghaddm et al.[156]	EDM	AISI 2312 hot worked steel	Ip, V, Ton, Toff, Duty factor	MRR TWR SR	ANN GRA	The addition of Taguchi technique GRA and SA algorithm is quit efficient in Estimating the optimal EDM process.
2013/Zhang Y.et al.[157]	EDM	Mold steel, 8407	Pulse duration ,Polarity , V, Ip	MRR	FEM	A new technique of research of the characteristic of EDM plasma proposed.
2013/Dhanabalan. S et al.[158]	EDM	Inconal 718	Ton, Toff, Ip	MRR EWR	GRA	Adapted algorithm adopted here is utilized successfully for both detraining the optimum setting of input parameter.
2013/Agrawal A et al.[159]	PMEDM	Al/Sic MMC	Ip, Ton, Pulse-off-time, Powder concentration	TWR	ANN	Mixing graphite powder in dielectric effectively reduces The TWR at times of machining of MMC

2014/P. Sivaprakasam et al.[160]	Micro -WEDM	Ti-6Al-4v	V, Capacitance, Feed rate	MRR SR kw	RSM GA	Model developed can be utilized as GA to estimate the optimal machining conditions using multi-objective optimization methods.
2014/Kumar Sanjeev, et al.[161],	EDM	Titanium alloy	PeakIp, Ton, Pulse-of- time	SR	ANN, Taguchi method	Predicted outcomes gotten were confirmed by comparing with the outcomes & found to be in a cohesive agreement with each other.
2015/Dewangan et al.[162],	EDM	AISI P20	Ip, Pulse-on time, Tool-work time, Tool-lift time	WLT SCD SR	GRA Fuzzy logic	Grey-fuzzy based hybrid optimization methods to optimal settings of EDM Parameters to enhance outer layer integrity.
2015/Patowari et al.[163]	EDM	W-Cu P/M coating on work piece	Compaction pressure, Sintering temperature, Ip, Ton, Toff,	MRR WLT	ANN	Effect of process variables on the responses was clearly showcased through many plots
Note : Ip: Discharge Current, Peak Current, Ton: Pulse on Time, Toff : Off-time of discharging						

2.14 Objective of the Thesis

From the research papers in this classification, it was observed that few works have reported data on EDM on the material Al-Sic, AISI H13**,** AISI D6 tool steel, and various composite materials. Study on EDM of different material and different mathematical model can be used to validate the experimental results.

The objective of the present study is to find the feasibility of machining AISI D6 tool steel using copper electrode. The machining parameter selection for discharge current, pulse on time, and pulse on time of the tool using RSM approach for analyzing the responses material removal rate (MRR), tool wear ratio (TWR) and surface roughness (Ra).

Chapter 3

METHODOLOGY

3.1 Introduction

Methodology includes the problem identification and answering, detail experimental design and Design of Experiment (DOE). This Present chapter generally confers methodology of the plan, with an attention on electric discharge machine (EDM) experiment and machining is my material tools of AISI D6, input parameter consist of pulse on-time 4 levels, Pulse current 4 levels and voltage in 2 levels. Pertinent data group is achieved in order for further investigation analysis in following chapter. Thus, parameters and corroboration with DOE was applied as a setup experiment parameters and used as a response surface method to predict and model the parameters. Figure 3.1 shows the step by step experimental methodology.

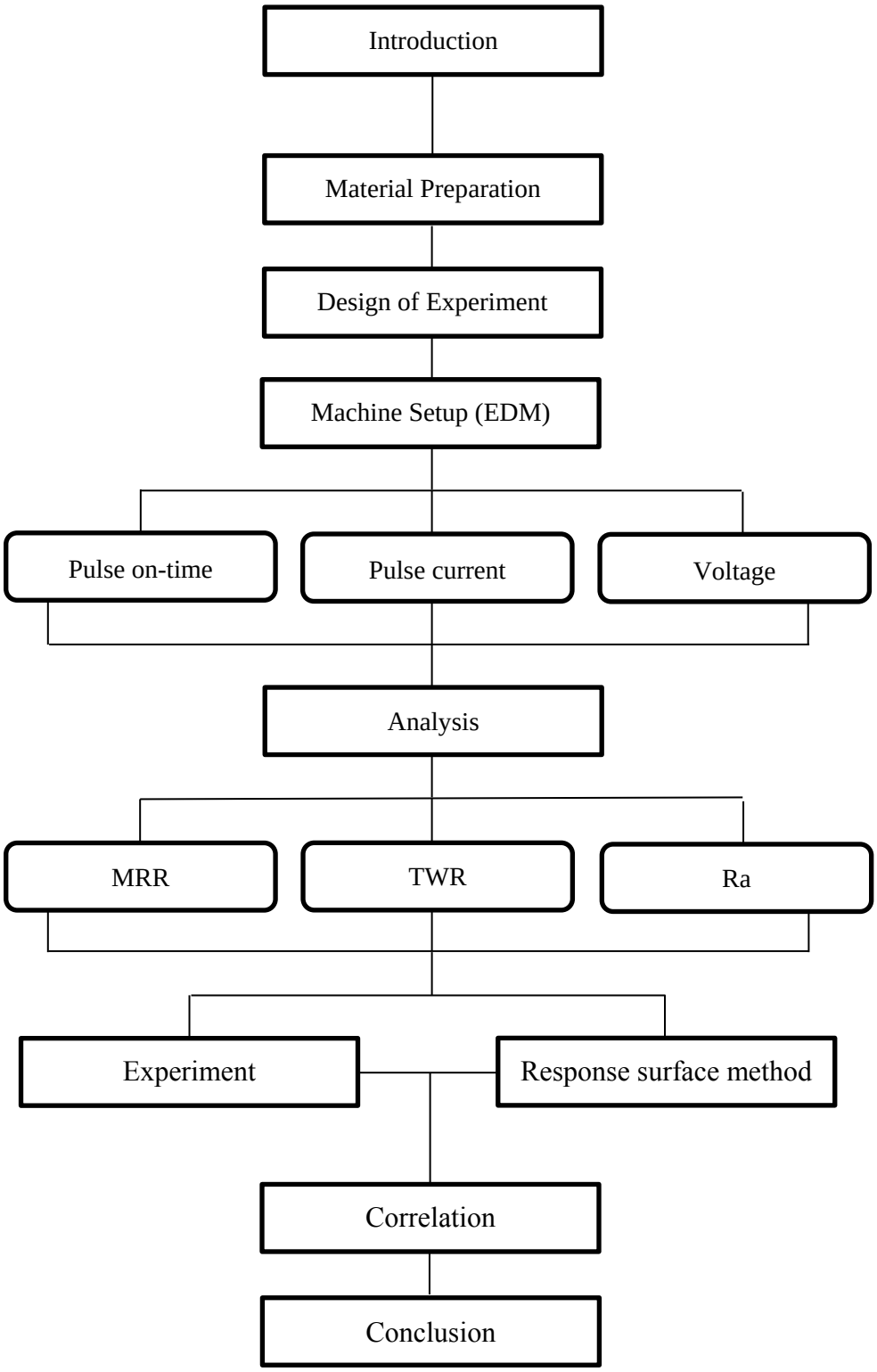

Figure 3.1: Flow chart of methodology

3.2 Material Preparation

The instrument steels that utilized in this investigation is high speed tools steel (AISI D6). Tool steels as work pieces was used, which are primarily used to make tools used in manufacturing processes as well as for machining metals, woods, and plastics. Tool steels are generally ingot-cast wrought products, and must be able to withstand high specific loads as well as be stable at elevated temperatures [164].

This is a tool steel grade offering very high wear resistance with edge holding quality. It is an air hardening alloy tool steel with excellent resistance to wear and abrasion. As high carbon high chromium tool steel 1.2436 has well through hardening properties and dimensional stability combined with high resistance to tempering [165]. Table 3.1, table 3.2 and table 3.3 shown respectively standards tool steel, chemical composition and heat treatment for tool steel.

Table 3.1: Standards Tool Steel [164]

	Germany	**USA**	**Japan**
Standards	DIN	AISI	JIS
	1.2436	D6	SKD2

Table 3.2 Chemical Composition (typical analysis in %)

C	**Si**	**Mn**	**P**	**S**	**Cr**	**W**
2.00-2.30	0.10-0.40	0.15-0.45	≤0.030	≤0.030	11.0-12.0	0.60-0.80

Table 3.3: Heat Treatment [164,165]

Soft annealing	Temperature(°C)	Cooling	Hardness
	870 - 900	furnace	max. 255 HB

Forging	Temperature(°C)	Cooling
	850 - 1050	furnace

Hardening	Temperature(°C)	Cooling	Tempering
	930 - 980	oil or air	see tempering diagram usually 100 - 400°C

3.3 Electrodes

The important factors in selecting cooper is their high strength-to-weight ratio, resistance to corrosion by many chemicals, high thermal and electrical conductivity, non-toxicity, reflectivity, appearance and ease of formability and of machinability; they are also nonmagnetic [123].

Copper is a chemical element with the symbol Cu (Latin: cuprum) and atomic number 29. It is a ductile metal with excellent electrical conductivity. Copper is malleable and ductile, when very pure, a good conductor of electricity and a great conductor of heat [58]. Copper is rather supple in its pure state and has a pinkish luster which is (beside gold) unusual for metals, which are normally silvery white. Table 3.4 shown material properties for copper tool.

Copper has been extensively utilized as industrial structure materials due to their distinctive properties, such as formability and ductility, corrosion resistance, heat transfer and electrical conductivity [166].

Table 3.4: Material properties

Material	Thermal conductivity (W/m-K)	Boiling point (K)	Melting point (K)
Copper	401	2835.15	1357.77

3.4 Experimental Setup

The following equipments were utilized in this experimental investigation:

Please refer 3.5.1 material procedure for the parameters.

3.4.1 Electrical Discharge Machining

This machine was utilized to create cylindrical shape on the workpiece for experiment in the electrical discharge machining process.

Brand: Azarakhsh

Model: CNC 204

Number of axis: Three

Figure 3.2: Electrical Discharge Machining

3.4.2 Balance

Precision balance was employed to amount the weight of the tool and workpiece before and later the machining process. We repeated the measurement twice to ensure accuracy in the data acquired.

Brand: METTLER TOLEDO

Model: AB265

Resolution: 0.00001 gram

Figure 3.3: Balancing Machine with accuracy equal to 0.00001 gram

3.4.3 Measuring Surface Roughness

The ability to perform surface roughness measurements is critical to maintaining component quality within predefined limits. The perthomete machine is used to measure the surface roughness of surfaces.

Brand : perthomete

Model :S6P

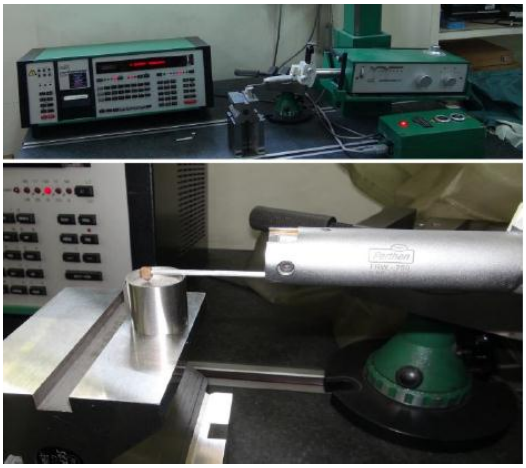

Figure 3.4: The surface roughness measurement machine (perthomete)

3.5 Experiment Method

In machining any material with any parameters utilizing Electro Discharge Machine, there is still a problem for this device in the first part. So as to examine this investigation, the plan of test will be made to taking care of the parameters issue. This section, in addition to the information parameters that should be selected for this research, is examined.

3.5.1 Material Procedure

The electrode needs to be cut its diameter same for all material. For the work piece, the lathe machine and grinding machines are utilized for cutting all samples in same measurement. Before run the trial, the electrode and work piece is cut with respect to their measurement. Figure 3.5 and figure 3.6 and table 3.5 allude to all the material measurement that should cut and shape. The lathe machine and center less grinding machine are used to cut the electrode.

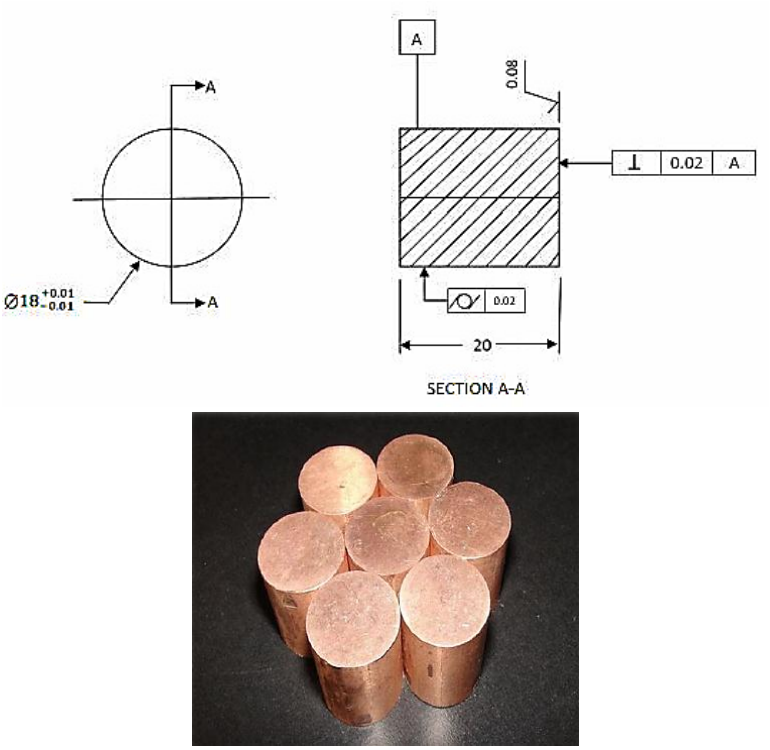

Figure 3.5: Measurement for the Tool Production

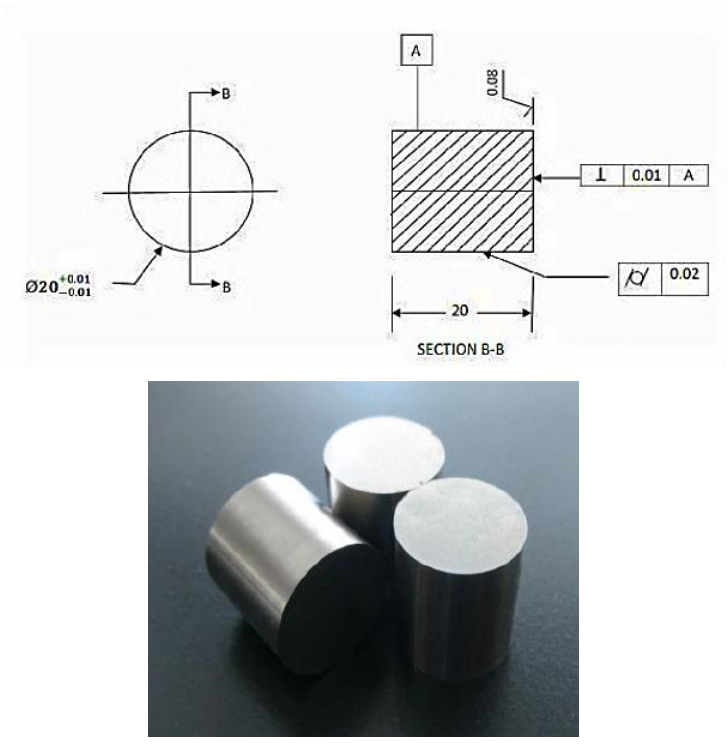

Figure 3.6: Measurement for the work piece production

Table 3.5: Tool and work-piece specifications

Material	Gender	Length (mm)	Diameter (mm)
Tool	Copper	20	18
Work-piece	AISI D6	20	20

3.5.2 EDM Machining

Kerosene will utilized as dielectric fluid. The electric discharge machine, typical CNC 204 (die sinking type) with servo-head (constant gap) and positive polarity for electrode (reverse polarity) will used to lead the test. These are the method of this trial:

1) Experiment will led with positive polarity of copper. The anode copper is taken. The diameter and length of tool are measured with a micrometer. Ensure its measurement is as per detail.
2) Take the copper mass amount and the work piece mass amount. An initial mass is estimated with a mettler toledo balance (AB265).
3) The work material (tool steel) was mounted on the T-slot table and situated at the longing place and clasped. The tool was clasped on the holder, and its arrangement was checked with the assistance of the attempt square.

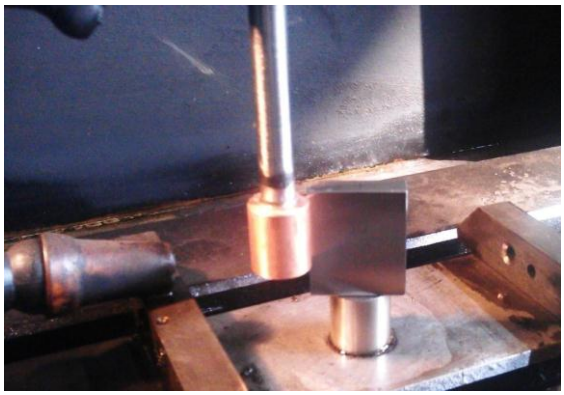

Figure 3.7: Tool and workpiece setting in EDM.

4) Set the parameters of the test with respect to table 3.6

5) Machining time of 20 min was set for the machining of all workpiece. At long last, switches 'ON' for working the craving release current qualities.

6) After machining activity, the copper tool was taken out and weight again on Precisa balance. Likewise take the mass estimation of work piece subsequent to machining.

7) The same trial was repetitive with other different parameters.

3.5.3 Machining Parameters

The parameters that are associated with this study are appeared table 3.6

Table 3.6: Input parameters

Parameters	Unit	levels			
		1	2	3	4
Pulse on time	µs	10	20	30	40
Pulse current	A	8	10	12	14
Input voltage	V	150	250	-	-

3.6 Information Collection

The information that will be taken is:

1) Mass of work piece before and after machining
2) Mass of tool before and after

3.6.1 Analyzed Method

A mettler toledo balance (AB265) was employed to amount the weight of the copper tool and workpiece required. Parallel process for determining the weight of work piece was utilized to define the weight of the copper tool beforehand and afterward machining. After completion of every machining method, the work piece was blown by compressed gas air gun to make sure no scrap and dielectrics were present. The present work highlights the event of mathematical answer to calculate the EDM machining parameters such as: mass of conductor, pulse length and voltage on the metal removal rate, wear quantitative relation and surface roughness. The MRR in mm3/min of the work piece was measured by dividing the burden of labor piece before and once machining (found by advisement technique exploitation balance) against the machining time that was achieved. This work has been established supported the mathematical equation (3.1).The equation (3.0) can used for confirm the TWR in g/g value:

$$\%TWR=\frac{(M_{T1}-M_{T2})\times\rho_W}{(M_{W1}-M_{W2})\times\rho_T}\times 100 \qquad \text{Eq (3.0)}$$

$$MRR=\frac{(M_{W1}-M_{W2})}{(\rho_W\times t)}\times 10^3 \qquad \text{Eq (3.1)}$$

where MRR is the material removal rate; TWR is the tool wear ratio; M_{W1}, M_{W2} are the weight of workpiece (in grams) before and after machining, M_{T1}, M_{T2} are the tool weight (in grams) beforehand and after machining; ρ_W is the density of the workpiece in g/cm^3; t is the machining time in min and ρ_T is the density of the Cu tool (i.e., 93.8 g/cm3).

Also, a perthomete measuring roughness (S6P) was used to measure the surface roughness of the work piece required.

Response surface methodology is used to optimize the performance of the process in order to obtain the maximum benefit from the EDM. The software of Design Expert was performed to carry out the design of the experiments and develop resource models. The analysis of variance (ANOVA) was used to confirm the established equations.

Due to the result, the most effective parameters for EDM machining method are determined. While, the lower TWR relation within the EDM machine is that the higher and correct performance characteristic. The higher material removal rate in the EDM machine, the better is the machining performance.

3.7 Summary

These results are being interpreted in Chapter 4 Results and Discussion. Graphs were drawn to illustrate the tool wear growth at every experiment. Then, from the graphs we were able to confirm the simplest choice and correct conductor. The electrical discharge machine (EDM) method experiment has been utilized beneath experimental founded and procedure.

Chapter 4

RESULTS AND DISCUSSIONS

4.1 Introduction

Chapter four is mostly discuss the results obtained throughout the experimental analysis on the tool wear ratio (TWR), surface roughness (Ra) and material removal rate (MRR) for different machining parameters (Pulse on time, Pulse current and voltage).

4.2 Experimental Work

The AISI-D6 steel hardened to 60 HRC and Cu were respectively employed as the experimental and electrode materials. The test pieces and electrodes were precisely machined to the sizes defined in Table 3.5. Tables 3.6 demonstrate the test plan carried out in this investigation. The controlling parameters pulse current (I) and pulse on-time (Ton) each was varied over four levels. The steels are usually cut in the range of 150 V to 250 V [167]; therefore, this specific parameter was varied over only two levels so that the number of tests could be minimized. The other parameters were set fixed as: machining gap = 2 mm; duty cycle = 20; and polarity = positive. Kerosene oil was used as the dielectric medium. In all, 32 experiments as listed in Table 4.1 were performed on the Azarakhsh Ayzvpals CNC EDM system shown in Figure 3.2.

Table 4.1: Information parameters and their levels utilized in the present investigation

NO.	Pulse current (I)	Pulse on time (T_{on})	Pulse off time (T_{off})	GAP VOLT	JAM LENG	WORK TIME	HIGH VOLT
1	8	10	5 (50/)	40 v	5 (0.5)	10 (1.0s)	1(150)
2	8	20	5 (50/)	40 v	5 (0.5)	10 (1.0s)	1(150)
3	8	30	5 (50/)	40 v	5 (0.5)	10 (1.0s)	1(150)
4	8	40	5 (50/)	40 v	5 (0.5)	10 (1.0s)	1(150)
5	10	10	5 (50/)	40 v	5 (0.5)	10 (1.0s)	1(150)
6	10	20	5 (50/)	40 v	5 (0.5)	10 (1.0s)	1(150)
7	10	30	5 (50/)	40 v	5 (0.5)	10 (1.0s)	1(150)
8	10	40	5 (50/)	40 v	5 (0.5)	10 (1.0s)	1(150)
9	12	10	5 (50/)	40 v	5 (0.5)	10 (1.0s)	1(150)
10	12	20	5 (50/)	40 v	5 (0.5)	10 (1.0s)	1(150)
11	12	30	5 (50/)	40 v	5 (0.5)	10 (1.0s)	1(150)
12	12	40	5 (50/)	40 v	5 (0.5)	10 (1.0s)	1(150)
13	14	10	5 (50/)	40 v	5 (0.5)	10 (1.0s)	1(150)
14	14	20	5 (50/)	40 v	5 (0.5)	10 (1.0s)	1(150)
15	14	30	5 (50/)	40 v	5 (0.5)	10 (1.0s)	1(150)
16	14	40	5 (50/)	40 v	5 (0.5)	10 (1.0s)	1(150)
17	8	10	5 (50/)	40 v	5 (0.5)	10 (1.0s)	3(250)
18	8	20	5 (50/)	40 v	5 (0.5)	10 (1.0s)	3(250)
19	8	30	5 (50/)	40 v	5 (0.5)	10 (1.0s)	3(250)
20	8	40	5 (50/)	40 v	5 (0.5)	10 (1.0s)	3(250)
21	10	10	5 (50/)	40 v	5 (0.5)	10 (1.0s)	3(250)
22	10	20	5 (50/)	40 v	5 (0.5)	10 (1.0s)	3(250)
23	10	30	5 (50/)	40 v	5 (0.5)	10 (1.0s)	3(250)
24	10	40	5 (50/)	40 v	5 (0.5)	10 (1.0s)	3(250)
25	12	10	5 (50/)	40 v	5 (0.5)	10 (1.0s)	3(250)
26	12	20	5 (50/)	40 v	5 (0.5)	10 (1.0s)	3(250)
27	12	30	5 (50/)	40 v	5 (0.5)	10 (1.0s)	3(250)
28	12	40	5 (50/)	40 v	5 (0.5)	10 (1.0s)	3(250)
29	14	10	5 (50/)	40 v	5 (0.5)	10 (1.0s)	3(250)
30	14	20	5 (50/)	40 v	5 (0.5)	10 (1.0s)	3(250)
31	14	30	5 (50/)	40 v	5 (0.5)	10 (1.0s)	3(250)
32	14	40	5 (50/)	40 v	5 (0.5)	10 (1.0s)	3(250)

After each test, the related performance measures including MRR, TWR and R_a were measured. In order to determine MRR and TWR, the weight of steel and copper tools was measured before and after machining using a digital precision scale Mettler Toledo-AB265 in an accuracy of ±0.00001 gram. Table 4.2 and 4.3 shown that the weight of steel and copper tools before and after machining.

Table 4.2: The weight of copper tools before and after machining

NO.	Part Name	First Weight	Second Weight	Subtraction Weight	Density
1	CU	45.74251	45.52098	0.22153	8.94
2	CU	45.69722	47.50718	0.19004	8.94
3	CU	45.74584	45.69367	0.05217	8.94
4	CU	45.73948	45.71387	0.02561	8.94
5	CU	45.74186	45.53023	0.21163	8.94
6	CU	45.72057	45.45709	0.26348	8.94
7	CU	45.78121	45.69152	0.08969	8.94
8	CU	45.68920	45.63283	0.05637	8.94
9	CU	45.73351	45.37812	0.35539	8.94
10	CU	45.72510	45.23344	0.49166	8.94
11	CU	45.74103	45.53916	0.20187	8.94
12	CU	45.63981	45.49702	0.14279	8.94
13	CU	45.70567	45.29937	0.40630	8.94
14	CU	45.68219	45.01756	0.66463	8.94
15	CU	45.69588	45.36449	0.33139	8.94
16	CU	45.76586	45.42539	0.34047	8.94
17	CU	45.76270	45.59169	0.17101	8.94
18	CU	45.62079	45.48452	0.13627	8.94
19	CU	45.72600	45.68610	0.03990	8.94
20	CU	45.64065	45.61764	0.02292	8.94
21	CU	45.68575	45.55089	0.13486	8.94
22	CU	45.73934	45.62716	0.11218	8.94
23	CU	45.74622	45.69417	0.05205	8.94
24	CU	45.72601	45.69607	0.02994	8.94
25	CU	45.73237	45.52478	0.20759	8.94
26	CU	45.72738	45.49012	0.23726	8.94
27	CU	45.74404	45.63633	0.10771	8.94
28	CU	45.77167	45.69059	0.08108	8.94
29	CU	45.75920	45.49625	0.26295	8.94
30	CU	45.78193	45.78754	0.29439	8.94
31	CU	45.68979	45.45292	0.14687	8.94
32	CU	45.76280	45.64248	0.12032	8.94

Table 4.3: The weight of AISI D6 tools steel before and after machining

NO.	Part Name	First Weight	Second Weight	Subtraction Weight	Density
1	1.2436 (D6)	48.13278	47.19340	0.93938	7.77
2	1.2436 (D6)	48.14914	46.79771	1.35143	7.77
3	1.2436 (D6)	48.11768	45.46707	2.65061	7.77
4	1.2436 (D6)	48.15148	45.38924	2.76224	7.77
5	1.2436 (D6)	48.18775	46.95828	1.22947	7.77
6	1.2436 (D6)	48.11948	46.35648	1.76300	7.77
7	1.2436 (D6)	48.11023	44.59120	3.51903	7.77
8	1.2436 (D6)	48.17583	44.39298	3.78285	7.77
9	1.2436 (D6)	48.09536	46.37020	1.72516	7.77
10	1.2436 (D6)	48.14876	45.52053	2.62823	7.77
11	1.2436 (D6)	48.11651	43.44242	4.67409	7.77
12	1.2436 (D6)	48.14123	43.04570	5.09553	7.77
13	1.2436 (D6)	48.20194	46.16361	2.03833	7.77
14	1.2436 (D6)	48.15992	44.56997	3.58995	7.77
15	1.2436 (D6)	48.12504	42.58590	5.53914	7.77
16	1.2436 (D6)	48.13315	41.19488	6.93827	7.77
17	1.2436 (D6)	48.11549	47.07233	1.04316	7.77
18	1.2436 (D6)	48.17731	46.46436	1.71295	7.77
19	1.2436 (D6)	48.15178	45.69530	2.45648	7.77
20	1.2436 (D6)	48.19106	45.62108	2.56998	7.77
21	1.2436 (D6)	48.07332	46.89591	1.17741	7.77
22	1.2436 (D6)	48.11880	45.84033	2.27847	7.77
23	1.2436 (D6)	48.20819	45.16122	3.04697	7.77
24	1.2436 (D6)	48.19582	44.85934	3.33648	7.77
25	1.2436 (D6)	48.17540	46.68181	1.49359	7.77
26	1.2436 (D6)	48.08601	45.11456	2.97145	7.77
27	1.2436 (D6)	48.15535	44.07895	4.07640	7.77
28	1.2436 (D6)	48.18573	43.65352	4.53221	7.77
29	1.2436 (D6)	48.19517	46.29816	1.89701	7.77
30	1.2436 (D6)	48.17351	44.77128	3.40223	7.77
31	1.2436 (D6)	48.14540	43.57095	4.57445	7.77
32	1.2436 (D6)	48.11795	43.01065	5.10739	7.77

Table 4.4 shows the output parameters of the tool wear ratio (TWR), material removal rate (MRR) and surface roughness (R_a). TWR and MRR are calculated by using Equations 3.0 and 3.1 respectively, while the surface roughness is measured from surface machine tool directly.

Table 4.4: Output parameters (MRR, TWR,R_a)

NO	MRR	TWR	Ra (µm)
1	6.044916345	20.49627549	3.43
2	8.696461746	12.2217946	4.01
3	17.05669241	1.710639534	4.92
4	17.77503218	0.805808174	5.91
5	7.911647362	14.96039589	3.17
6	11.34492634	12.98909348	4.50
7	22.6449807	2.215157216	5.84
8	24.34266409	1.295127169	7.05
9	11.1014257	17.90438152	4.01
10	16.91268696	16.25866971	4.92
11	30.07779923	3.75368835	6.18
12	32.78977834	2.435521293	5.95
13	13.11667667	17.32431519	3.81
14	23.10135135	16.09070381	5.06
15	35.644440154	5.199727174	5.65
16	44.6478121	4.264923605	5.99
17	6.712741313	14.24801574	3.24
18	11.02284427	6.914154337	3.89
19	15.80746461	1.411702433	5.34
20	16.53784784	0.775118977	5.15
21	7.576640927	9.954947613	3.24
22	14.66196911	4.279131384	4.08
23	19.60727156	1.484690931	5.19
24	21.47027027	0.779914096	5.80
25	9.611261261	12.07977628	3.09
26	19.12129987	6.939682466	4.77
27	26.23166023	2.296480346	5.61
28	29.16480051	1.554845408	5.87
29	12.20727156	12.04723593	3.74
30	21.89337194	7.520434647	5.43
31	29.43662519	2.790472262	5.57
32	32.86609752	2.047492414	6.29

4.3 Influence of Pulse on Time (Ton) on the Material Removal Rate (MRR)

Figure 4.1 up to 4.4 shown the influence of material removal rate (The material removal rate (MRR) is defined as the volume of material removed over a unit period of time) on the pulse on time (The duration of time (µs) the current is allowed to flow per cycle) in two levels for voltage and four levels for pulse current. The result had showed the material removal rate increases with increasing of pulse on time. It took 40µs for the maximum MRR when voltage and pulse current were 150V and 14A respectively. Keeping the current constant but varying the voltage from 150V to 250V, the minimum MRR is found when pulse on time is 10 µs.

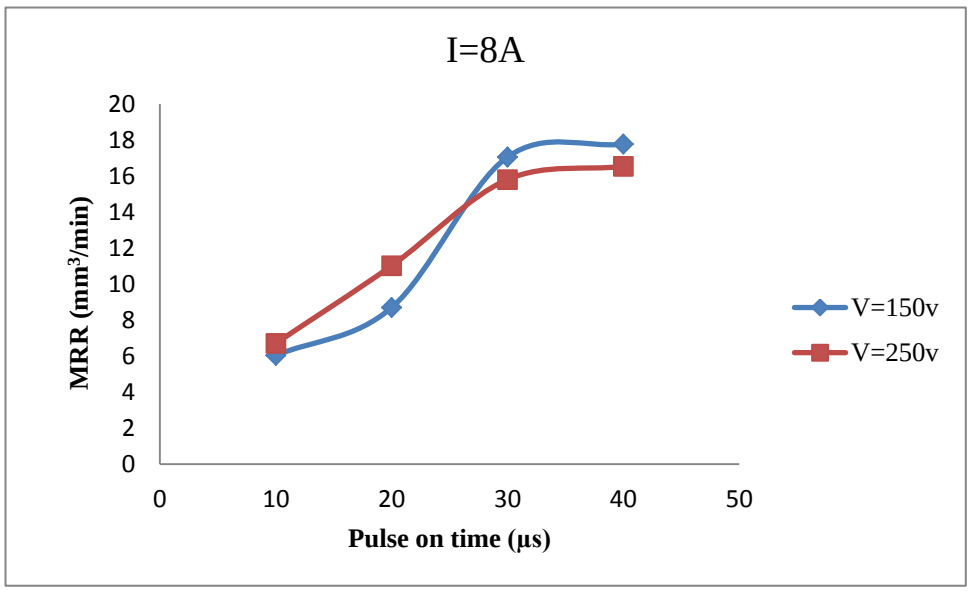

Figure 4.1: The effect of the pulse on time on the material removal rate at varying voltage (I=8A).

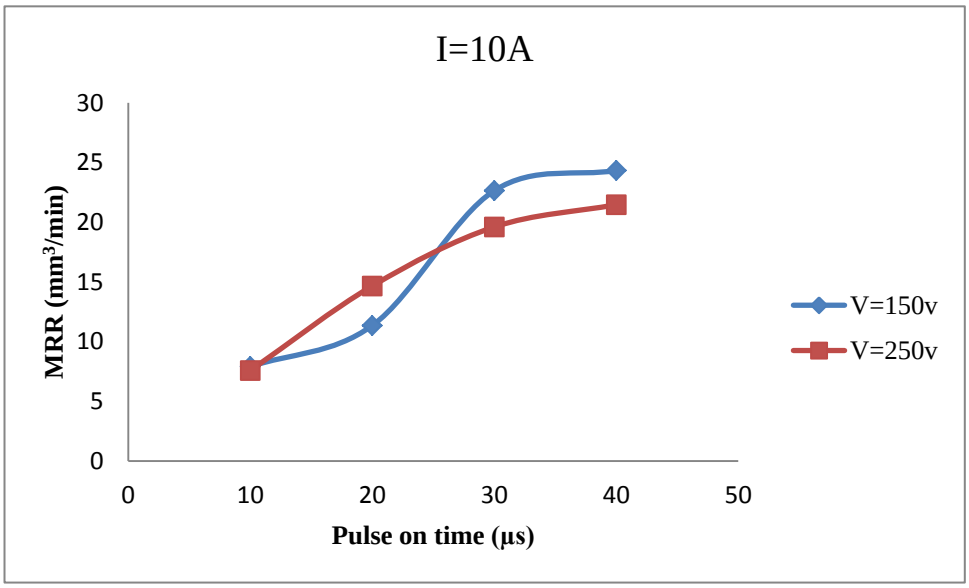

Figure 4.2: The effect of the pulse on time on the material removal rate at varying voltage (I=10A).

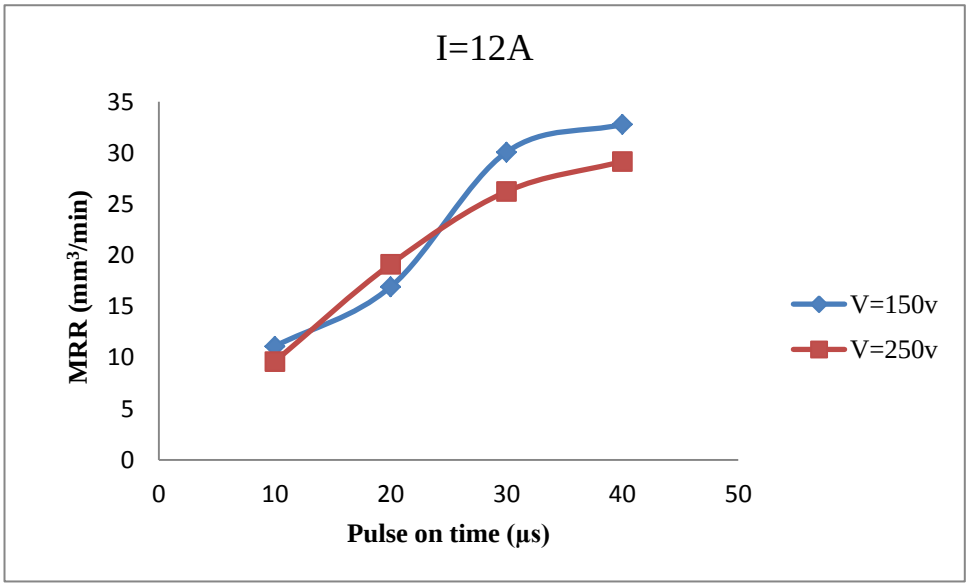

Figure 4.3: The effect of the pulse on time on the material removal rate at varying voltage (I=12A).

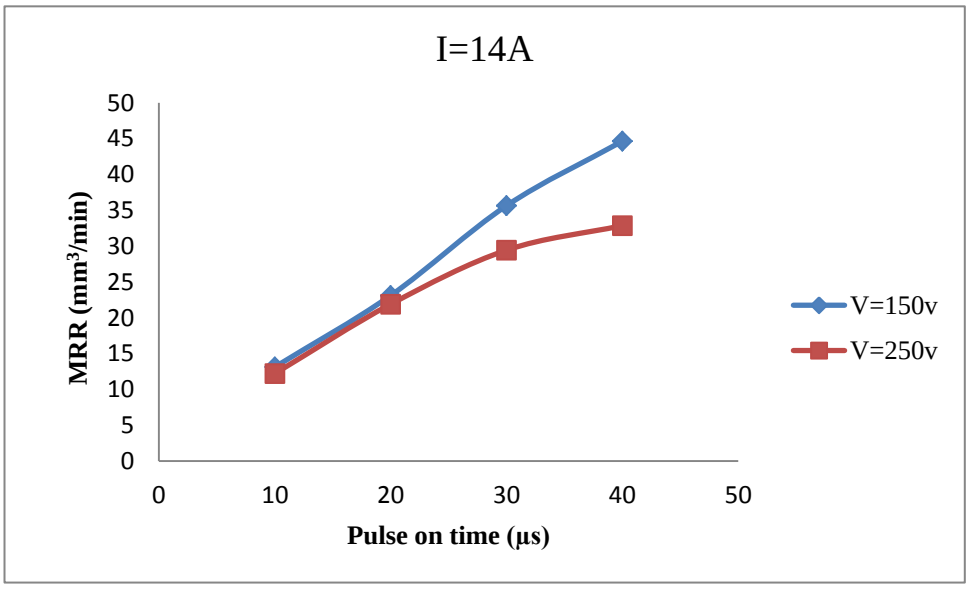

Figure 4.4: The effect of the pulse on time on the material removal rate at varying voltage (I=14A).

Figure 4.1 up to 4.4 demonstrates the effect of pulse on-time on the material removal rate. As can be noticed from Figure 4.1 up to Figure 4.4, the MRR gradually increases with the increasing of T_{on} and this effect becomes increasingly pronounced as the pulse on-time increases that can be seen more clearly from Figure 4.1 and Figure 4.2. This finding can be attributed to increase in the ignition energy, defined by Eq. 4.1 [168], which in turn increases the melting rate and hence results in the increased MRR.

$$W_{IF} = \int_{T_d}^{T_{on}} V_{sp}.I_{sp}.dt \qquad \text{Eq (4.1)}$$

Where W is the ignition energy, I is the pulse current, T is the pulse time and V is the voltage.

4.4 Influence of Pulse Current (I) on the Material Removal Rate (MRR)

Figure 4.5 up to 4.8 shown influence of material removal rate (The material removal rate (MRR) is defined as the volume of material removed over a unit period of time) on the pulse current in two levels for voltage and four levels for pulse on time.

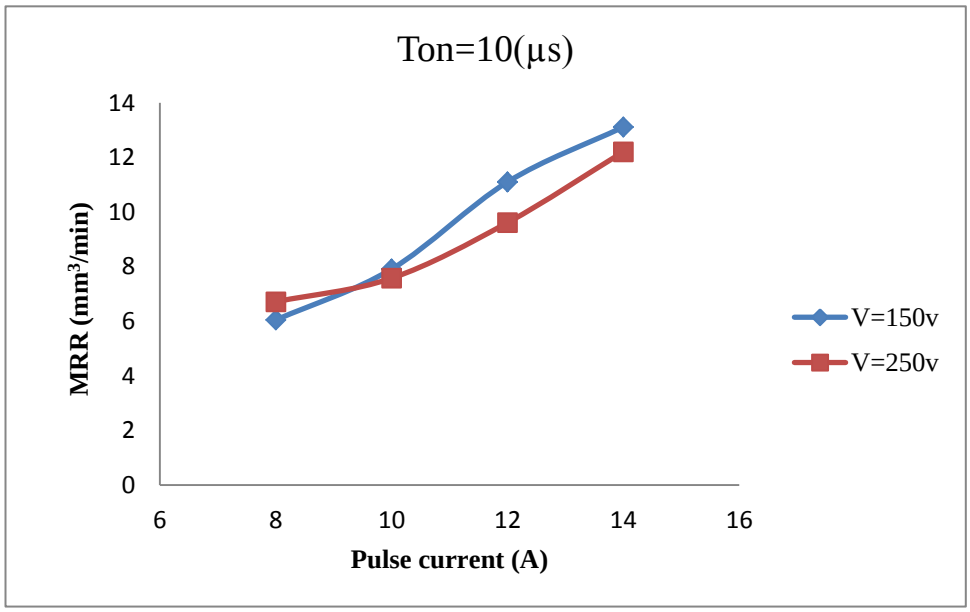

Figure 4.5: The effect of the pulse current (I) on the material removal rate (MRR) at varying voltage (T_{on}=10µs).

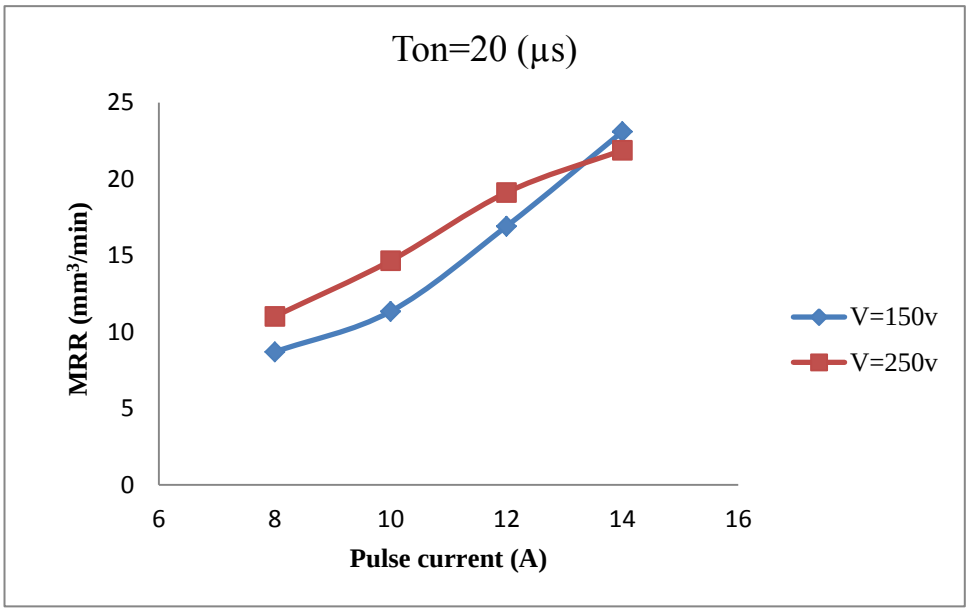

Figure 4.6: The effect of the pulse current on the material removal rate at varying voltage (T_{on}=20µs).

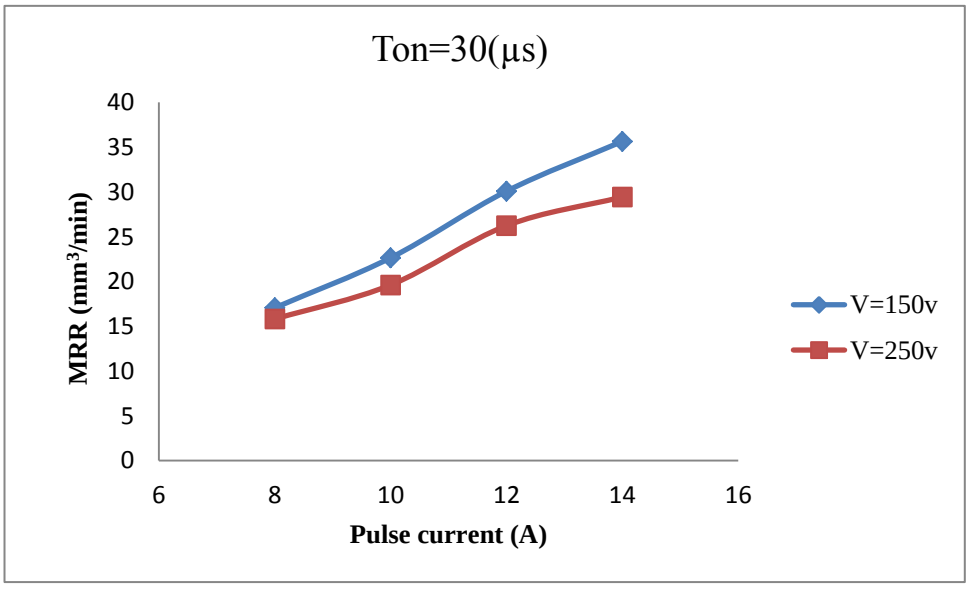

Figure 4.7: The effect of the pulse current on the material removal rate at varying voltage (T_{on}=30µs).

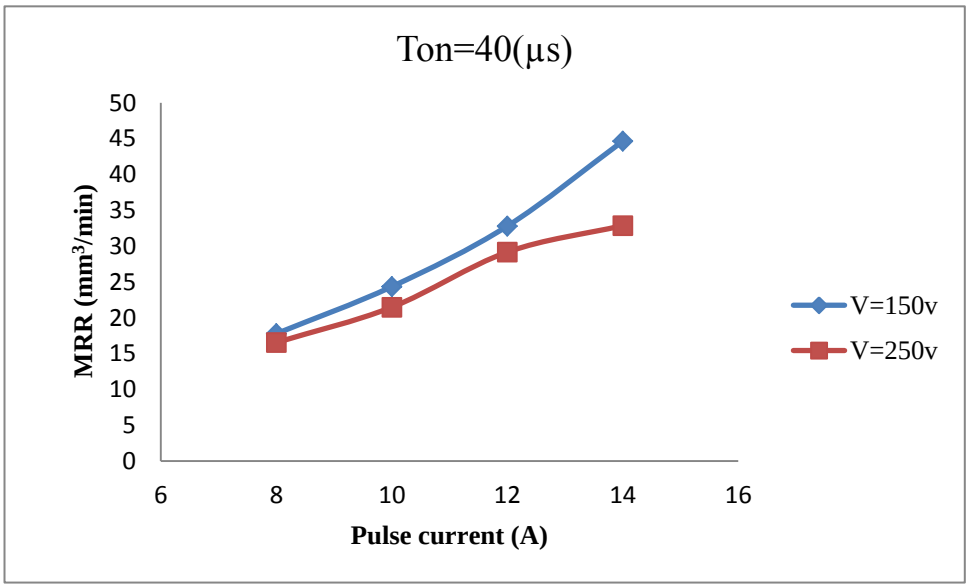

Figure 4.8: The effect of the pulse current on the material removal rate at varying voltage (T_{on}=40µs).

Figure 4.5 up to 4.8 illustrates the effectiveness of pulse current on the material removal rate. As can be noticed from Figure 4.5 up to Figure 4.8, the MRR gradually increases with the increasing of pulse current and this effect becomes increasingly pronounced as the pulse current increases that can be seen more clearly from Figure 4.7 and Figure 4.8. This finding can be attributed to increase in the ignition energy, defined by Eq. 4.1 [168], which in turn increases the melting rate and hence results in the increased MRR.

More in detail, the mechanism involved in affecting the MRR is different for the pulse current and the pulse on-time. In the former case, the increase in the MRR owes to increase in the current density which speeds up ionization of dielectric fluid thus leading to rapid material melting [169]. In the latter case, the MRR increases as

the volume of melt-hole increases which is reasoned to a fact that the surface temperature of the work-piece rises at a higher pulse current.

4.5 Influence of Voltage (V) on the Material Removal Rate (MRR)

Figure 4.8 and 4.3 respectively portray the effect of the pulse current and pulse on-time at varying voltage. For each level of voltage, the MRR increases as the current increases (Figure 4.8). It is worth noticing that interestingly a low voltage (150 V) offers higher MRR than a high voltage (250 V), which is observed 45 and 35 respectively. The same fact can be observed for the pulse on time when its value exceeds 30 μs (Figure 4.3). On the other hand, the Eq. (4.1) dictates that the material removal rate increases due to increase in the voltage. In fact, for some materials multi-sparking phenomenon occurs at low input voltage that leads to the increased MRR [167, 170]. However, this phenomenon is closely linked to the pulse on-time and becomes evident in the present material when the time exceeds 30 μs. From the above discussion, it follows that the EDM of AISI-D6 steel needs to be performed employing high pulse current, pulse on-time and low voltage to achieve high productivity

4.6 Influence of Pulse on Time (Ton) on the Tool Wear Ratio (TWR)

Figure 4.9 up to 4.12 shown influence of tool wear ratio (TWR or electrode wear ratio (EWR) or relative electrode wear (REW) is defined as the ratio of volume of materials removed from the tool electrode to work piece) on the pulse on time (The duration of time (μs) the current is allowed to flow per cycle) in two levels for voltage and four levels for pulse current.

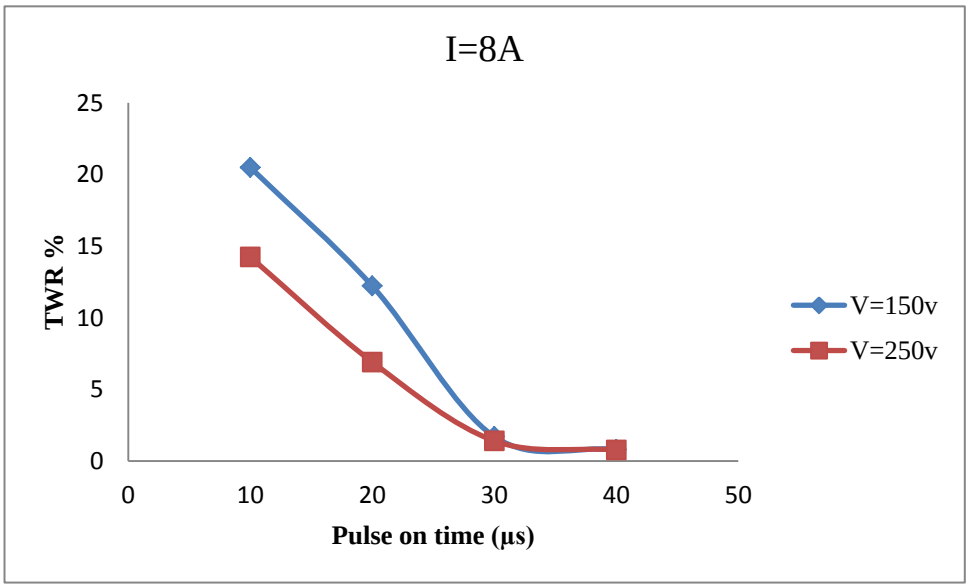

Figure 4.9: The effect of the T_{on} on the tool wear ratio at varying voltage (I=8A).

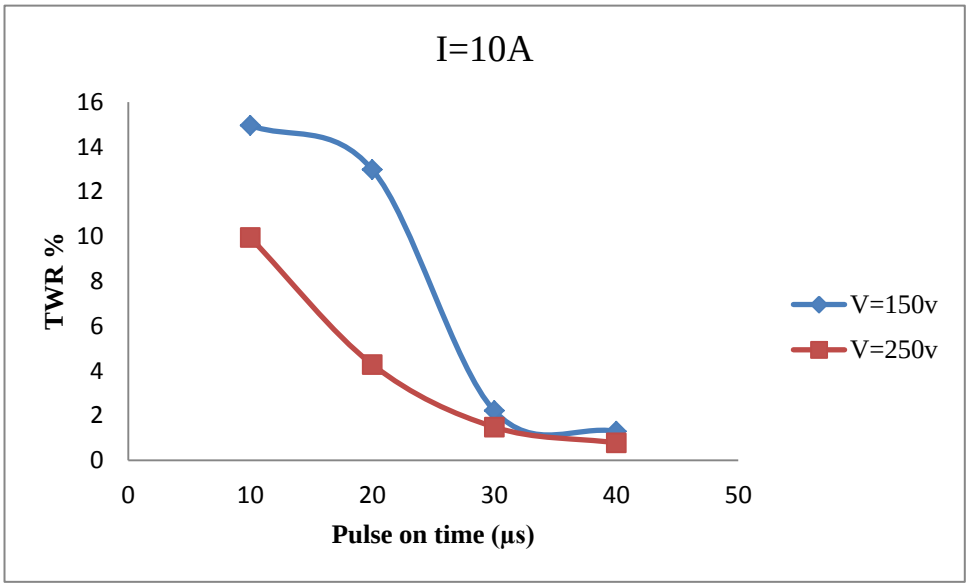

Figure 4.10: The effect of the T_{on} on the tool wear ratio at varying voltage (I=10A).

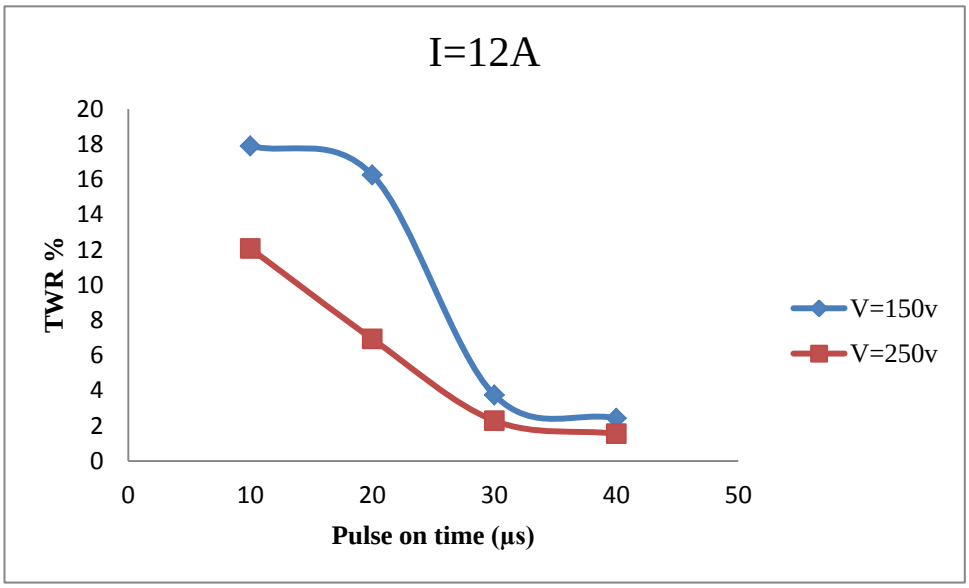

Figure 4.11: The effect of the T_{on} on the tool wear ratio at varying voltage (I=12A).

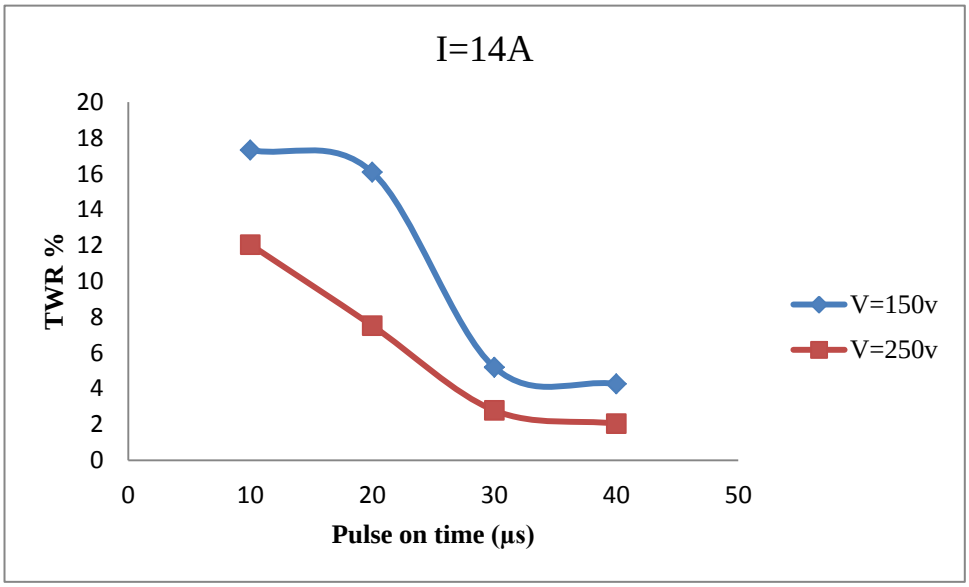

Figure 4.12: The effect of the T_{on} on the tool wear ratio at varying voltage (I=14A).

Figure 4.9 and 4.12 illustrates the influence of pulse on-time on TWR. As can be observed, there is a decrease in the TWR as the pulse on-time increases. For different pulse current (I), the maximum TWR is obtained from 150V.The highest TWR is found when T_{on} and pulse current are 10µs and 8A respectively. In fact, the electrode was connected to the positive terminal in this work. And for the low time, the

electrons flow from the work-piece to the tool causing high tool wear value. For long pulse on-time, on the other hand, the positive ions flow from tool towards the workpiece due to the expansion of plasma channel radius [171]. As a result, the material removal mechanism becomes positive ions collide, and the TWR reduces. This is to point out that high pulse on-time yields high MRR as found before. Thus, setting large pulse on-time value could be a good strategy to simultaneously improve the MRR and to reduce the TWR. This is to be seen from the curves in Figure 4.8 that the TWR further reduces as the current decreases to value, which can be seen more clearly from Figure 4.15 and 4.16. This can be reasoned to increase in the input energy to the Cu tool that in turn causes corresponding increase in the tool melt [172,173].

4.7 Influence of Pulse Current (I) on the Tool Wear Ratio (TWR)

Figure 4.13 up to 4.16 shown influence of tool wear ratio (TWR is defined as the ratio of volume of materials removed from the tool electrode to that of work piece) on the pulse current in two levels for voltage (150v and 250v) and four levels for pulse on time (10, 20, 30, 40μs).

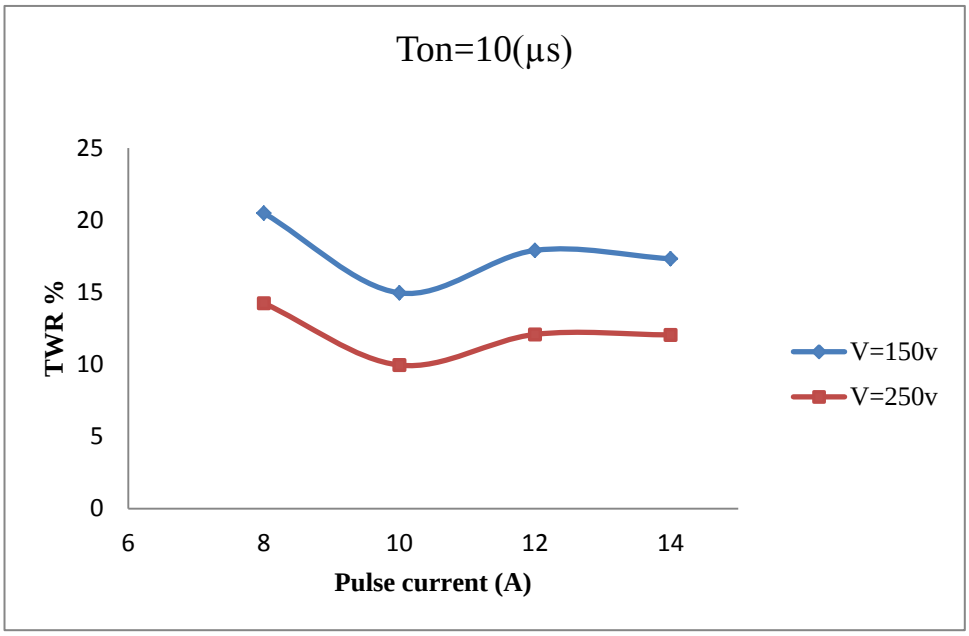

Figure 4.13: The influence of the (I) on the tool wear ratio at varying voltage (Ton =10 µs).

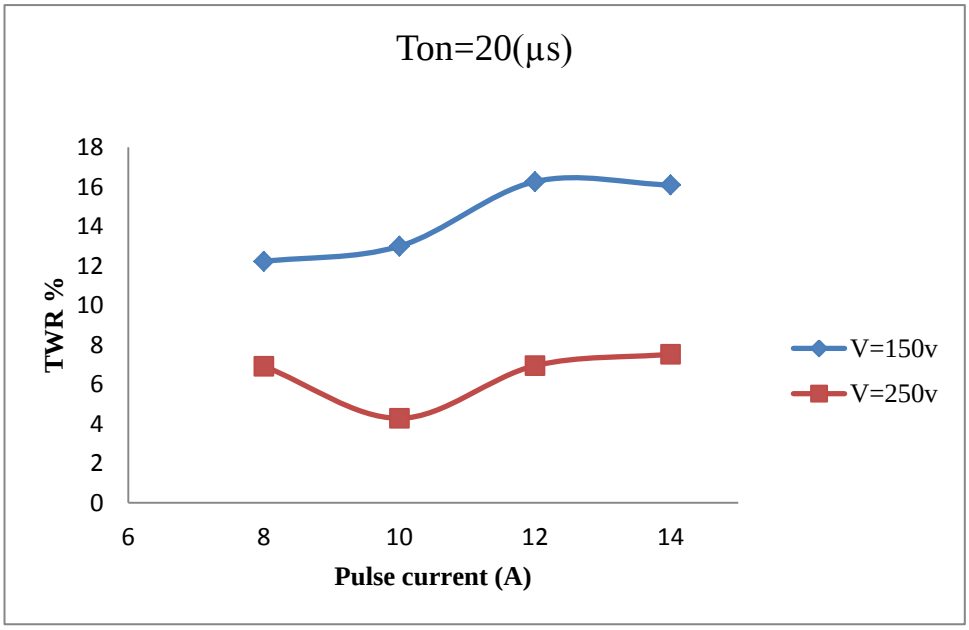

Figure 4.14: The effect of the pulse current on the tool wear ratio at varying voltage (Ton =20 µs).

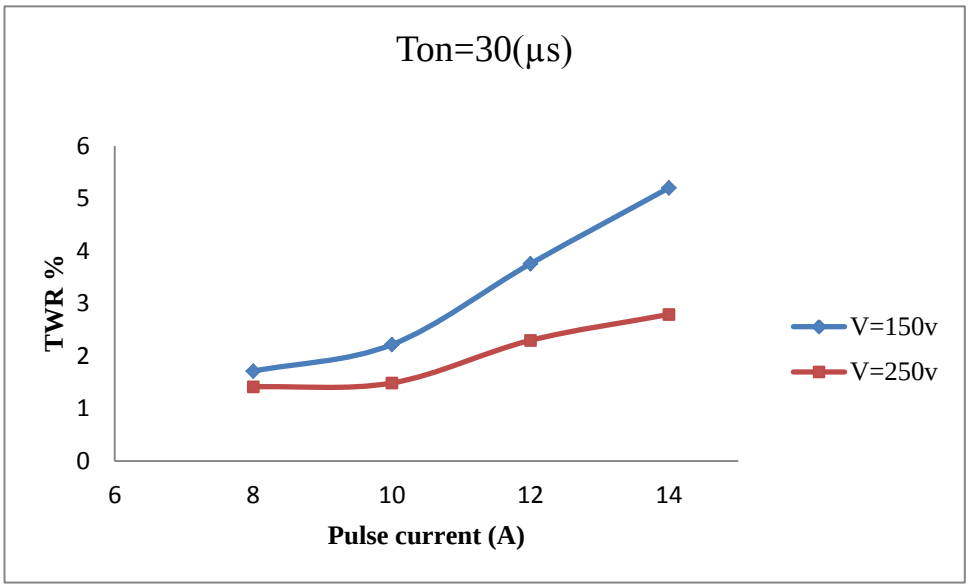

Figure 4.15: The effect of the pulse current on the tool wear ratio at varying voltage (Ton =30 µs).

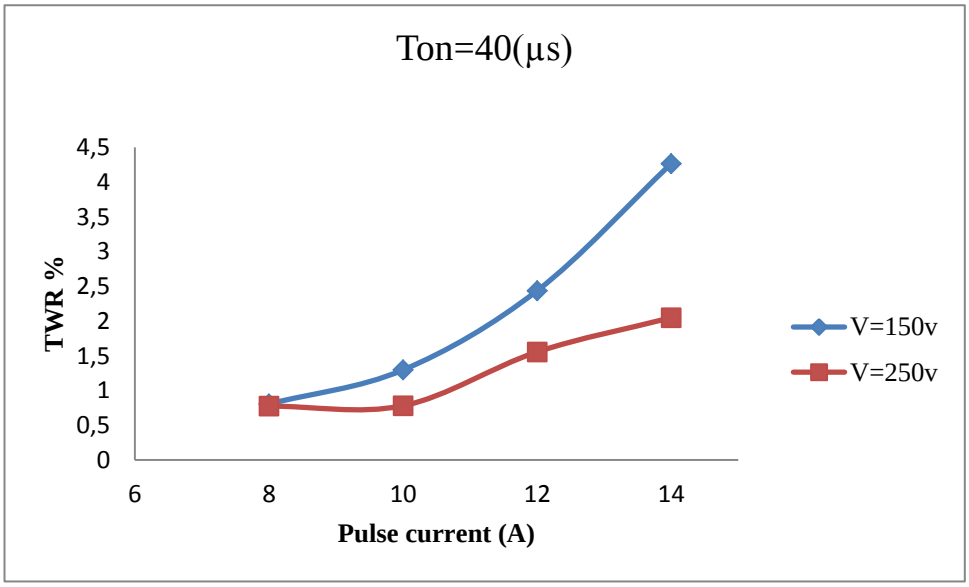

Figure 4.16: The influence of the pulse current on the tool wear ratio at varying voltage (Ton =40 µs).

Figure 4.13 up to 4.16 shown influence of tool wear ratio (TWR) on the pulse current (I) in two levels for voltage (150V, 250V) and four levels for pulse current (8A, 10A, 12A, 14A). As shown at the same time with increase of the pulse current, tool wear ratio increases. In figure 4.13 the TWR obtained high value at 8A and decrease at

10A. The reason for this can be justified due to the lower melting point of copper (1084 degrees) relative to the melting temperature of the workpiece , with increase of the pulse current due to increases flow density and create high-energy sparks, much more of the tool melts over the workpiece. And for the reason withe increases pulse current, the tool wear ratio increases than workpiece. This can be reasoned to increase in the input energy to the Cu tool that in turn causes corresponding increase in the tool melt.

4.8 Influence of Voltage (V) on the Tool Wear Ratio (TWR)

Figure 4.13 up to 4.16 and 4.9 up to 4.12 respectively portray the effect of the pulse current and pulse on-time at varying voltage. For each level of voltage, the TWR increases as the pulse current increases (Figure 4.15) and the TWR decreases as the pulse on time increases (Figure 4.9). It is worth noticing that interestingly a low voltage (150 V) offers higher TWR than a high voltage (250 V) does.

As found for MRR, TWR is also high for low voltage which can be attributed to multi-sparking phenomenon at low voltage. Based on the findings discussed in this sub-section, it can be said that to reduce Cu tool wear in EDM of AISI-D6 steel, low pulse current, and high pulse on-time may be employed.

4.9 Effect of the Pulse on Time (Ton) on the Surface Roughness (Ra)

Figure 4.17 up to 4.20 shown influence of surface roughness (The surface harshness is displayed by the 'average surface roughness (R_a)', which is measured in micron [µm]) on the pulse on time (The duration of time (µs) the current is allowed to flow per cycle) in two levels for voltage (150V, 250V) and four levels for pulse current (8, 10, 12, 14 Ampere). As the pulse on time increases the surface roughness increases as well. The maximum Ra is obtained when the pulse on time and voltage is 40 µs and 150V. In figure 4.28, it is observed that the surface roughness decreases as the voltage increases.

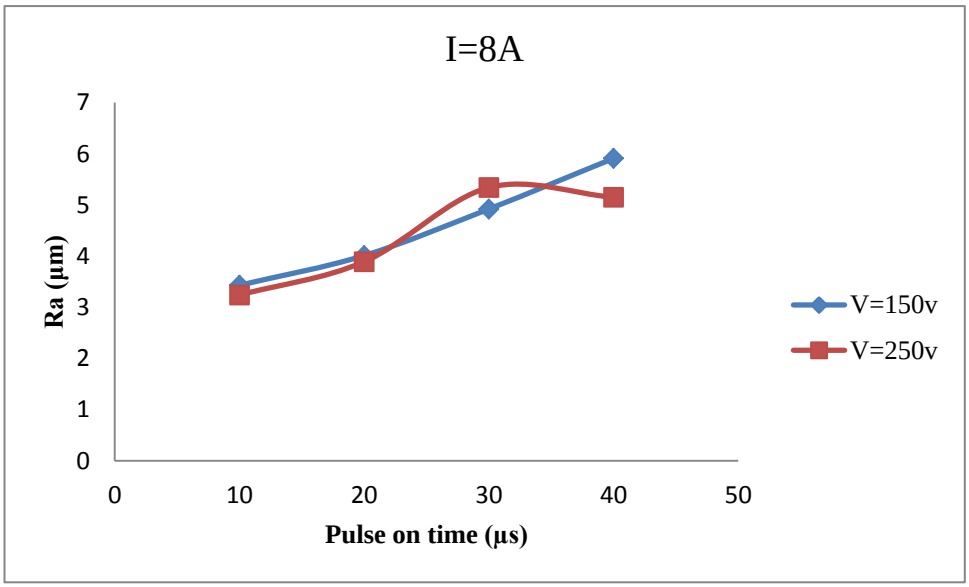

Figure 4.17: The influence of the pulse on time on R_a at varying voltage (I =8A).

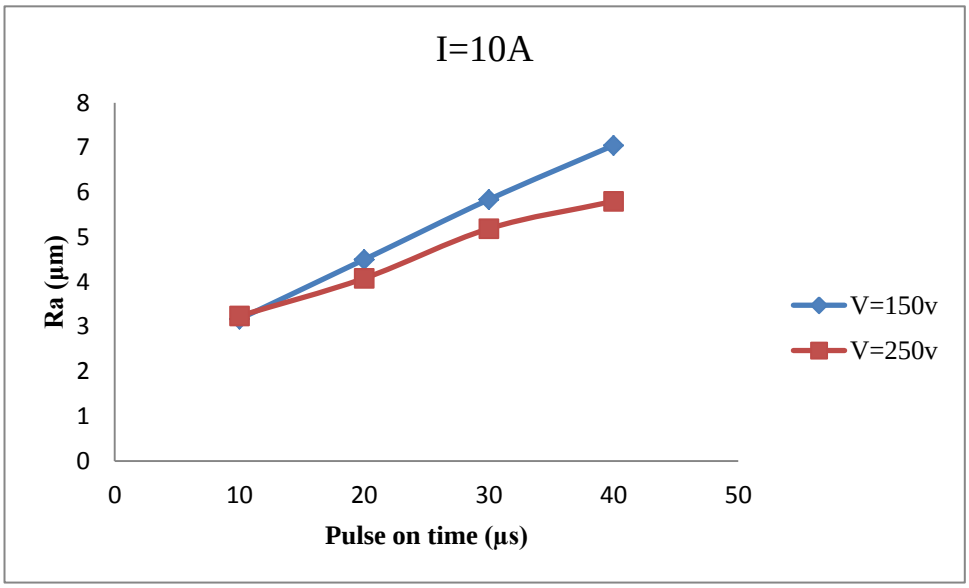

Figure 4.18: The influence of the pulse on time on R_a at varying voltage (I=10 A).

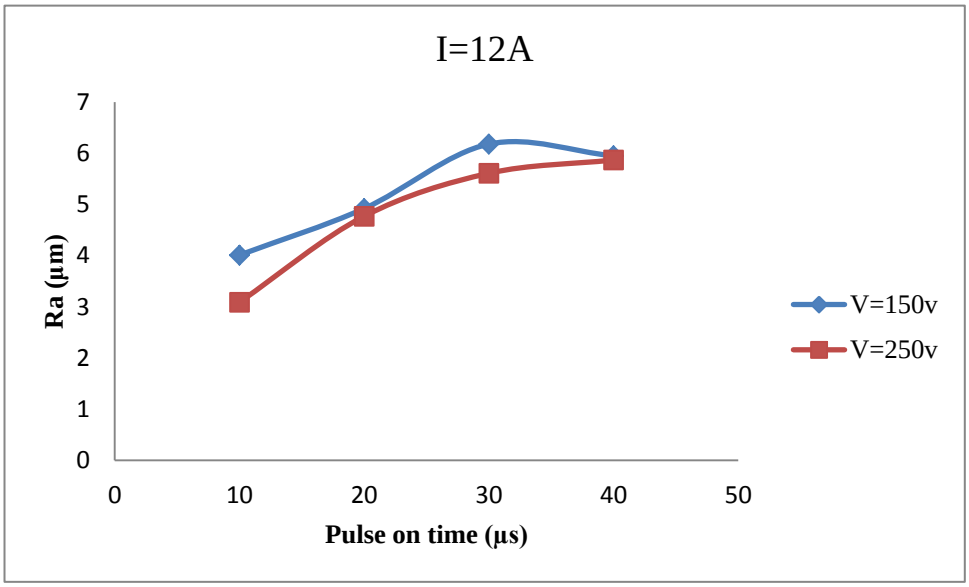

Figure 4.19: The influence of the pulse on time on surface roughness at varying voltage (I =12 A).

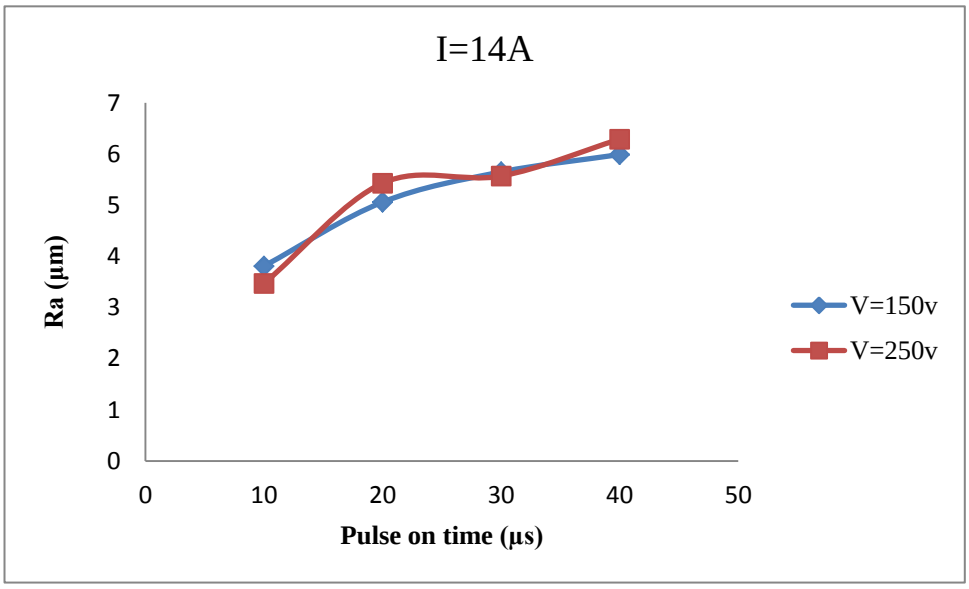

Figure 4.20: The influence of the pulse on time on surface roughness at varying voltage (I =14 A).

4.10 Influence of Pulse Current (I) on the Surface Roughness (Ra)

Figure 4.21 up to 4.22 shown influence of surface roughness (Ra) on the pulse current (I) in two levels for voltage (150v, 250v) and four levels for pulse on time (10, 20, 30, 40µs). The surface roughness increases as the result of pulse current increase. The minimum Ra is detected when the pulse current, voltage and pulse on time are 12A, 250V and 10 µs respectively.

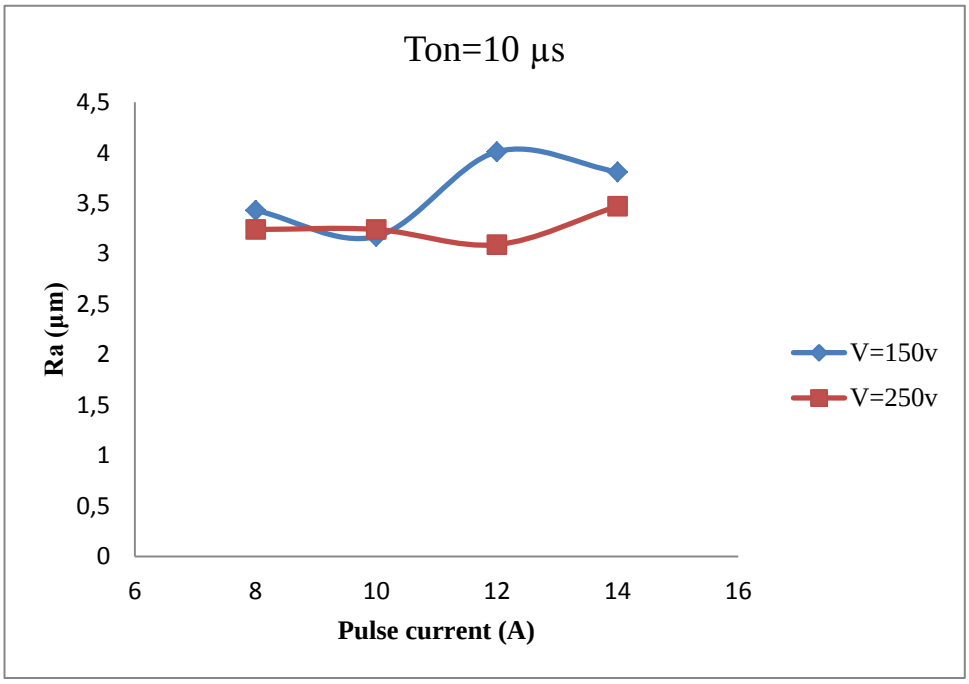

Figure 4.21: The influence of the pulse current on R_a at varying voltage (Ton =10 µs).

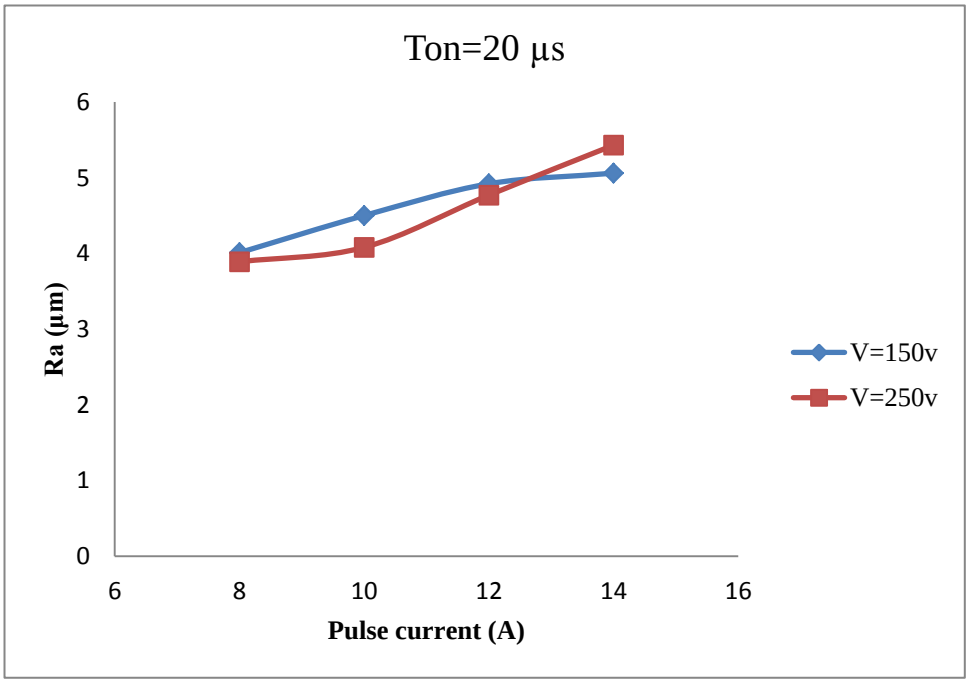

Figure 4.22: The influence of the pulse current on R_a at varying voltage (Ton =20 µs).

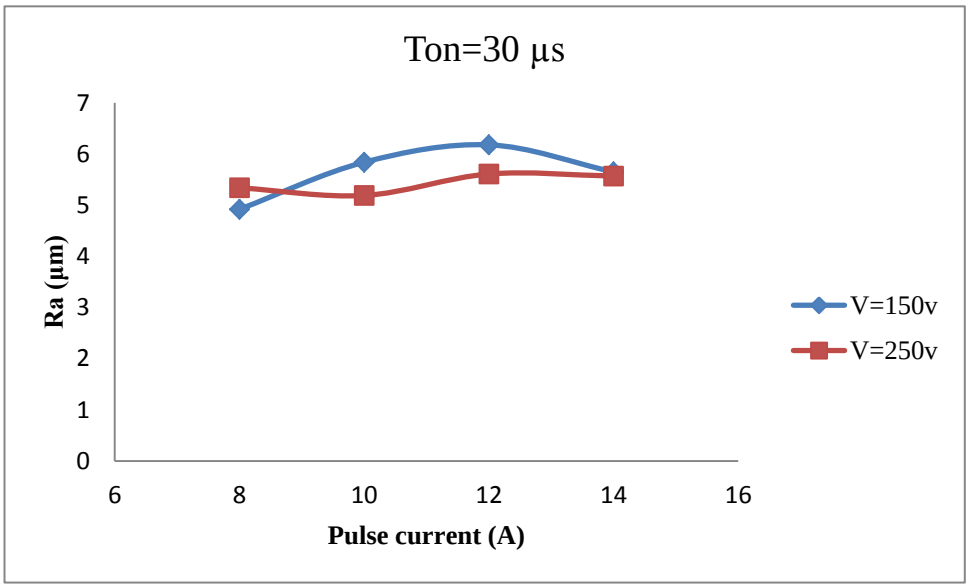

Figure 4.23: The influence of the pulse current on R_a at varying voltage (Ton =30 µs).

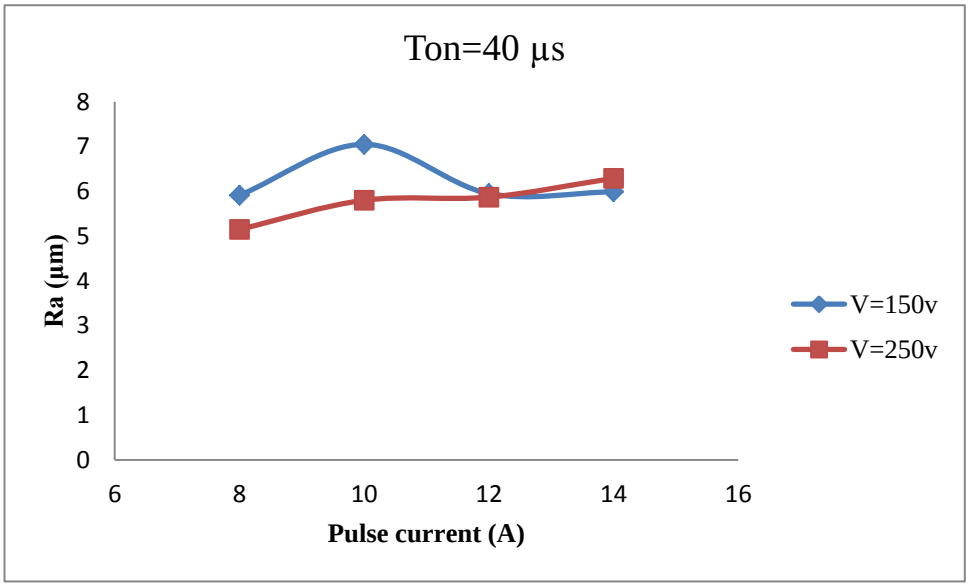

Figure 4.24: The influence of the pulse current on R_a at varying voltage (Ton =40 µs).

Figure 4.17 up to Figure 4.20 shows the influence of variation in the pulse on-time on the surface roughness at varying pulse current. It can be seen that, for the entire range of pulse current, the surface roughness increases as the pulse on-time increases. This is also evident from the curves that the surface quality deteriorates

not only when the pulse on-time is increased but also when the current is increased [174]. This is due to a fact that the ignition energy increases by increasing both of these parameters; as a result the radius of the plasma channel and the size of melt-hole increases and the surface quality deteriorates consequently [175]. From Figure 4.24, it very well may be seen that the surface roughness is low for high voltage, which can be reasoned to low sparking.

In summary, the effect of process parameters on the performance measures of EDM of AISI-D6 steel is opposing in nature.

It is more appropriate to set pulse current, pulse on-time to high values and voltage to low values if productivity is the prime objective through EDM of tool steel. However, contrarily, the pulse current and pulse on-time need to be set to high values and voltage must be kept low when TWR is the major objective. For obtaining good surface quality, low values of the pulse on-time and pulse current while large values of voltage should be opted. In view of obtained interactive effects on various outputs, it is proposed to choose intermediate settings of the parameters so as to attain a trade-off among all of the considered performance measures.

Next chapter represents the optimization methods used in EDM, with response surface method and gives some examples of optimization for EDM process parameters.

Chapter 5

OPTIMIZATION

5.1 Introduction

Response surface methodology is used to optimize the performance of the process in order to obtain the maximum benefit from the EDM. The software of Design Expert was performed to carry out the design of the experiments and develop resource models. The analysis of variance (ANOVA) was used to confirm the established equations. The experimental parameters align with their units and levels are collected in Table 5.1.

5.2 Theory of RSM and Full Factorial Design

5.2.1 Steps of RSM

RSM was invented by Box and Wilson in 1951, and it has been used to model and optimize the various processes [176]. The RSM has two main aims. The first one is optimizing the responses which are a function of various input parameters. The second one is predicting the mathematical relationships between the process parameters and the measured responses [177]. The RSM would include following steps for EDM process: Identifying the EDM effective parameters; Considering a reasonable limits of the identified parameters; Developing a desired experimental design; Performing the tests according to the developed experimental design; Measuring the responses; Establishing the mathematical models; Controlling the

model adequacy using analysis of variance (ANOVA), and exploring the influence of the parameters on responses and optimizing them. In Sections 5.2.2 and 5.2.3, the choosing of effective parameters and their limitations, and developing experimental designs and mathematical models will be discussed in details. The ANOVA, effect of parameters and optimizing will be explained in their related sections.

5.2.2 Choosing Parameters and Their Limitations

Various parameters could affect the considered responses, and it is almost difficult to recognize and control the small contributions from each one. Consequently, it is essential to choice those parameters with major effects and their limitations. For this purpose, one can act in two different ways.

In first way, screening designs could be carried out to determine which of the numerous experimental parameters and their interactions present more significant effects. In this regard, full or fractional two-level factorial designs may be used mainly because they are well organized [178,179]. In this way, a very large number of the experiments should be done which may be very time consuming and expensive. In second way, one can use the literature in the related field of study and use the obtained results to identify the effective parameters and their limitations.

5.2.3 Selecting the Experimental Design and Modeling

Modeling the simplest model that can be utilized in RSM is based on linear function. For its use, it is essential that the responses acquired be well fitted to the following relationship [179]:

$$Y = \beta o + \sum_{i=0}^{k} \beta i\, Xi + \varepsilon \qquad Eq(5.1)$$

Where k is the number of parameters, βo is the constant term, βi belongs to the coefficients of the linear parameters, Xi represents the parameters and ε is the residual related to the experiments. Thus, the responses would not present any curvature. To assess curvature, a second-order model should be applied. This type of model should contain both the first-order effects and the interaction between the different experimental parameters. In this regard, the following equation will be used [178,179]:

$$Y = \beta o + \sum_{i=0}^{k} \beta_i X_i + \sum_{1 \le i \le j}^{k} \beta_{ij} X_i X_j + \varepsilon \qquad \text{Eq (5.2)}$$

Where β_{ij} belongs to the coefficients of the interaction parameters.Furthermore, to define a critical point (maximum, minimum, or saddle), it is needed for the polynomial equation to cover quadratic terms as follows [179–182]:

$$Y = \beta o + \sum_{i=0}^{k} \beta_i X_i + \sum_{i=1}^{k} \beta_{ii} X_i^2 + \sum_{1 \le i \le j}^{k} \beta_{ij} X_i X_j + \varepsilon \qquad \text{Eq(5.3)}$$

Where β_{ii} stands for the coefficients of the quadratic parameter. Inaddition, the coefficients of the Eq. (5.3) can be computed using the Eqs. (5.4)–(5.7).

$$\beta_O = 0.142857(\sum Y) - 0.035714 \sum \sum (X_{ii}\, Y) \qquad \text{Eq (5.4)}$$

$$\beta_i = 0.041667\ (\sum X_i\, Y) \qquad \text{Eq (5.5)}$$

$$\beta_{ii} = 0.03125 \sum (X_{ii} Y) + 0.00372 \sum \sum (X_{ii}\, Y) - 0.035714\ (\sum Y) \qquad \text{Eq (5.6)}$$

$$\beta_{ij} = 0.0625 \sum (X_{ij} Y) \qquad \text{Eq (5.7)}$$

For evaluation the parameters in Eq. (5.3), different second order experimental design are available. In this regard, full or partial factorial design, Box–Behnken design, central composite design, and Doehlert design are frequently used [178,179]. These experimental designs differ from one another according to their selection of experimental points, number of levels for parameters, and number of runs. Due to application of the full factorial design in current study, it is explained in summary in this section. Full factorial design, as can realize from its name, covers all the possible conditions, and hence the number of experiments required for this type of design will very large. However, when the number of factors and their levels is not large, it will result in the most accurate models [178,179].

5.3 Materials and Methods

5.3.1 Design of Experiments

In this investigation, full factorial design including 32 runs, three EDM parameters including pulse on time (at four levels), pulse cur-rent (at four levels) and voltage (at two levels) was employed to design of experiments. The levels and actual values of EDM parameters are shown in Table 5.1. In addition, the evaluated and measured responses were the MRR and TWR. Moreover, Design-Expert Version 8.0 software was used for preparing the experimental design which is presented in Table 5.2.

Table 5.1: Coded and actual values of EDM parameters

Parameters	Symbol	Unit	Levels			
			1	2	3	4
Pulse on	*A*	μs	10	20	30	40
Pulse current	*B*	A	8	10	12	14
Input voltage	*C*	V	150	250	–	–

Table 5.2: Design layout including experimental and predicted values for MRR and TWR

No.	**Run**	**Coded values of parameters**			**Responses**			
		(*A*)	**(*B*)**	**(*C*)**	**MRR (mm^3/min)**		**TWR (%)**	
					Experimental	**Predicted**	**Experimental**	**Predicted**
1	16	10	8	150	6.044916	5.482303	20.49627	19.54081
2	23	20	8	150	8.696461	9.14349	12.22179	11.33076
3	24	30	8	150	17.05669	16.18345	1.71064	2.06891
4	8	40	8	150	17.77503	18.08385	0.805808	0.66908
5	15	10	10	150	7.911647	7.353789	14.96039	16.0065
6	18	20	10	150	11.34492	12.94661	12.98909	10.58851
7	20	30	10	150	22.64498	21.05618	2.215157	3.24059
8	6	40	10	150	24.34266	25.12277	1.295127	0.98047
9	31	10	12	150	11.10142	10.71295	17.90438	18.3588
10	7	20	12	150	16.91268	18.61025	16.25867	15.55784
11	17	30	12	150	30.0778	28.88321	3.753688	4.34659
12	32	40	12	150	32.78977	33.28974	2.435521	2.10934
13	10	10	14	150	13.11667	13.21345	17.32431	18.07385
14	26	20	14	150	23.10135	24.22426	16.0907	15.09925
15	22	30	14	150	35.64444	35.13187	5.199727	6.77201
16	27	40	14	150	44.64781	43.89593	4.264923	4.21877
17	29	10	8	250	6.712741	7.053654	14.24801	13.55991
18	25	20	8	250	11.02284	11.73944	6.914154	6.87793
19	9	30	8	250	15.80746	15.47627	1.411702	1.98571
20	13	40	8	250	16.53784	16.26753	0.775119	0.54813
21	30	10	10	250	7.576641	7.996519	9.954947	10.31685
22	11	20	10	250	14.66197	14.71329	4.279131	5.16263
23	2	30	10	250	19.60727	19.42621	1.484691	1.81238
24	5	40	10	250	21.47027	21.80084	0.779914	0.45266
25	21	10	12	250	9.611261	9.740073	12.07977	11.58621
26	12	20	12	250	19.1213	18.61017	6.939682	6.23762
27	4	30	12	250	26.23166	24.99409	2.29648	2.37309
28	3	40	12	250	29.1648	28.89020	1.554845	1.04123
29	28	10	14	250	12.20727	11.98709	12.04723	11.91908
30	19	20	14	250	21.89337	21.71730	7.520434	7.34001
31	1	30	14	250	29.43662	29.47398	2.790472	3.24317
32	14	40	14	250	32.86609	34.00657	2.047492	2.47659

5.3.2 EDM Process and Experimental Details

The experiments were carried out according to the design matrix (table 5.2 and table 5.3) on a spark system which is shown in Figure 5.1, and performed for 20 min to obtain more precise results. The AISI D6tool steels with 20 mm diameter and 20 mm thick were used as workpieces. Also, circular electrolytic copper with 18 mm diameter were utilized as electrodes. The workpieces before EDM, electrodes and final productions in this study are illustrated in Figure 5.2. The circular electrode is favored over the other shapes, because it results in higher MRR and lower EWR [183]. Commercial kerosene was used as the dielectric fluid and impulse jet flushing system was employed to remove the eroded materials from the sparking area. The work-pieces and electrodes materials were weighed before and after the EDM using a digital weighing scale of 0.001-g precision. The MRR and TWR amounts were calculated using the following equations 3.0 and 3.1. Also the surface roughness of the electrical discharge machined samples was measured using a Kosaka Surfcoder SE 1200.

Table 5.3**:** Design layout including experimental and predicted values for Ra.

Standard run no.	***Run***	***Coded values of parameters***			***Ra (µm)***		
		A	B	C	Experimental	Predicted	Error %
1	16	10	8	150	3.43	3.12	-9.04
2	23	20	8	150	4.01	4.39	9.48
3	24	30	8	150	4.92	5.33	8.33
4	8	40	8	150	5.91	5.95	0.68
5	15	10	10	150	3.17	3.47	9.46
6	18	20	10	150	4.5	4.7	4.44
7	20	30	10	150	5.84	5.61	-3.94
8	6	40	10	150	7.05	6.19	-12.2
9	31	10	12	150	4.01	3.7	-7.73
10	7	20	12	150	4.92	4.9	-0.41
11	17	30	12	150	6.18	5.77	-6.63
12	32	40	12	150	5.95	6.31	6.05
13	10	10	14	150	3.81	3.82	0.26
14	26	20	14	150	5.06	4.98	-1.58
15	22	30	14	150	5.65	5.82	3.01
16	27	40	14	150	5.99	6.33	5.68
17	29	10	8	250	3.24	3.11	4.01
18	25	20	8	250	3.89	4.01	3.08
19	9	30	8	250	5.34	4.89	-8.43
20	13	40	8	250	5.15	5.44	5.63
21	30	10	10	250	3.24	3.26	0.62
22	11	20	10	250	4.08	4.43	8.58
23	2	30	10	250	5.19	5.27	1.54
24	5	40	10	250	5.8	5.79	-0.17
25	21	10	12	250	3.09	3.3	-6.79
26	12	20	12	250	4.77	4.73	-0.84
27	4	30	12	250	5.61	5.53	-1.43
28	3	40	12	250	5.87	6.01	2.39
29	28	10	14	250	3.74	3.82	2.14
30	19	20	14	250	5.43	4.91	-9.58
31	1	30	14	250	5.57	5.68	1.97
32	14	40	14	250	6.29	6.12	-2.7

Figure5.1: The used spark system

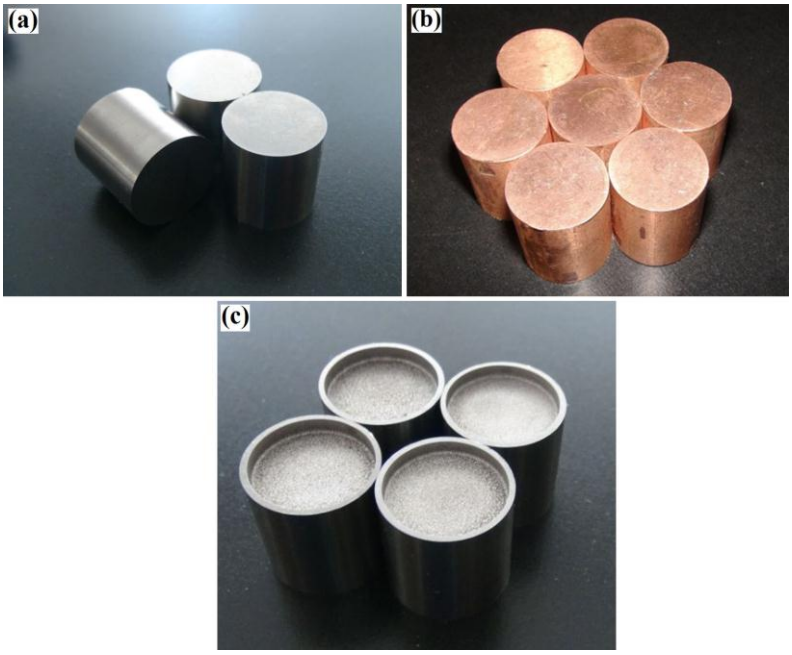

Figure 5.2: (a) The workpieces before EDM, (b) copper electrodes and (c) final productions.

5.3.3 Establishing Mathematical Model

A second order polynomial regression model with the main and interaction effects of the EDM parameters developed the mathematical relationships. If the measured responses (Y) i.e. MRR and TWR are a function of EDM parameters i.e. Pulse on

time (A), pulse current (B) and voltage (C), the response surface can be explored as Eq. (5.8):

Y= $f(A, B, C)$ Eq (5.8)

Considering the employed regression equation in this study (Eq.(5.3)), the selected polynomials for the three EDM parameters (A,B and C) will be presented as Eq. (5.9). Furthermore, the Design-Expert software at 95% confidence level was used to calculate the coefficients of the models. Moreover, the sufficiency of the models was confirmed using ANOVA, and models were presented using contour and 3D plots.

Y=$b_0 + b_1(A) + b_2(B) + b_3(C) + b_{11}(A^2) + b_{22}(B^2) + b_{33}(C^2) + b_{12}(AB) +$

$b_{13}(AC) + b_{23}(BC)$ Eq (5.9)

5.4 Results and discussion

5.4.1 Numerical Relationships and ANOVA Analysis for MRR and TWR and Ra

The FDS (fraction of design space) graph is illustrated in Figure 5.3.This graph is a line graph showing the relationship between the volume of the design space (area of interest) and amount of prediction error. The curve indicates what fraction (percentage) of the design space has a given prediction error or lower.

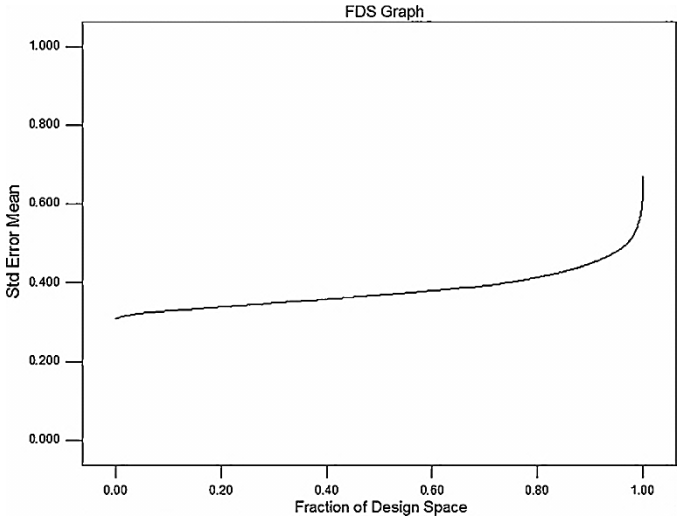

Figure 5.3: The FDS graph of the developed design matrix.

In general, a lower (approximately 1.0 or lower) and flatter FDS curve is better, and lower is more important than flatter. Moreover, the Std Err (standard error) of design graph is depicted in Figure 5.4. This graph is a contour (Figure 5.4a) or 3D (Figure 5.4b) plot showing the standard error of prediction for areas in the design space.

By default, these values are reflective of the design only, not of the response data. Generally, it is better this graph to have relatively low standard error across the region of interest. Low is approximately 1.0 or lower.

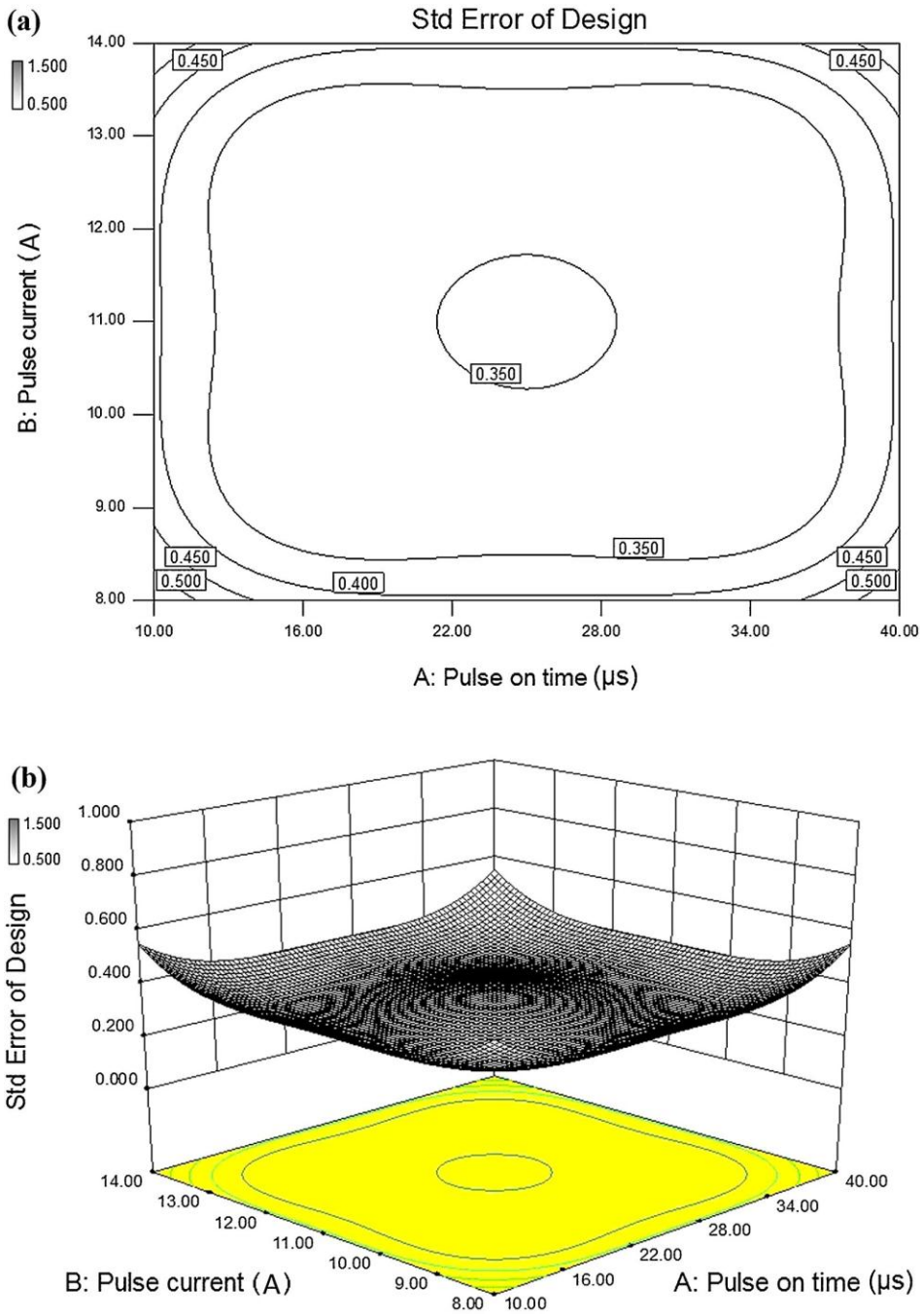

Figure 5.4: The Std Err of design graph: (a) contour plot, and (b) 3D plot.

The numerical relationships between the EDM parameters and the responses MRR and TWR and R_a have been obtained as follows:

$$\text{MRR } (mm^3/min) = 20.12 + 9.98A + 7.22B - 0.91C + 3.75AB - 1.38AC - 1.23BC - 2.07A^2 + 0.56B^2 \quad \text{Eq (5.10)}$$

$$\text{TWR } (\%) = 5.71 - 7.08A + 0.78B - 1.96C + 0.89AB + 1.56\,AC - 0.42BC - 2.03A^2 + 1.03B^2 \quad \text{Eq (5.11)}$$

$$Ra(\mu m) = 5.17 + 1.28A + 0.35B - 0.13C - 0.083AB - 0.049AC + 0.076BC - 0.37A^2 - 0.13B^2 \quad \text{Eq(5.12)}$$

Eqs. (5.10) - (5.12) predict the MRR, TWR and R_a for the EDM of the AISI D6 tool steels. The normal plot of residuals, the predicted versus actual response plot, the residuals versus the predicted response plot, and the residuals versus the experimental run plot are respectively illustrated in Figures 5.5–5.8, for MRR, TWR and R_a. The normal probability plot indicates whether the residuals follow anormal distribution, in which case the points will follow a straight line. Figures 5.5 demonstrate that errors are extended normally because the residuals follow a straight line. Figures 5.6 reveals that the predicted responses values are in good agreement with the actual ones within the ranges of the EDM process parameters, because the data points are split evenly by the 45◦line. Figures 5.7, 5.8 reveal that numerical models predict the responses adequately due to randomly scattered residuals.

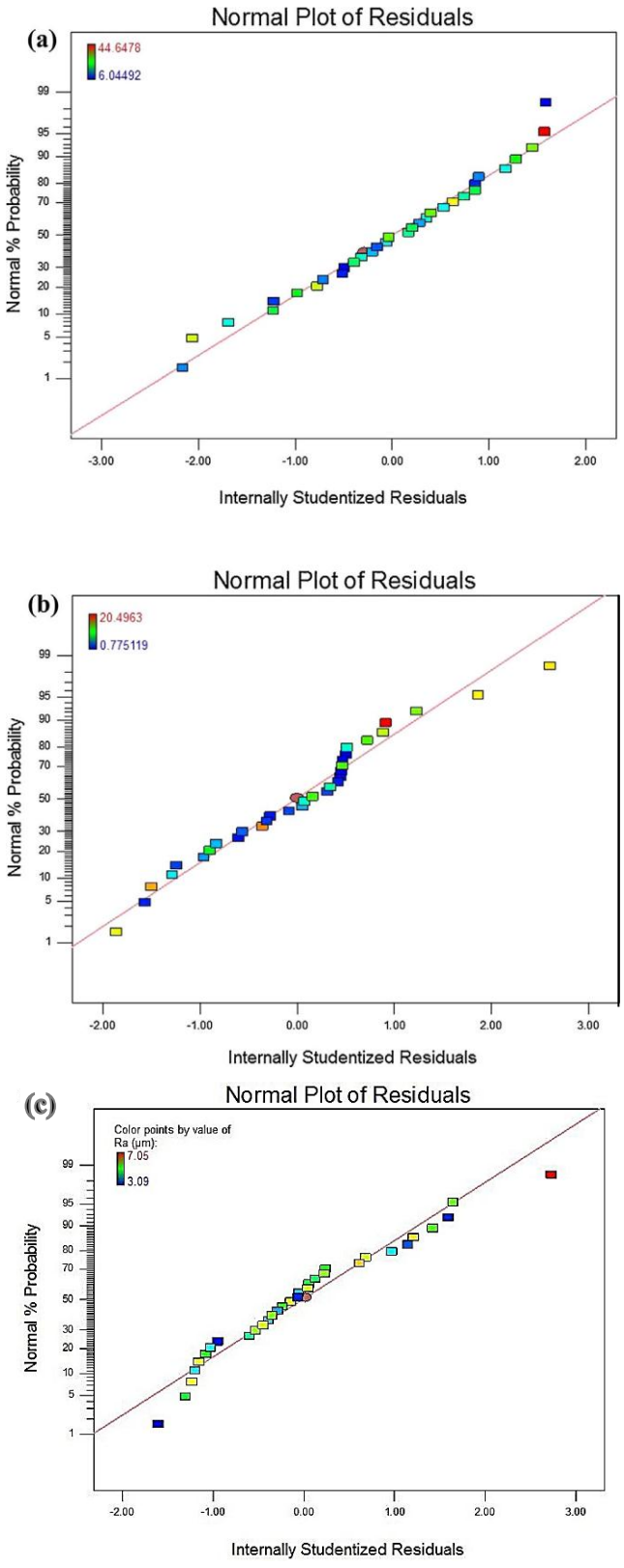

Figure 5.5: Normal probability plot of residuals for: (a) MRR, and (b) TWR, and (c) R_a

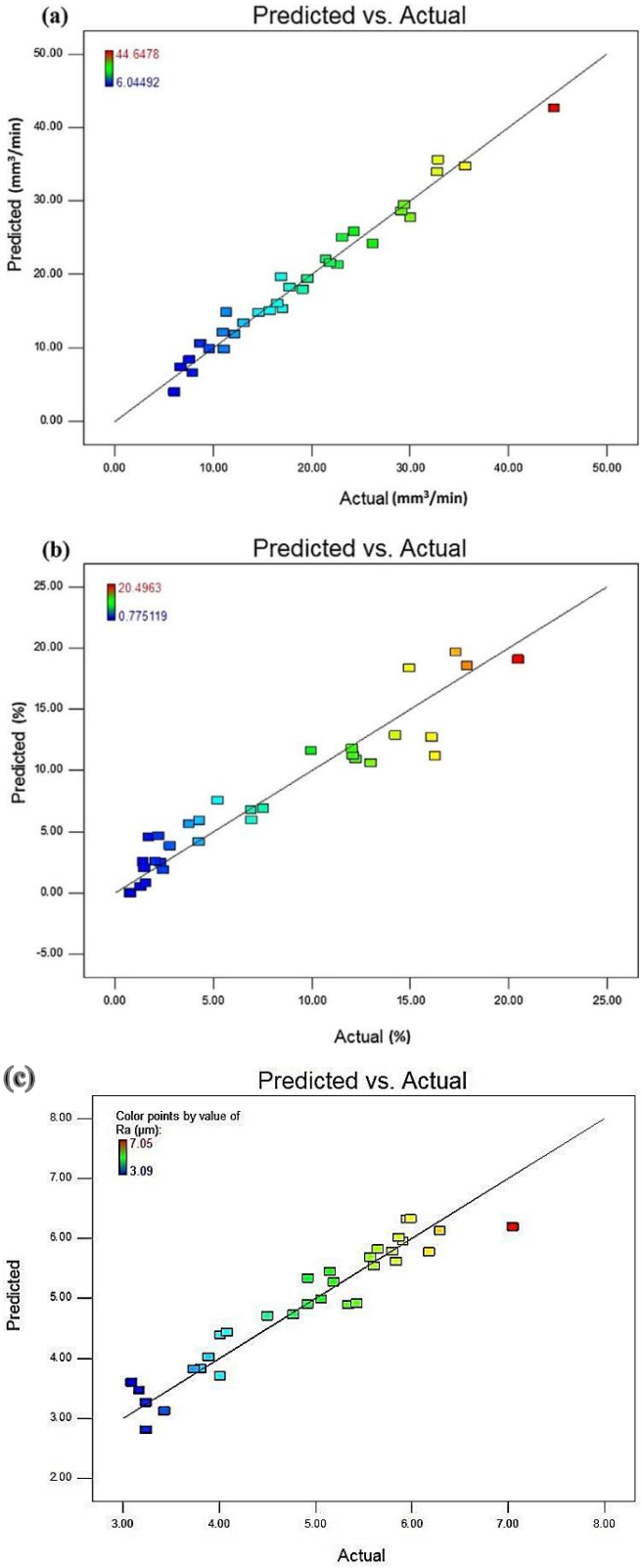

Figure 5.6: Predicted versus actual response plot for: (a) MRR, and (b) TWR, and (c) R_a

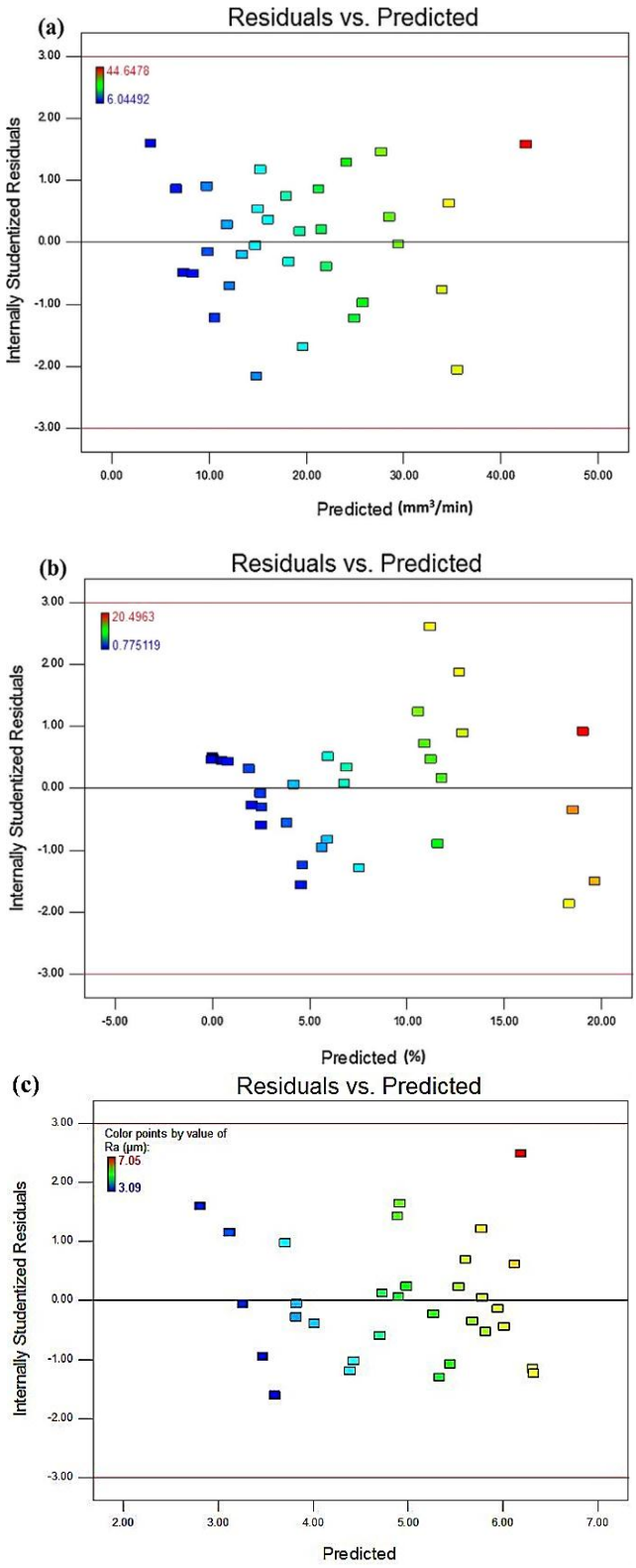

Figure 5.7: Residuals versus the predicted response plot for: (a) MRR, and (b) TWR, and (c) R_a

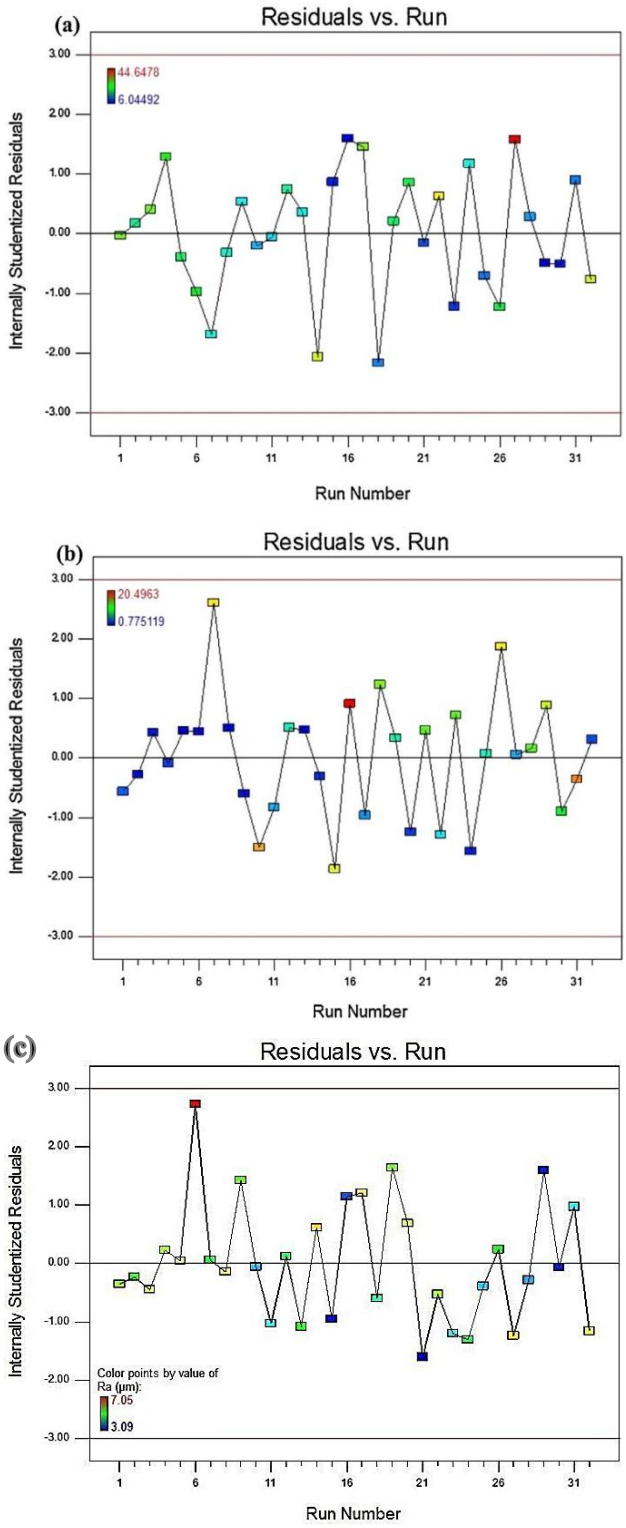

Figure 5.8: Residuals versus the experimental run plot for: (a) MRR, and (b) TWR, and (c) R_a

The ANOVA for the responses MRR, TWR and R_a are summarized in Tables 5.4, 5.5 and 5.7. The F-value, P-value, R2 and adjusted R2 are employed for identifying the more significant model and coefficients. Larger F-value, $R^2$and adjusted R^2, and smaller P-value show that the model or a coefficient is significant. According to Tables 5.4 and 5.5, the F-value, P-value, R^2 and adjusted R^2 for the predicted MRR and TWR models are 112.43,<0.0001, 0.9751, 0.9664, and 31.11, <0.0001, 0.9154, 0.8860, respectively. Thus, it can be concluded that the models predict adequately.

Table 5.4: ANOVA table for response MRR.

Source	Sum of Squares	Degree of freedom	Mean Square	F-Value	P-Value	
Model	2780.97	8	347.6213	112.4285	<0.0001	**significant**
A	1598.247	1	1598.247	516.9091	<0.0001	
B	927.5096	1	927.5096	299.9775	<0.0001	
C	26.79089	1	26.79089	8.664779	0.0073	
AB	138.877	1	138.877	44.91594	<0.0001	
AC	33.61138	1	33.61138	10.87068	0.0032	
BC	26.95237	1	26.95237	8.717005	0.0071	
A^2	26.98366	1	26.98366	8.727123	0.0071	
B^2	1.998282	1	1.998282	0.646289	0.4297	
C^2	0	0	-	-	-	
Residual	71.1144	23	3.091931			
R^2	0.9751					
Adjusted R^2	0.9664					

Table 5.5: ANOVA table for response TWR

Source	Sum of Squares	Degree of freedom	Mean Square	F-Value	P-Value	
Model	1111.677	8	138.9596	31.11112	<0.0001	**significant**
A	890.7618	1	890.7618	199.4292	<0.0001	
B	10.69672	1	10.69672	2.394846	0.1354	
C	123.2534	1	123.2534	27.59471	<0.0001	
AB	7.816224	1	7.816224	1.749944	0.1989	
AC	43.20697	1	43.20697	9.673441	0.0049	
BC	3.104142	1	3.104142	0.694974	0.4131	
A^2	26.09636	1	26.09636	5.842612	0.024	
B^2	6.74114	1	6.74114	1.509248	0.2317	
C^2	0	0		31.11112		
Residual	102.7308	23	4.466557	199.4292		
R^2	0.9154			2.394846		
Adjusted R^2	0.8860		138.9596	27.59471		

As well, P-values <0.05 reveal that the coefficients are significant and P-values >0.1 mean that the coefficients are not significant. Thus, according to the P-values, A, B, C, AB, AC, BC and A2 are significant terms for predicted MRR model. Similarly, A, C, AC and A2 are significant terms for TWR model. After reduction of the models by considering only the significant terms, the following mathematical relationships are obtained:

MRR (mm3 /min) = 20.43 + 9.98A + 7.22B - 0.91C + 3.75AB

$$- 1.38AC - 1.23BC - 2.07A^2 \qquad \text{Eq (5.13)}$$

$$TWR (\%) = 6.28 - 7.08A - 1.96C + 1.56AC - 2.03A^2 \qquad \text{Eq (5.14)}$$

Furthermore, the F-values demonstrate that the order of the more significant terms in MRR and TWR models are as follows, correspondingly:

$$A > B > AB > AC > A^2 > BC > C,\ A > C > AC > A^2.$$

According to the table 5.6, the F-value, P-value, R^2 and adjusted R^2 for the predicted Ra model are 30.82, <0.0001, 0.9147, 0.8850. Therefore, the predicted models are adequate and significant. Additionally, P-values < 0.05 verify that the coefficients are significant and P-values > 0.1 mean that the coefficients are not significant. Thus, according to the P-values, A, B, and A^2 are significant terms for predicted Ra model. After reduction of the models by considering only the significant terms, the following mathematical models are achieved:

$$Ra(\mu m) = 5.10 + 1.28A + 0.35B - 0.37A^2 \qquad \text{Eq (5.15)}$$

Furthermore, the F-values prove that the order of the more significant terms in Ra is as follows:

$A>B>A^2>$.

Table 5.6: ANOVA table for response Ra.

Source	Sum of Squares	Degree of freedom	Mean Square	F-Value	P-Value	
Model	33.13811	8	4.142264	30.82063	< 0.0001	**significant**
A	29.30944	1	29.30944	218.0777	< 0.0001	
B	2.13444	1	2.13444	15.88136	0.0006	
C	0.525313	1	0.525313	3.908603	0.0601	
AB	0.067344	1	0.067344	0.501079	0.4861	
AC	0.04225	1	0.04225	0.314362	0.5804	
BC	0.10201	1	0.10201	0.759008	0.3926	
A^2	0.851512	1	0.851512	6.335704	0.0193	
B^2	0.1058	1	0.1058	0.787208	0.3841	
C^2	0	0				
Residual	3.091178	23	0.134399			
R^2	0.9147					
Adjusted R^2	0.8850					

5.4.2 Effect of EDM Parameters on MRR

The perturbation plot for MMR is illustrated in Figure 5.9. Also, Figure 5.10 a–f show the contour and 3D surface plots. These plots illustrate the interaction effect of any two EDM parameters on the MMR when the other parameter is on its level zero (center level). Figures5. 9 and 5.10a–f reveal that increase in pulse on time and pulse cur-rent, and decrease in input voltage all cause to higher amounts of MMR. The

correlation between the three main parameters affecting the EDM discharge energy (W) can be stated as follow [184]:

$$W = \int_0^{T_{on}} U(T_i) I(T_i) dT_i \quad \text{Eq (5.16)}$$

Where U, I and T_i stand for the input voltage (V), the peak current (A) and the pulse on time (μs), respectively. In fact, increasing the pulse on time increases the machining time and consequently the workpiece surface temperature; thus, the volume of melt holes and the MRR increase. Also, increasing the pulse current, based on the increased current density, cause to faster dielectric fluid ionization, and hence higher MRR. Based on Eq. (5.14), by increasing the input voltage, the material removal rate must have increased. However, according to Figures 5.9 and 5.10a–f, the MRR decrease as the input voltage increases. Increasing the input voltage to an appropriate level can increase MRR, but at low input voltage, the plasma channels generated on compact work piece surface, that is more compact, cause the multi sparking phenomenon. Therefore, this speed up the machining process and increases the MRR at lower voltages.

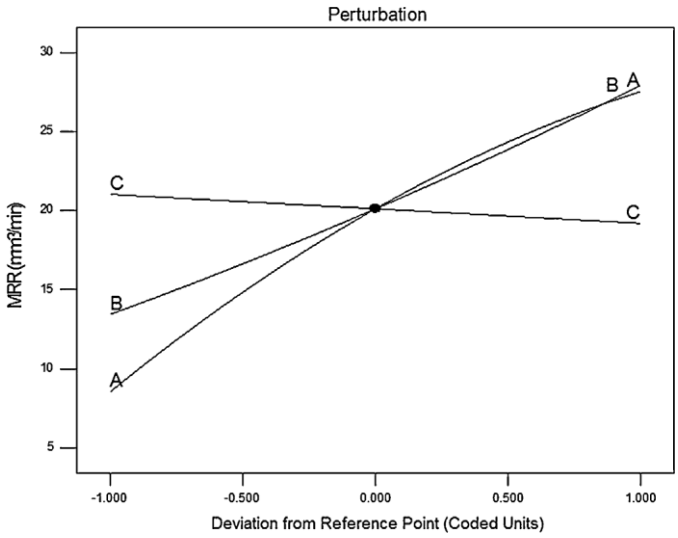

Figure 5.9: Perturbation plot illustrating the influence of EDM parameters on the MRR

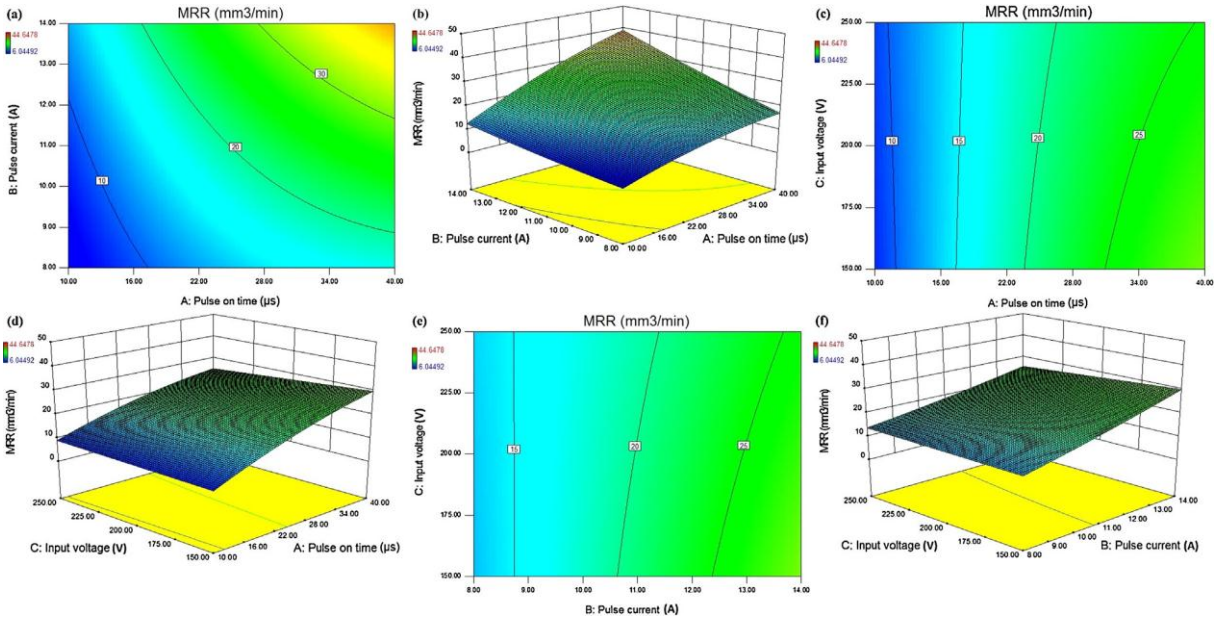

Figure 5.10: Contour and 3D plots for the response MRR.

5.4.3 Effect of EDM Process Parameters on TWR

The perturbation, counter and 3D surface plots for the TWR are shown in Figures 5.11 and 5.12a–f. According to Figures 5.11 and 5.12a–f, three main results can be achieved. First, lower values of pulse on time cause to higher TWR, continuously. In EDM process with positive polarity when the pulse on-time is lesser, the material removal dominant mechanism for the movement of electrons from the cathode (work piece) to the positive pole (tool) causes high tool wear ratio. However, increasing the pulse on-time, due to the expansion of the plasma channel radius, the movement of positive ions from tool side (positive polarity) toward work piece (cathode) is more comfortable and material removal dominant mechanism become positive ions collide. This causes a reduction in TWR while increases the pulse on-time [185]. Second, with increasing the pulse current, the TWR increases. Due to lower melting temperature of copper tool (1084◦C) than the melting temperature of steel work piece, an increase in pulse current and W, the surface of tool melts relative to the work piece. Therefore, by increasing the pulse current, the tool wear ratio increases. Third, the values of TWR decrease with increase of input voltage. This is due to the compression of the plasma channel, which is associated with lower voltage. In this case, multi-sparking phenomenon increases the speed of machining. In fact, due to caused ignition energy between tool and work piece, tool wear ratio increases.

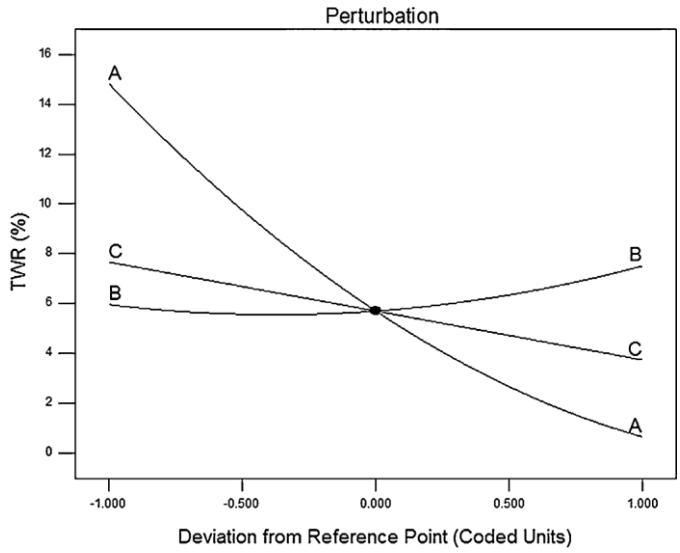

Figure 5.11: Perturbation plot illustrating the influence of EDM parameters on the TWR.

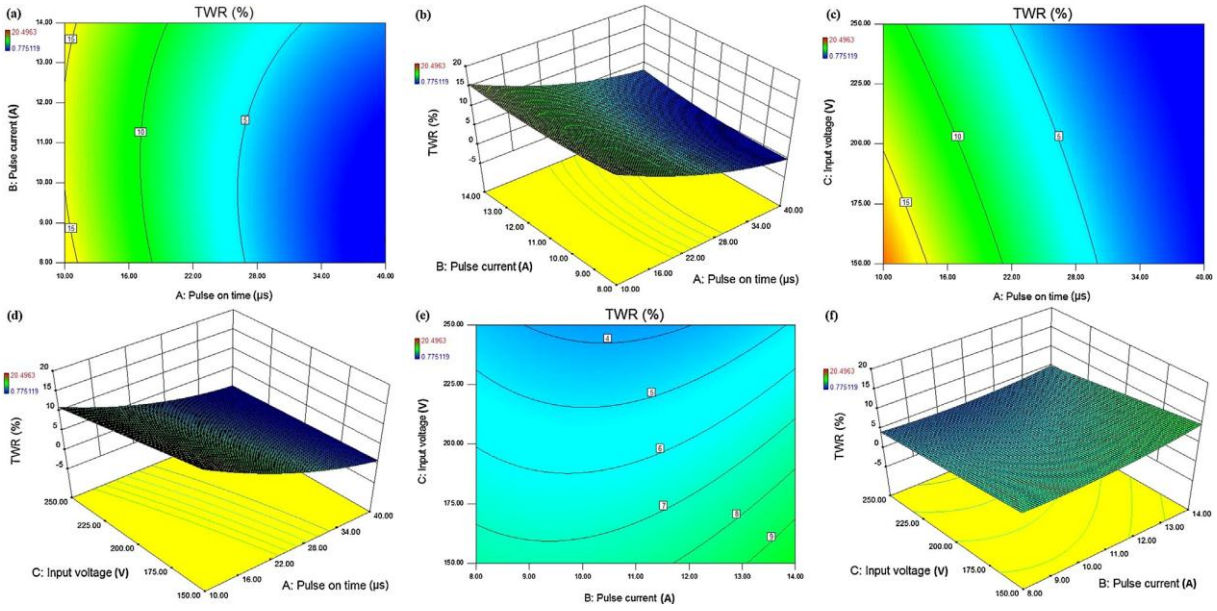

Figure 5.12: Contour and 3D plots for the response TWR.

5.4.4 Effect of EDM Parameters on Ra

The perturbation plot for Ra is presented in Figure 5.13. Also, Figures 5.14a-f show the contour and 3D surface plots. These plots illustrate the interaction effect of any two EDM parameters on the Ra when the other parameter is on its level zero (center level). Figures 5.13 and 5.14a-f reveal that increase in pulse on time and pulse current, and decrease in input voltage all cause to higher amounts of Ra. On the surface of the electrical discharge machined materials there are a lot of microscopic craters which are due to random spark discharge between the electrodes. The most effective parameter on the size of these craters is the energy of the discharge. The higher energetic pulses result in higher material removal, and hence a deeper cavity produces. The deeper the cavity depths, the higher the roughness. The correlation between the three main parameters affecting the EDM discharge energy (W) can be stated as follow equation (5.16).

In fact, increasing the pulse on time increases the machining time and consequently the workpiece surface temperature; thus, the volume of melt holes increase. Also, with increasing the pulse current, based on the increased current density, cause to faster dielectric fluid ionization, and hence higher material removal and bigger craters on the surfaces.

Based on equation 5.16, by increasing the input voltage the discharge energy rate must have increased, and hence the Ra should be increased, too. But, according to Figures 5.13 and 5.14a-f, the Ra decreases as the input voltage increases. Increasing the input voltage to an appropriate level can increase material removal rate, but at

low input voltage, the plasma channels generated on compact work piece surface that is more compact cause the multi sparking phenomenon. Therefore, this speeds up the machining process and increases the material removal rate at lower voltages, which cause to formation of the bigger craters on the machined surfaces.

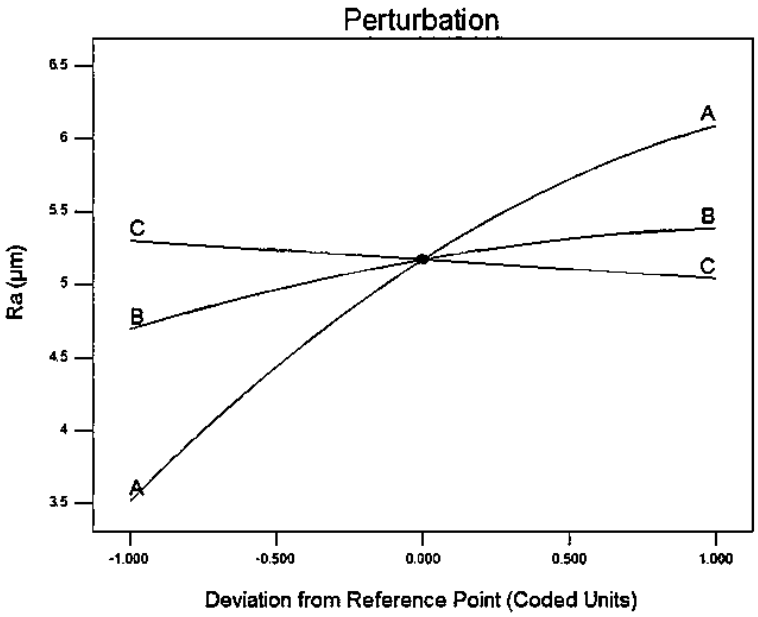

Figure 5.13: Perturbation plot illustrating the influence of EDM parameters on the Ra.

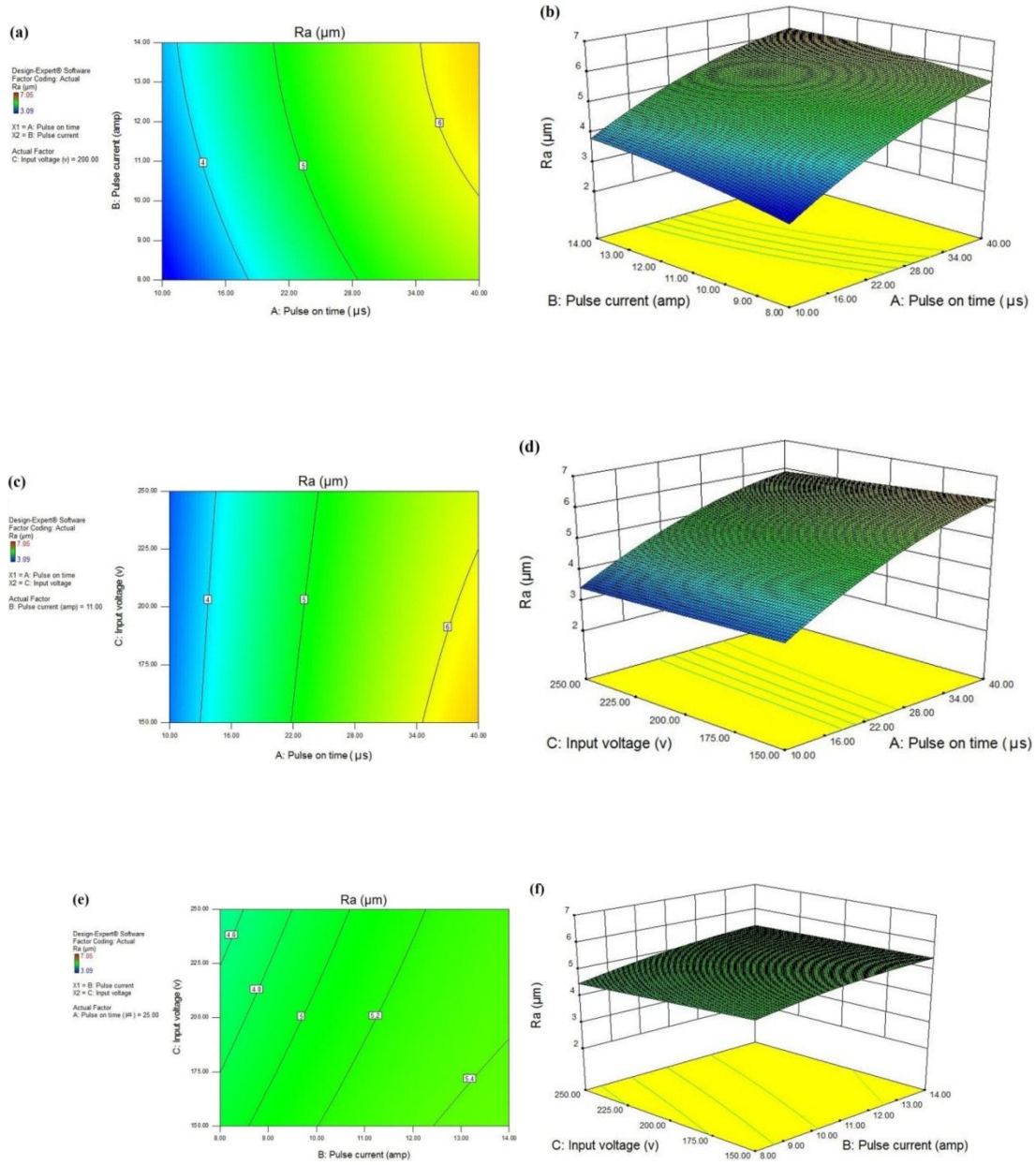

Figure 5.14: Contour and 3D plots for the response Ra

Figure 5.15 up to 5.17 respectively shown experimental and predicted values for material removal rate (MRR), tool wear ratio (TWR) and surface roughness (Ra).

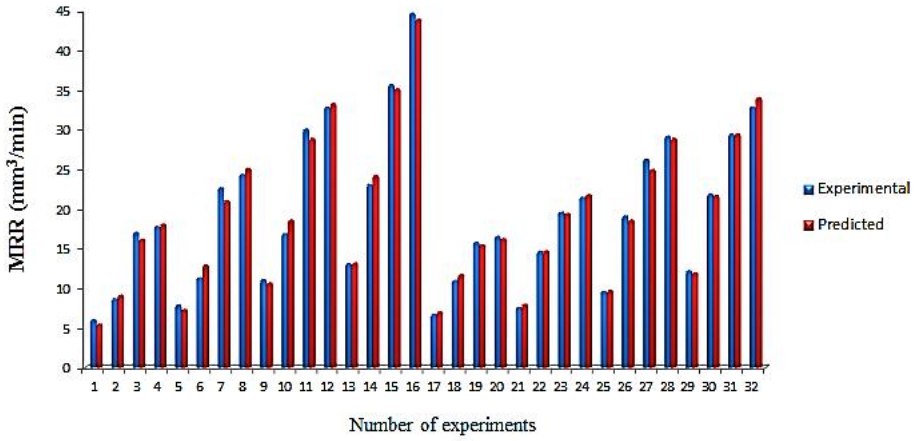

Figure 5.15: Experimental and predicted values for MRR

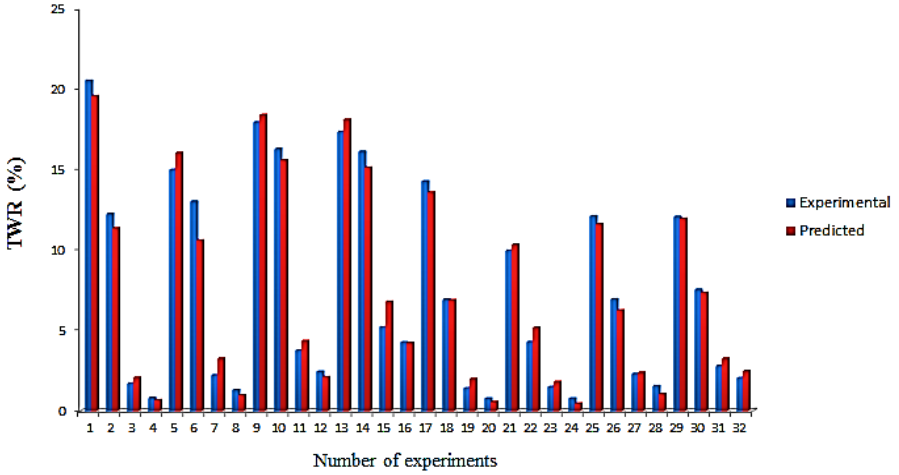

Figure 5.16: Experimental and predicted values for TWR

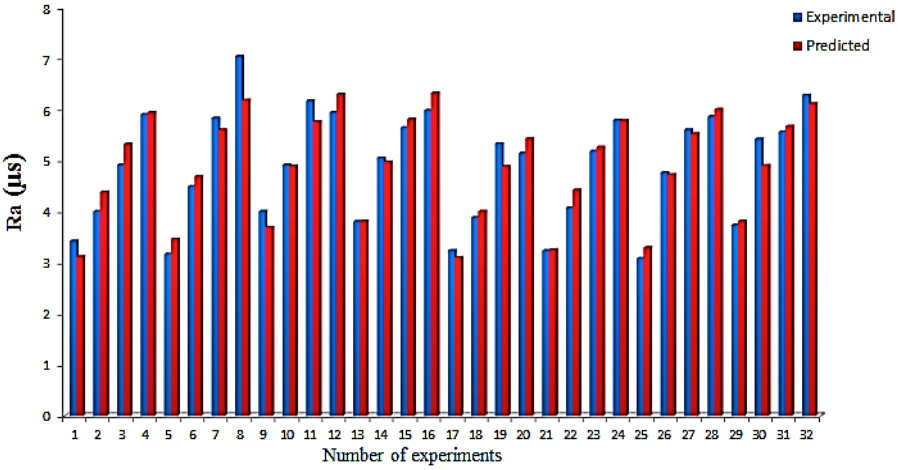

Figure 5.17: Experimental and predicted values for Ra

5.4.5 Optimization of EDM Parameters

In this study, a multiple response method called desirability was used for optimization of EDM parameters. This method employs an objective function, called the desirability function, and transforms (by desirability function) an estimated response into a scale-free amounts called desirability. The desirability varies between 0 and1. An amount of 1 signifies the ideal case, where 0 represents that the response is outside its acceptable limits. Combined desirability is the weighted statistical mean of the individual desirability for the all responses. The parameters settings with highest total desirability are regarded to be the best possible parameter conditions. The optimization process has been conducted using the Design Expert Software in which the MRR, TWR and R_a optimized concurrently using the established models (Eqs. (5.13), (5.14) and (5.15)). In multi response optimization, a calculation of how the solution satisfies the combined objectives for the responses should be assured. The optimality solution is to calculate the process parameters for maximizing the MRR and minimizing the TWR illustrated in Figures 5.18 and 5.19.

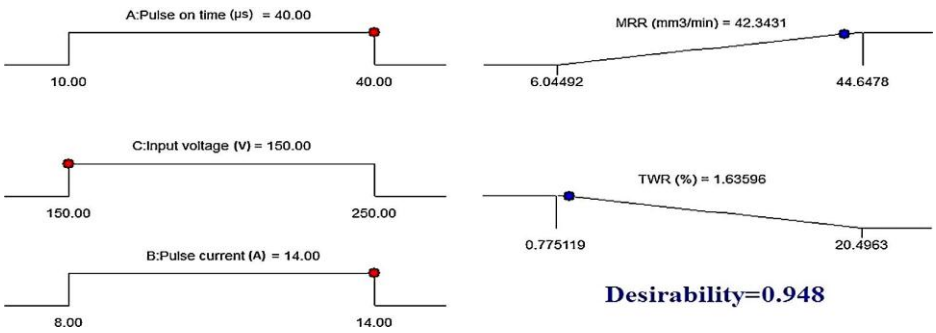

Figure 5.18: Ramps graphs showing the optimality solution

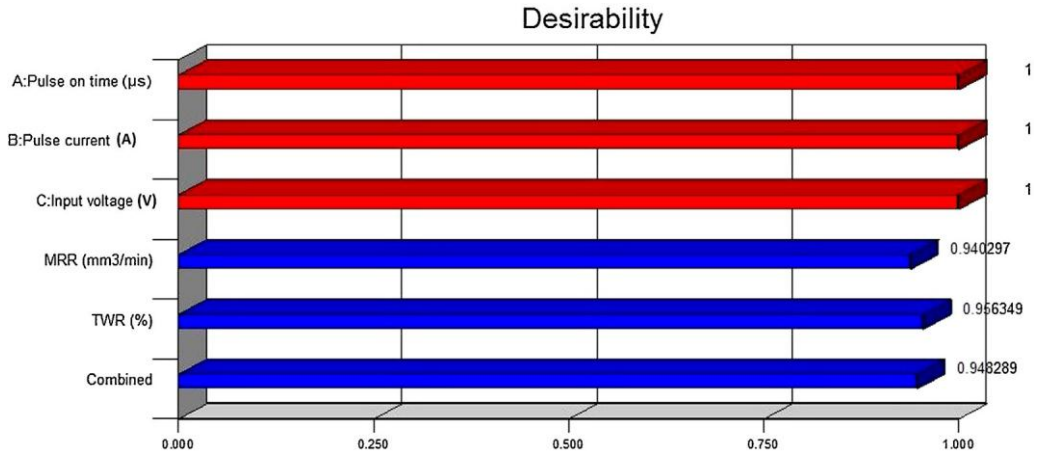

Figure 5.19: Bar graph showing the maximum desirability of 0.948 for the combined objective.

Also the optimality solution to calculate the process parameters for minimizing the Ra is illustrated in Figures 5.20 and 5.21.

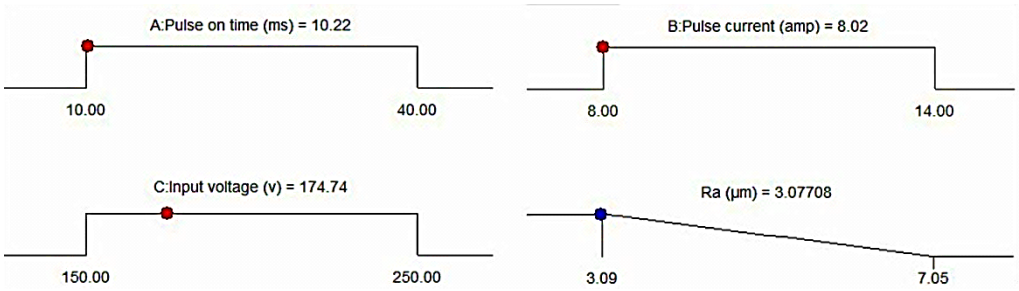

Figure 5.20: Ramps graphs showing the optimality solution.

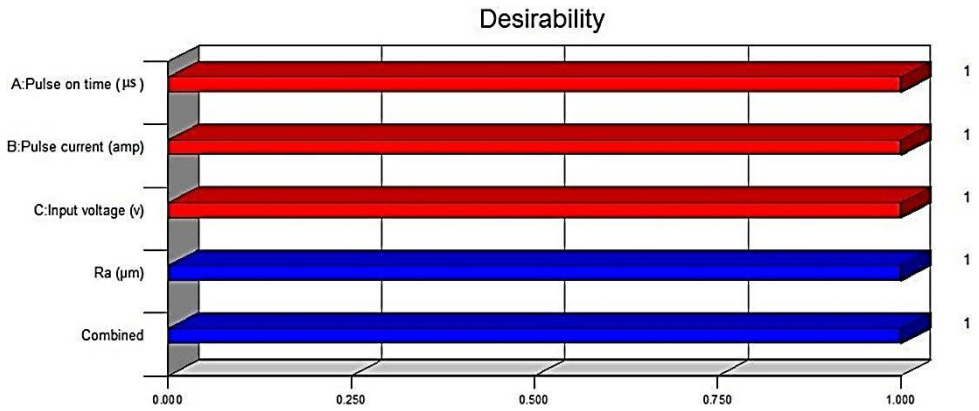

Figure 5.21: Bar graph showing the maximum desirability of 1 for the combined objective.

Table 5.7**:** Constraint of input parameters, and optimum value for parameters and MRR, TWR

Parameter or response	**Goal**	**Optimum value**
Pulse on time	**In range**	**40 µs**
Pulse current	**In range**	**14 A**
Input voltage	**In range**	**150 V**
MMR	**Maximize**	**42.34 mm^3/min**
TWR	**Minimize**	**1.63%**

The amounts of constraints, optimum amounts of EDM parameters and the predicted amounts of MRR, TWR and R_a are summarized in Table 5.7 and table 5.8.

Table 5.8: Constraint of input parameters, and optimum values for parameters and Ra.

Parameter or response	**Goal**	**Optimum value**
Pulse on time	in range	10.43 µs
Pulse current	in range	8.05 A
Input voltage	in range	242.8 V
Ra	minimize	2.9 µm

The pulse on time recognized as the most impressive factor on affecting of the Ra. Moreover the Ra decreased due to decreasing of the pulse current and pulse on time and also increasing of the input voltage. In order to get minimum amount of Ra (3.07µm), the optimized values for pulse current, pulse on time and input voltage were respectively 8.02 A, 10.22 µs and 174.74 V.

Chapter 6

CONCLUSION

6.1 Introduction

In this chapter the main outcomes of this research study that mainly includes the machining characteristics of EDM is summarized. Furthermore, it gives an overview of the results of prediction and modeling of the material removal rate, tool wear ratio and surface roughness. Finally as a result of findings, some recommendations have been proposed briefly for the future studies.

6.2 Conclusion

In the current study, the effect of some controlling parameters on the performance measures in the EDM of AISI-D6 steel was investigated. Based on the results of the experimental work conducted, the following conclusions were drawn:

i. The material removal rate increased as the pulse current and pulse on-time increased and contrarily decreased as the voltage, especially when the pulse current is above 30 A, increased.

ii. The tool wear ratio increased as the pulse current increased and decreased when the voltage increased, and contrary to increase in the material removal rate decreased as the pulse on-time increased.

iii. The surface quality in terms of roughness improved as the pulse current and pulse on-time are decreased and improved as the voltage is increased.

iv. The trends presented in this study were expected to act as guideline for the users to set the parameters to achieve the desired objective. Furthermore, from the above findings, the effect of input parameters on various performance measures of the process are opposing in nature. Therefore, to acquire a trade-off among all of the considered measures, the parameters should be set to intermediate values of the settings employed in this work.

v. The results showed that the EDM parameters of AISI D6 tool steel achieved in this study. Furthermore the numerical models developed and utilized to predict and optimize the TWR, Ra and MMR. Also, the result of ANOVA analysis proved that these numerical models could be applied for prediction of TWR, Ra and MMR. Moreover due to increasing of the pulse on time over EDM process, the TWR decreased while the MMR was increased.

vi. In addition, the increasing of pulse current resulted in increasing of both MMR and TWR, on the other hand the increase of input voltage caused decreasing of MMR and TWR. Furthermore, over EDM of AISI D6 tool steels the highest value of 42.34 mm^3/min for MMR and lowest value of 1.63% for TWR predicted by developed models. Finally the optimized pulse on time of 40μ, optimized pulse current of 14A and optimized input voltage

of 150V acquired for maximum amount of MMR and minimum amount of TWR.

vii. The pulse on time recognized as the most impressive factor on affecting of the Ra. Moreover the Ra decreased due to decreasing of the pulse current and pulse on time and also increasing of the input voltage. In order to get minimum amount of Ra (3.07μm), the optimized values for pulse current, pulse on time and input voltage were respectively 8.02 A, 10.22 μs and 174.74 V.

6.3 Future Recommendation

- The variation in parameters may affect the microstructure of the work-piece. Therefore, there is a need of microscopic studies to clarify this point; however, it is left for future.
- The mathematical model can be developed for different work piece and electrode materials for EDM processes.
- Responses like roundness, circularity, cylindricity, machining cost etc .are to be considered in further research.
- The standard optimization procedure can be developed and the optimal results are to be validated

REFERENCES

[1] Kumar, A., Maheshwari, S., Sharma, C., & Beri, N. (2010). Research developments in additives mixed electrical discharge machining (AEDM): a state of art review. *Materials and Manufacturing processes*, 25(10), 1166-1180.

[2] Abbas, N. M., Solomon, D. G., & Bahari, M. F. (2007). A review on current research trends in electrical discharge machining (EDM). *International Journal of machine tools and Manufacture*, 47(7-8), 1214-1228.

[3] Kumar, S., Batish, A., Singh, R., & Bhattacharya, A. (2017). Effect of cryogenically treated copper-tungsten electrode on tool wear rate during electro-discharge machining of Ti-5Al-2.5 Sn alloy. Wear, 386, 223-229.

[4] Huang, S. F., Liu, Y., Li, J., Hu, H. X., & Sun, L. Y. (2014). Electrochemical discharge machining micro-hole in stainless steel with tool electrode high-speed rotating. *Materials and Manufacturing Processes*, *29*(5), 634-637.

[5] Adrian, I., Eugen, A., & Florin, N. (2010). A study about micro-drilling by electrical discharge method of an Al/Sic hybrid composite. *International journal of academic research*, *2*(3).

[6] Batish, A., Bhattacharya, A., Singla, V. K., & Singh, G. (2012). Study of material transfer mechanism in die steels using powder mixed electric discharge machining. *Materials and Manufacturing Processes*, *27*(4), 449-456.

[7] Sidhu, S. S., Batish, A., & Kumar, S. (2014). Study of surface properties in particulate-reinforced metal matrix composites (MMCs) using powder-mixed electrical discharge machining (EDM). *Materials and Manufacturing Processes*, *29*(1), 46-52.

[8] Yeh, C. C., Wu, K. L., Lee, J. W., & Yan, B. H. (2014). Processing Characteristics Using Phosphorous Dielectric on Wire Electrical Discharge Machining of Polycrystalline Silicon. *Materials and Manufacturing Processes*, 29(2), 146-152.

[9] Radhika, N., Sudhamshu, A. R., & Chandran, G. K. (2014). Optimization of electrical discharge machining parameters of Aluminium hybrid composites using Taguchi method. *Journal of Engineering Science and Technology*, *9*(4), 502-512.

[10] Gangil, M., Pradhan, M. K., & Purohit, R. (2017). Review on modelling and optimization of electrical discharge machining process using modern Techniques. *Materials Today: Proceedings*, *4*(2), 2048-2057.

[11] Rengasamy, N. V., Rajkumar, M., & Kumaran, S. S. (2016). An analysis of mechanical properties and optimization of EDM process parameters of Al 4032 alloy reinforced with Zrb2 and Tib2 in-situ composites. *Journal of Alloys and Compounds*, *662*, 325-338.

[12] Moghaddam, M. A., & Kolahan, F. (2015). An optimised back propagation neural network approach and simulated annealing algorithm towards optimisation of EDM process parameters. *International Journal of Manufacturing Research*, *10*(3), 215-236.

[13] Gopalakannan, S., & Senthilvelan, T. (2014). Optimization of machining parameters for EDM operations based on central composite design and desirability approach. *Journal of Mechanical Science and Technology*, *28*(3), 1045-1053.

[14] Kumar, S., Singh, R., Singh, T. P., & Sethi, B. L. (2009). Surface modification by electrical discharge machining: A review. *Journal of Materials Processing Technology*, *209*(8), 3675-3687.

[15] Jameson, E. C. (2001). *Electrical discharge machining*. Society of Manufacturing Engineers.

[16] Izquierdo, B., Plaza, S., Sánchez, J. A., Pombo, I., & Ortega, N. (2012). Numerical prediction of heat affected layer in the EDM of aeronautical alloys. *Applied Surface Science*, *259*, 780-790.

[17] Jahan, M. P. (Ed.). (2014). *Electrical Discharge Machining (EDM): Types, Technologies and Applications*. Nova Science Publishers, Incorporated.

[18] Descoeudres, A. (2006). Characterization of electrical discharge machining plasmas.

[19] Schumacher, B. M. (2004). After 60 years of EDM the discharge process remains still disputed. *Journal of Materials Processing Technology*, *149*(1-3), 376-381.

[20] Rajurkar, K. P., Levy, G., Malshe, A., Sundaram, M. M., McGeough, J., Hu, X., ... & DeSilva, A. (2006). Micro and nano machining by electro-physical and chemical processes. *CIRP Annals-Manufacturing Technology*, *55*(2), 643-666.

[21] Amorim, F. L., Weingaertner, W. L., & Bassani, I. A. (2010). Aspects on the optimization of die-sinking EDM of tungsten carbide-cobalt. *Journal of the Brazilian Society of Mechanical Sciences and Engineering*, *32*(SPE), 496-502.

[22] Chakraborty, S., Dey, V., & Ghosh, S. K. (2015). A review on the use of dielectric fluids and their effects in electrical discharge machining characteristics. *Precision Engineering*, *40*, 1-6.

[23] Puri, A. B., & Bhattacharyya, B. (2003). An analysis and optimisation of the geometrical inaccuracy due to wire lag phenomenon in WEDM. *International journal of Machine tools and manufacture*, *43*(2), 151-159.

[24] Singh, S., & Bhardwaj, A. (2011). Review to EDM by using water and powder-mixed dielectric fluid. *Journal of Minerals and Materials Characterization and Engineering*, *10*(02), 199.

[25] Mandaloi, G., Singh, S., Kumar, P., & Pal, K. (2016). Effect on crystalline structure of AISI M2 steel using tungsten–thorium electrode through MRR, EWR, and surface finish. *Measurement*, *90*, 74-84.

[26] Yan, M. T., & Lai, Y. P. (2007). Surface quality improvement of wire-EDM using a fine-finish power supply. *International journal of machine tools and manufacture*, *47*(11), 1686-1694.

[27] Goswami, A., & Kumar, J. (2014). Optimization in wire-cut EDM of Nimonic-80A using Taguchi's approach and utility concept. *Engineering Science and Technology, an International Journal*, *17*(4), 236-246.

[28] Pallav, K., Han, P., Ramkumar, J., & Ehmann, K. F. (2014). Comparative assessment of the laser induced plasma micromachining and the micro-EDM processes. *Journal of Manufacturing Science and Engineering*, *136*(1), 011001.

[29] Banu, A., & Ali, M. Y. (2016). Electrical discharge machining (EDM): a review. *Int J Engineering Materials Manufacture*, *1*(1), 3-10.

[30] Dewangan, S. K. (2010). experimental investigation of machining parameters for EDM using U-shaped electrode of AISI P20 tool steel. *Department of Mechanical Engineering, National Institute of Technology Rourkela (India)*.

[31] Tsai, Y. Y., & Masuzawa, T. (2004). An index to evaluate the wear resistance of the electrode in micro-EDM. *Journal of Materials Processing Technology*, *149*(1-3), 304-309.

[32] Klocke, F., Lung, D., Antonoglou, G., & Thomaidis, D. (2004). The effects of powder suspended dielectrics on the thermal influenced zone by electrodischarge machining with small discharge energies. *Journal of materials processing technology*, *149*(1-3), 191-197.

[33] Jahan, M. P., Wong, Y. S., & Rahman, M. (2009). A study on the fine-finish die-sinking micro-EDM of tungsten carbide using different electrode materials. *Journal of materials processing technology*, *209*(8), 3956-3967.

[34] Puertas, I., Luis, C. J., & Alvarez, L. (2004). Analysis of the influence of EDM parameters on surface quality, MRR and EW of WC–Co. *Journal of Materials Processing Technology*, *153*, 1026-1032.

[35] Kucukturk, G., & Cogun, C. (2010). A new method for machining of electrically nonconductive workpieces using electric discharge machining technique. *Machining Science and Technology*, *14*(2), 189-207.

[36] Smith, C., & Koshy, P. (2013). Applications of acoustic mapping in electrical discharge machining. *CIRP Annals-Manufacturing Technology*, *62*(1), 171-174.

[37] Goodlet, A., & Koshy, P. (2015). Real-time evaluation of gap flushing in electrical discharge machining. *CIRP Annals*, *64*(1), 241-244.

[38] Shabgard, M., Oliaei, S. N. B., Seyedzavvar, M., & Najadebrahimi, A. (2011). Experimental investigation and 3D finite element prediction of the white layer thickness, heat affected zone, and surface roughness in EDM process. *Journal of mechanical science and technology*, *25*(12), 3173-3183.

[39] Yildiz, Y. (2016). Prediction of white layer thickness and material removal rate in electrical discharge machining by thermal analyses. *Journal of Manufacturing Processes*, *23*, 47-53.

[40] Zhang, G., Guo, J., Ming, W., Huang, Y., Shao, X., & Zhang, Z. (2014). Study of the machining process of nano-electrical discharge machining based on combined atomistic-continuum modeling method. *Applied Surface Science*, *290*, 359-367.

[41] Sabouni, H. R., & Daneshmand, S. (2012). Investigation of the parameters of EDM process performed on smart NiTi alloy using graphite tools. *Life Science Journal*, *9*(4), 504-510.

[42] Zhao, Y., Kunieda, M., & Abe, K. (2013). Experimental investigations into EDM behaviors of single crystal silicon carbide. *Procedia CIRP*, *6*, 135-139.

[43] Zhang, M., Zhang, Q., Zhu, G., Liu, Q., & Zhang, J. (2016). Effects of some process parameters on the impulse force in single pulsed EDM. *Procedia CIRP*, *42*, 627-631.

[44] Klocke, F., Garzón, M., Dieckmann, J., & Klink, A. (2011). Process force analysis on sinking-EDM electrodes for the precision manufacturing. *Production Engineering*, *5*(2), 183-190.

[45] Zhang, Y., Liu, Y., Shen, Y., Ji, R., Li, Z., & Zheng, C. (2014). Investigation on the influence of the dielectrics on the material removal characteristics of EDM. *Journal of Materials Processing Technology*, *214*(5), 1052-1061.

[46] Li, J., Zhang, Y., & Yu, Z. (2011, April). Influence of reaction force on the electrode in micro hole drilling by micro EDM. In *Consumer Electronics, Communications and Networks (CECNet), 2011 International Conference on* (pp. 414-417). IEEE.

[47] Klocke, F., Garzon, M., & Klink, A. (2010). Effects of process parameters on single discharge forces measured during sinking-EDM. In *Proceedings of the 16th International Symposium on Electromachining.*

[48] Saravanan, M., Kumar, A. V., Kannan, V. N., & Thangaiah, I. S. (2017). Optimization of process parameters during wire electrical discharge machining of Ti Gr 2 for improving corner accuracy. *Materials Today: Proceedings*, *4*(2), 2105-2113.

[49] Rajagopal, S. P., Ganesh, V., Lanjewar, A. V., & Sankar, M. R. (2013). Past and current status of hybrid electric discharge machining (H-EDM) processes. *Advanced Materials Manufacturing & Characterization*, *3*(1), 111-118.

[50] Nayak, S. K., Patro, J. K., Dewangan, S., & Gangopadhyay, S. (2014). Multi-objective optimization of machining parameters during dry turning of AISI 304 austenitic stainless steel using grey relational analysis. *Procedia Materials Science*, *6*, 701-708.

[51] Sevvel, P., & Jaiganesh, V. (2014). Characterization of mechanical properties and microstructural analysis of friction stir welded AZ31B Mg alloy thorough optimized process parameters. *Procedia Engineering*, *97*, 741-751.

[52] Sevvel, P., Stephan Thangaiah, I. S., Mars Mukesh, S., & Mohammed Anif, G. (2015). Laboratory Scale Testing of Thermoelectric Regenerative Braking System. *International Journal of Vehicle Structures & Systems (IJVSS)*, *7*(4).

[53] Sevvel, P., & Jaiganesh, V. (2015). Effect of tool shoulder diameter to plate thickness ratio on mechanical properties and nugget zone characteristics during FSW of dissimilar Mg alloys. *Transactions of the Indian Institute of Metals*, *68*(1), 41-46.

[54] Manpreet Singh, Amandeep Singh Bansal, Sanjeev Kumar. (2014). Effect of different wire electrodes on the MRR of MS workpiece using WEDM Process. *International Journal of Mechanical Engineering and Technology*, pp.180–188.

[55] Jaiganesh, V., & Sevvel, P. (2015). Effect of Process Parameters on the Microstructural Characteristics and Mechanical Properties of AZ80A Mg Alloy During Friction Stir Welding. *Transactions of the Indian Institute of Metals*, *68*(1), 99-104.

[56] Ramesh, N. N., Harinarayana, K., & Naik, B. B. (2014). Machining Characteristics of HSS & Titanium Using Electro Discharge Sawing and Wire–Electrodischarge Machining. *Procedia materials science*, *6*, 1253-1259.

[57] Sevvel, P., & Jaiganesh, V. (2015). Influence of tool profile during FSW of Mg alloy using optimized parameters. *Int. J. of App. Eng. Research*, *10*, 159-164.

[58] Anand, G., Satyanarayana, S., & Hussain, M. M. (2017). Optimization of Process Parameters in EDM with Magnetic Field Using Grey Relational Analysis with Taguchi Technique. *Materials Today: Proceedings*, *4*(8), 7723-7730.

[59] Gangil, M., & Pradhan, M. K. (2017). Optimization the machining parameters by using VIKOR Method during EDM process of Titanium alloy.

[60] Selvarajan, L., Mouri, P., & Raja, R. R. (2018). Experimental Investigation of EDM Parameters on Machining Si 3 N 4-TiN Conductive Ceramic Composite

Using Hallow Tube Electrode for Improving Geometrical Accuracy. *Materials Today: Proceedings*, *5*(2), 8080-8088.

[61] Saha, N., Chakraborty, S., Dey, P. P., & Das, P. K. (2014). Machining of ZrB2-SiC Composites by Wire-EDM Technique. *Transactions of the Indian Ceramic Society*, *73*(2), 94-97.

[62] Muttamara, A., Fukuzawa, Y., Mohri, N., & Tani, T. (2009). Effect of electrode material on electrical discharge machining of alumina. *Journal of materials processing technology*, *209*(5), 2545-2552.

[63] Gaikwad, V., & Jatti, V. S. (2016). Optimization of material removal rate during electrical discharge machining of cryo-treated NiTi alloys using Taguchi's method. *Journal of King Saud University-Engineering Sciences.*

[64] Prihandana, G. S., Mahardika, M., Hamdi, M., & Mitsui, K. (2011). Effect of low-frequency vibration on workpiece in EDM processes. *Journal of mechanical science and technology*, *25*(5), 1231.

[65] Manjaiah, M., Narendranath, S., Basavarajappa, S., & Gaitonde, V. N. (2015). Effect of electrode material in wire electro discharge machining characteristics of Ti50Ni50− xCux shape memory alloy. *Precision Engineering*, *41*, 68-77.

[66] Rajmohan, T., Prabhu, R., Rao, G. S., & Palanikumar, K. (2012). Optimization of machining parameters in electrical discharge machining (EDM) of 304 stainless steel. *Procedia engineering*, *38*, 1030-1036.

[67] Dwivedi, A. P., & Choudhury, S. K. (2016). Increasing the Performance of EDM Process Using Tool Rotation Methodology for Machining AISI D3 Steel. *Procedia CIRP*, *46*, 131-134.

[68] Muthuramalingam, T., & Mohan, B. (2015). A review on influence of electrical process parameters in EDM process. *Archives of civil and mechanical engineering*, *15*(1), 87-94.

[69] Torres, A., Puertas, I., & Luis, C. J. (2015). Modelling of surface finish, electrode wear and material removal rate in electrical discharge machining of hard-to-machine alloys. *Precision Engineering*, *40*, 33-45.

[70] Dhakar, K., & Dvivedi, A. (2017). Experimental Investigation on Near-dry EDM using Glycerin-Air Mixture as Dielectric Medium. *Materials Today: Proceedings*, *4*(4), 5344-5350.

[71] Ubale, S. B., & Deshmukh, S. D. (2018). Experimental Investigation and Modelling of Wire Electrical Discharge Machining Process on W-Cu Metal Matrix Composite. *Materials Today: Proceedings*, *5*(1), 84-90.

[72] [72] Lin, M. Y., Tsao, C. C., Hsu, C. Y., Chiou, A. H., Huang, P. C., & Lin, Y. C. (2013). Optimization of micro milling electrical discharge machining of Inconel 718 by Grey-Taguchi method. *Transactions of Nonferrous Metals Society of China*, *23*(3), 661-666.

[73] Chandramouli, S., & Eswaraiah, K. (2018). Experimental investigation of EDM process parameters in machining of 17-4 PH Steel using taguchi method. *Materials Today: Proceedings*, *5*(2), 5058-5067.

[74] Kumar, A., & Maheshwari, S. (2015). Optimization of Submerged Arc Welding Rutile Based Flux constituents by Hybrid Grey, Fuzzy and Taguchi Analysis. *Advanced Materials Manufacturing & Characterization*, *5*(2), 63-70.

[75] Siddiquee, A. N., Khan, Z. A., Goel, P., Kumar, M., Agarwal, G., & Khan, N. Z. (2014). Optimization of deep drilling process parameters of AISI 321 steel using Taguchi method. *Procedia materials science*, *6*, 1217-1225.

[76] Rao, P. S., Ramji, K., & Satyanarayana, B. (2014). Experimental investigation and optimization of wire EDM parameters for surface roughness, MRR and white layer in machining of aluminium alloy. *Procedia Materials Science*, *5*, 2197-2206.

[77] Assarzadeh, S., & Ghoreishi, M. (2013). Statistical modeling and optimization of process parameters in electro-discharge machining of cobalt-bonded tungsten carbide composite (WC/6% Co). *Procedia Cirp*, *6*, 463-468.

[78] Choudhary, R., & Singh, G. (2018). Effects of process parameters on the performance of electrical discharge machining of AISI M42 high speed tool steel alloy. *Materials Today: Proceedings*, *5*(2), 6313-6320.

[79] Izwan, N. S. L. B., Feng, Z., Patel, J. B., & Hung, W. N. (2016). Prediction of Material Removal Rate in Die-Sinking Electrical Discharge Machining. *Procedia Manufacturing*, *5*, 658-668.

[80] Goswami, A., & Kumar, J. (2014). Investigation of surface integrity, material removal rate and wire wear ratio for WEDM of Nimonic 80A alloy using GRA and Taguchi method. *Engineering Science and Technology, an International Journal*, *17*(4), 173-184.

[81] Pramanik, A., Basak, A. K., Islam, M. N., & Littlefair, G. (2015). Electrical discharge machining of 6061 aluminium alloy. *Transactions of Nonferrous Metals Society of China*, *25*(9), 2866-2874.

[82] Dave, H. K., Mathai, V. J., Desai, K. P., & Raval, H. K. (2015). Studies on quality of microholes generated on Al 1100 using micro-electro-discharge

machining process. *The International Journal of Advanced Manufacturing Technology*, *76*(1-4), 127-140.

[83] Selvakumar, G., Sornalatha, G., Sarkar, S., & Mitra, S. (2014). Experimental investigation and multi-objective optimization of wire electrical discharge machining (WEDM) of 5083 aluminum alloy. *Transactions of Nonferrous Metals Society of China*, *24*(2), 373-379.

[84] Singh, S. (2012). Optimization of machining characteristics in Electrical discharge machining of Al2O3 p/6061 Al cast metal matrix composites. *International Journal of Advanced Manufacturing Technology*.

[85] Kandpal, B. C., & Singh, H. (2015). Machining of aluminium metal matrix composites with electrical discharge machining-a review. *Materials Today: Proceedings*, *2*(4-5), 1665-1671.

[86] Marafona, J., & Chousal, J. A. G. (2006). A finite element model of EDM based on the Joule effect. *International Journal of Machine Tools and Manufacture*, *46*(6), 595-602.

[87] Selvarajan, L., Rajavel, J., Prabakaran, V., Sivakumar, B., & Jeeva, G. (2018). A Review Paper on EDM Parameter of Composite material and Industrial Demand Material Machining. *Materials Today: Proceedings*, *5*(2), 5506-5513.

[88] Muttamara, A., Fukuzawa, Y., Mohri, N., & Tani, T. (2009). Effect of electrode material on electrical discharge machining of alumina. *Journal of materials processing technology*, *209*(5), 2545-2552..

[89] Kumar, S. S., Uthayakumar, M., Kumaran, S. T., & Parameswaran, P. (2014). Electrical discharge machining of Al (6351)–SiC–B4C hybrid composite. *Materials and Manufacturing Processes*, *29*(11-12), 1395-1400.

[90] Singh, J., Walia, R. S., Satsangi, P. S., & Singh, V. P. (2012). Hybrid electric discharge machining process with continuous and discontinuous ultrasonic vibrations on workpiece. *Int. J. Mech. Syst. Eng*, *2*(1), 22-33.

[91] Dastagiri, M., & Kumar, A. H. (2014). Experimental Investigation of EDM Parameters on Stainless Steel&En41b. *Procedia Engineering*, *97*, 1551-1564.

[92] Niamat, M., Sarfraz, S., Aziz, H., Jahanzaib, M., Shehab, E., Ahmad, W., & Hussain, S. (2017). Effect of Different Dielectrics on Material Removal Rate, Electrode Wear Rate and Microstructures in EDM. *Procedia CIRP*, *60*, 2-7.

[93] Gostimirovic, M., Kovac, P., Skoric, B., & Sekulic, M. (2011). Effect of electrical pulse parameters on the machining performance in EDM.

[94] Sarosh, M., Jahanzaib, M., Mumtaz, J., & Sarfraz, S. (2016). Investigation of Electric Disharge Machining Parameters To Minimize Surface Roughness. *Pakistan Journal of Science*, *68*(3), 315.

[95] Zhang, Y., Liu, Y., Ji, R., & Cai, B. (2011). Study of the recast layer of a surface machined by sinking electrical discharge machining using water-in-oil emulsion as dielectric. *Applied surface science*, *257*(14), 5989-5997.

[96] Chakraborty, S., Dey, V., & Ghosh, S. K. (2015). A review on the use of dielectric fluids and their effects in electrical discharge machining characteristics. *Precision Engineering*, *40*, 1-6.

[97] Zhang, Y., Liu, Y., Shen, Y., Ji, R., Li, Z., & Zheng, C. (2014). Investigation on the influence of the dielectrics on the material removal characteristics of EDM. *Journal of Materials Processing Technology*, *214*(5), 1052-1061.

[98] Wang, X., Liu, Z., Xue, R., Tian, Z., & Huang, Y. (2014). Research on the influence of dielectric characteristics on the EDM of titanium alloy. *The International Journal of Advanced Manufacturing Technology*, *72*(5-8), 979-987.

[99] Liu, Y., Zhang, Y., Ji, R., Cai, B., Wang, F., Tian, X., & Dong, X. (2013). Experimental characterization of sinking electrical discharge machining using

water in oil emulsion as dielectric. *Materials and Manufacturing Processes*, *28*(4), 355-363.

[100] Zhang, Y., Liu, Y., Ji, R., Cai, B., & Shen, Y. (2013). Sinking EDM in water-in-oil emulsion. *The International Journal of Advanced Manufacturing Technology*, *65*(5-8), 705-716.

[101] Valaki, J. B., & Rathod, P. P. (2016). Assessment of operational feasibility of waste vegetable oil based bio-dielectric fluid for sustainable electric discharge machining (EDM). *The International Journal of Advanced Manufacturing Technology*, *87*(5-8), 1509-1518.

[102] Shen, Y., Liu, Y., Zhang, Y., Dong, H., Sun, W., Wang, X., ... & Ji, R. (2015). High-speed dry electrical discharge machining. *International Journal of Machine Tools and Manufacture*, *93*, 19-25.

[103] Wang, J., Han, F., Cheng, G., & Zhao, F. (2012). Debris and bubble movements during electrical discharge machining. *International Journal of Machine Tools and Manufacture*, *58*, 11-18.

[104] Yongfeng, G., Yerui, F., Li, W., Kelie, D., Changjin, M., & Lin, T. (2018). Experimental Investigation of EDM Parameters for ZrB 2-SiC Ceramics Machining. *Procedia CIRP*, *68*, 46-51.

[105] Zapata-Solvas, E., Jayaseelan, D. D., Lin, H. T., Brown, P., & Lee, W. E. (2013). Mechanical properties of ZrB2-and HfB2-based ultra-high temperature ceramics fabricated by spark plasma sintering. *Journal of the European Ceramic Society*, *33*(7), 1373-1386.

[106] Sivasankar, S., & Jeyapaul, R. (2016). Characterization of ZrB2-SiC Composites With an Analytical Study on Material Removal Rate and Tool Wear Rate during Electrical Discharge Machining. *Transactions of the Canadian Society for Mechanical Engineering*, *40*(3), 331-349.

[107] Saha, N., Chakraborty, S., Dey, P. P., & Das, P. K. (2014). Machining of ZrB2-SiC Composites by Wire-EDM Technique. *Transactions of the Indian Ceramic Society*, *73*(2), 94-97.

[108] Singh, G., Singh, G., Singh, K., & Singla, A. (2017). Experimental studies on material removal rate, tool wear rate and surface properties of machined surface by powder mixed electric discharge machining. *Materials Today: Proceedings*, *4*(2), 1065-1073.

[109] Prasanna, P., Sashank, T. V., Manikanta, B., & Aluri, P. (2017). Optimizing The Process Parameters Of Electrical Discharge Machining On AA7075-SiC Alloys. *Materials Today: Proceedings*, *4*(8), 8517-8527.

[110] Chandramouli, S., Shrinivas Balraj, U., & Eswaraiah, K. (2014). Optimization of electrical discharge machining process parameters using Taguchi method. *International Journal of Advanced Mechanical Engineering*, *4*(4), 425-434.

[111] Singh, K., & Kumar, D. (2015). To Study The Effect of Copper Tungsten And Cryogenic Copper Tungsten Electrode on Material Removal Rate During Electrical Discharge Machining of H11 Tool Steel At Straight Polarity. *International Journal of Mechanical Engineering and Robotics Research*, *4*(1), 224.

[112] Baroi, B. K., Kar, S., & Patowari, P. K. (2018). Electric Discharge Machining of Titanium Grade 2 Alloy and its Parametric Study. *Materials Today: Proceedings*, *5*(2), 5004-5011.

[113] Torres, A., Puertas, I., & Luis, C. J. (2015). Modelling of surface finish, electrode wear and material removal rate in electrical discharge machining of hard-to-machine alloys. *Precision Engineering*, *40*, 33-45.

[114] Wang, A. C., Tsai, L., & Lin, Y. C. (2014). Characterizing the machining effects of lateral electrodes in electrical discharge machining. *International journal of precision engineering and manufacturing*, *15*(6), 1095-1100.

[115] Kar, S., Chakraborty, S., Dey, V., & Ghosh, S. K. (2017). Optimization of Surface Roughness Parameters of Al-6351 Alloy in EDC Process: A Taguchi Coupled Fuzzy Logic Approach. *Journal of The Institution of Engineers (India): Series C*, *98*(5), 607-618.

[116] Wang, X., Liu, Z., Xue, R., Tian, Z., & Huang, Y. (2014). Research on the influence of dielectric characteristics on the EDM of titanium alloy. *The International Journal of Advanced Manufacturing Technology*, *72*(5-8), 979-987.

[117] Shabgard, M., & Khosrozadeh, B. (2017). Investigation of carbon nanotube added dielectric on the surface characteristics and machining performance of Ti–6Al–4V alloy in EDM process. *Journal of Manufacturing Processes*, *25*, 212-219.

[118] Torres, A., Luis, C. J., & Puertas, I. (2017). EDM machinability and surface roughness analysis of TiB2 using copper electrodes. *Journal of Alloys and Compounds*, *690*, 337-347.

[119] Aghdeab, S. H., & Ahmed, A. I. (2016). Effect of Pulse on Time and Pulse off Time on Material Removal Rate and Electrode Wear Ratio of Stainless Steel AISI 316L in EDM. *Engineering and Technology Journal*, *34*(15 Part (A) Engineering), 2940-2949.

[120] Izquierdo, B., Plaza, S., Sánchez, J. A., Pombo, I., & Ortega, N. (2012). Numerical prediction of heat affected layer in the EDM of aeronautical alloys. *Applied Surface Science*, *259*, 780-790.

[121] Manjaiah, M., Narendranath, S., Basavarajappa, S., & Gaitonde, V. N. (2014). Wire electric discharge machining characteristics of titanium nickel shape memory alloy. *Transactions of Nonferrous Metals Society of China*, *24*(10), 3201-3209.

[122] Kumar, S. V., & Kumar, M. P. (2015). Machining process parameter and surface integrity in conventional EDM and cryogenic EDM of Al–SiCp MMC. *Journal of Manufacturing Processes*, *20*, 70-78.

[123] Kumar, K. M., & Hariharan, P. (2013). Experimental determination of machining responses in machining austempered ductile iron (ADI). *Procedia Engineering*, *64*, 1495-1504.

[124] Khan, M. A. R., Rahman, M. M., & Kadirgama, K. (2014). Neural network modeling and analysis for surface characteristics in electrical discharge machining. *Procedia Engineering*, *90*, 631-636.

[125] Manohar, M., Selvaraj, T., Sivakumar, D., Gopinath, S., & George, K. M. (2014). Experimental study to assess the effect of Electrode bottom profiles

while machining Inconel 718 through EDM Process. *Procedia materials science*, *6*, 92-104.

[126] Razak, M. A., Abdul-Rani, A. M., Rao, T. V. V. L. N., Pedapati, S. R., & Kamal, S. (2016). Electrical discharge machining on biodegradable AZ31 magnesium alloy using Taguchi method. *Procedia engineering*, *148*, 916-922.

[127] Dwivedi, A. P., & Choudhury, S. K. (2016). Improvement in the surface integrity of AISI D3 tool steel using rotary tool electric discharge machining process. *Procedia Technology*, *23*, 280-287.

[128] Gohil, V., & Puri, Y. M. (2018). Optimization of Electrical Discharge Turning Process using Taguchi-Grey Relational Approach. *Procedia CIRP*, *68*, 70-75.

[129] Nagaraju, N., Venkatesu, S., & Ujwala, N. G. (2018). Optimization of Process Parameters of EDM Process Using Fuzzy Logic and Taguchi Methods for Improving Material Removal Rate and Surface Finish. *Materials Today: Proceedings*, *5*(2), 7420-7428.

[130] Singh, N., Routara, B. C., & Das, D. (2018). Study of machining characteristics of Inconel 601in EDM using RSM. *Materials Today: Proceedings*, *5*(2), 3438-3449.

[131] Abhishek, K., Datta, S., Biswal, B. B., & Mahapatra, S. S. (2017). Machining performance optimization for electro-discharge machining of Inconel 601, 625, 718 and 825: An integrated optimization route combining satisfaction function, fuzzy inference system and Taguchi approach. *Journal of the Brazilian Society of Mechanical Sciences and Engineering*, *39*(9), 3499-3527.

[132] Buschaiah, K., JagadeeswaraRao, M., & Krishnaiah, A. (2018). Investigation On The Influence Of Edm Parameters On Machining Characteristics For Aisi 304. *Materials Today: Proceedings*, *5*(2), 3648-3656.

[133] Karthikeyan, P., & Arun, J. (2014). Machining characteristics analysis on EDM for Inconel 718 material using copper electrode. *International journal of research in engineering and technology*, *3*(11), 309-311.

[134] Vishnu, P., Kumar, N. S., & Manohar, M. (2018). Performance Prediction of Electric Discharge Machining of Inconel-718 using Artificial Neural Network. *Materials Today: Proceedings*, *5*(2), 3770-3780.

[135] Khundrakpam, N. S., Brar, G. S., & Deepak, D. (2018). Grey-Taguchi Optimization of Near Dry EDM Process Parameters on the Surface Roughness. *Materials Today: Proceedings*, *5*(2), 4445-4451.

[136] Mazarbhuiya, R. M., Choudhury, P. K., & Patowari, P. K. (2018). An Experimental Study on Parametric Optimization for Material Removal Rate and Surface Roughness on EDM by using Taguchi Method. *Materials Today: Proceedings*, *5*(2), 4621-4628.

[137] Aharwal, K. R., & Krishna, C. M. (2018). Optimization of Material Removal Rate and Surface Roughness in EDM Machining of Metal Matrix Composite using Genetic Algorithm. *Materials Today: Proceedings*, *5*(2), 5391-5397.

[138] Kumar, A., Maheshwari, S., Sharma, C., & Beri, N. (2010). A study of multiobjective parametric optimization of silicon abrasive mixed electrical discharge machining of tool steel. *Materials and Manufacturing processes*, *25*(10), 1041-1047.

[139] Jung, J. H., & Kwon, W. T. (2010). Optimization of EDM process for multiple performance characteristics using Taguchi method and Grey relational analysis. *Journal of Mechanical Science and Technology*, *24*(5), 1083-1090.

[140] Reza, M. S., Hamdi, M., Tomadi, S. H., & Ismail, A. R. (2010). Optimization of Control Parameters for EWR in Injection Flushing Type of EDM on Stainless Steel 304 Work Piece. *World Academy of Science, Engineering and Technology*, *72*, 2010.

[141] Chen, H. C., Lin, J. C., Yang, Y. K., & Tsai, C. H. (2010). Optimization of wire electrical discharge machining for pure tungsten using a neural network integrated simulated annealing approach. *Expert Systems with Applications*, *37*(10), 7147-7153.

[142] Pradhan, M. K., & Biswas, C. K. (2010). Neuro-fuzzy and neural network-based prediction of various responses in electrical discharge machining of AISI D2 steel. *The International Journal of Advanced Manufacturing Technology*, *50*(5-8), 591-610.

[143] Somashekhar, K. P., Ramachandran, N., & Mathew, J. (2010). Optimization of material removal rate in micro-EDM using artificial neural network and genetic algorithms. *Materials and Manufacturing Processes*, *25*(6), 467-475.

[144] Joshi, S. N., & Pande, S. S. (2011). Intelligent process modeling and optimization of die-sinking electric discharge machining. *Applied soft computing*, *11*(2), 2743-2755.

[145] Maji, K., & Pratihar, D. K. (2011). Modeling of electrical discharge machining process using conventional regression analysis and genetic algorithms. *Journal of materials engineering and performance*, *20*(7), 1121-1127.

[146] Amini, H., Soleymani Yazdi, M. R., & Dehghan, G. H. (2011). Optimization of process parameters in wire electrical discharge machining of TiB2 nanocomposite ceramic. *Proceedings of the Institution of Mechanical Engineers, Part B: Journal of Engineering Manufacture*, *225*(12), 2220-2227.

[147] Yang, R. T., Tzeng, C. J., Yang, Y. K., & Hsieh, M. H. (2012). Optimization of wire electrical discharge machining process parameters for cutting tungsten. *The International Journal of Advanced Manufacturing Technology*, *60*(1-4), 135-147.

[148] Somashekhar, K. P., Mathew, J., & Ramachandran, N. (2012). A feasibility approach by simulated annealing on optimization of micro-wire electric discharge machining parameters. *The International Journal of Advanced Manufacturing Technology*, *61*(9-12), 1209-1213.

[149] Bharti, P. S., Maheshwari, S., & Sharma, C. (2012). Multi-objective optimization of electric-discharge machining process using controlled elitist NSGA-II. *Journal of mechanical science and technology*, *26*(6), 1875-1883.

[150] Kumar, K., & Agarwal, S. (2012). Multi-objective parametric optimization on machining with wire electric discharge machining. *The International Journal of Advanced Manufacturing Technology*, *62*(5-8), 617-633.

[151] Shrivastava, P. K., & Dubey, A. K. (2013). Intelligent modeling and multiobjective optimization of electric discharge diamond grinding. *Materials and Manufacturing Processes*, *28*(9), 1036-1041.

[152] Baraskar, S. S., Banwait, S. S., & Laroiya, S. C. (2013). Multiobjective optimization of electrical discharge machining process using a hybrid method. *Materials and Manufacturing Processes*, *28*(4), 348-354.

[153] Shahali, H., Yazdi, M. R. S., Mohammadi, A., & Iimanian, E. (2012). Optimization of surface roughness and thickness of white layer in wire electrical discharge machining of DIN 1.4542 stainless steel using micro-genetic algorithm and signal to noise ratio techniques. *Proceedings of the Institution of Mechanical Engineers, Part B: Journal of Engineering Manufacture*, *226*(5), 803-812.

[154] Atefi, R., Javam, N., Razmavar, A., & Teimoori, F. (2012). The investigation of EDM parameters on electrode wear ratio. *Journal of Basic and Applied Scientific Research*, *4*(10), 1295-1299.

[155] Rajesh, R., & Anand, M. D. (2012). Determination of an optimum parametric combination using a surface roughness in EDM process through response surface methodology. *International Research Journal of Engineering Science, Technology and Innovation (IRJESTI)*, *1*(5), 145-151.

[156] Moghaddam, et al..: Application of grey relational analysis and simulated annealing algorithms for modeling and optimization for EDM parameters on 40 crmnmos 86 hot worked steel, ISME. In: Annual Int. Conference on Mechanical Engineering (2012)

[157] Zhang, Yet al..: A new method of investigation the characteristic of the heat Flux of EDM plasma. Procedia CIRP 6, 450–455 (2013)

[158] Dhanabalan, S., Sivakumar, K., & Narayanan, C. S. (2013). Optimization of machining parameters of EDM while machining Inconel 718 for form tolerance and orientation tolerance.

[159] [Agrawal, A., Dubey, A. K., & Shrivastava, P. K. (2013). Modeling and optimization of tool wear rate in powder mixed EDM of MMC. In *2nd International Conference on Mechanical and Robotics Engineering (ICMRE'2013) Dec* (pp. 17-18).

[160] Sivaprakasam, P., Hariharan, P., & Gowri, S. (2014). Modeling and analysis of micro-WEDM process of titanium alloy (Ti–6Al–4V) using response surface approach. *Engineering Science and Technology, an International Journal*, *17*(4), 227-235.

[161] Kumar, S., Batish, A., Singh, R., & Singh, T. P. (2015). A mathematical model to predict material removal rate during electric discharge machining of cryogenically treated titanium alloys. *Proceedings of the Institution of Mechanical Engineers, Part B: Journal of Engineering Manufacture*, *229*(2), 214-228.

[162] Dewangan, S., Gangopadhyay, S., & Biswas, C. K. (2015). Multi-response optimization of surface integrity characteristics of EDM process using grey-fuzzy logic-based hybrid approach. *Engineering Science and Technology, an International Journal*, *18*(3), 361-368.

[163] Mussada, E. K., & Patowari, P. K. (2015). Investigation of EDC parameters using W and Cu powder metallurgical compact electrodes. *International Journal of Machining and Machinability of Materials*, *17*(1), 65-78.

[164] Vieira, R. A., & Nono, M. D. C. D. A. (2005). Characterisation of Titanium Nitride Thin Films Deposited by Cathodic Arc Plasma Technique on AISI D6 Tool Steel. In *Materials science forum* (Vol. 498, pp. 717-721). Trans Tech Publications.

[165] Kacal, A., & Yıldırım, F. (2013). Application of grey relational analysis in high-speed machining of hardened AISI D6 steel. *Proceedings of the Institution of Mechanical Engineers, Part C: Journal of Mechanical Engineering Science*, *227*(7), 1566-1576.

[166] Khojastehnezhad, V. M., & Pourasl, H. H. (2018). Microstructural characterization and mechanical properties of aluminum 6061-T6 plates welded with copper insert plate (Al/Cu/Al) using friction stir welding. *Transactions of Nonferrous Metals Society of China*, *28*(3), 415-426.

[167] Abbas, N. M., Solomon, D. G., & Bahari, M. F. (2007). A review on current research trends in electrical discharge machining (EDM). *International Journal of machine tools and Manufacture*, *47*(7-8), 1214-1228.

[168] Boujelbene, M., Bayraktar, E., Tebni, W., & Salem, S. B. (2009). Influence of machining parameters on the surface integrity in electrical discharge machining. *Archives of Materials Science and Engineering*, *37*(2), 110-116.

[169] Huang, S. F., Liu, Y., Li, J., Hu, H. X., & Sun, L. Y. (2014). Electrochemical discharge machining micro-hole in stainless steel with tool electrode high-speed rotating. *Materials and Manufacturing Processes*, *29*(5), 634-637.

[170] Gohil, V., & Puri, Y. M. (2017). Turning by electrical discharge machining: A review. *Proceedings of the Institution of Mechanical Engineers, Part B: Journal of Engineering Manufacture*, *231*(2), 195-208.

[171] Her, M. G., & Weng, F. T. (2002). A study of the electrical discharge machining of semi-conductor BaTiO3. *Journal of materials processing technology*, *122*(1), 1-5.

[172] Marafona, J., & Wykes, C. (2000). A new method of optimising material removal rate using EDM with copper–tungsten electrodes. *International Journal of Machine Tools and Manufacture*, *40*(2), 153-164.

[173] Basha, S. K., Raju, M. J., & Kolli, M. (2018). Experimental Study of Electrical Discharge Machining of Inconel X-750 Using Tungsten-Copper Electrode. *Materials Today: Proceedings*, *5*(5), 11622-11627

[174] Choudhary, R., & Singh, G. (2018). Effects of process parameters on the performance of electrical discharge machining of AISI M42 high speed tool steel alloy. *Materials Today: Proceedings*, *5*(2), 6313-6320.

[175] Sarikavak, Y.; Cogun, C. Single discharge thermo-electrical modeling of micromachining mechanism in electric discharge machining. Journal of Mechanical Science and Technology 2012, 26 (5), 1591–1597.

[176] Heidarzadeh, A., & Saeid, T. (2013). Prediction of mechanical properties in friction stir welds of pure copper. *Materials & Design (1980-2015)*, *52*, 1077-1087.

[177] Heidarzadeh, A., Saeid, T., Khodaverdizadeh, H., Mahmoudi, A., & Nazari, E. (2013). Establishing a mathematical model to predict the tensile strength of friction stir welded pure copper joints. *Metallurgical and Materials Transactions B*, *44*(1), 175-183

[178] Lundstedt, T., Seifert, E., Abramo, L., Thelin, B., Nyström, Å., Pettersen, J., & Bergman, R. (1998). Experimental design and optimization. *Chemometrics and intelligent laboratory systems*, *42*(1-2), 3-40.

[179] Bezerra, M. A., Santelli, R. E., Oliveira, E. P., Villar, L. S., & Escaleira, L. A. (2008). Response surface methodology (RSM) as a tool for optimization in analytical chemistry. *Talanta*, *76*(5), 965-977.

[180] Heidarzadeh, A., Mousavian, R. T., Khosroshahi, R. A., Afkham, Y. A., & Pouraliakbar, H. (2017). Empirical model to predict mass gain of cobalt electroless deposition on ceramic particles using response surface methodology. *Rare Metals*, *36*(3), 209-219.

[181] Farhanchi, M., Neysari, M., Barenji, R. V., Heidarzadeh, A., & Mousavian, R. T. (2015). Mechanical activation process for self-propagation high-temperature synthesis of ceramic-based composites. *Journal of Thermal Analysis and Calorimetry*, *122*(1), 123-133.

[182] Heidarzadeh, A., Barenji, R. V., Esmaily, M., & Ilkhichi, A. R. (2015). Tensile properties of friction stir welds of AA 7020 aluminum alloy. *Transactions of the Indian Institute of Metals*, *68*(5), 757-767.

[183] Gopalakannan, S., & Senthilvelan, T. (2013). EDM of cast Al/SiC metal matrix nanocomposites by applying response surface method. *The International Journal of Advanced Manufacturing Technology*, *67*(1-4), 485-493.

[184] Boujelbene, M., Bayraktar, E., Tebni, W., & Salem, S. B. (2009). Influence of machining parameters on the surface integrity in electrical discharge machining. *Archives of Materials Science and Engineering*, *37*(2), 110-116.

[185] Sohani, M. S., Gaitonde, V. N., Siddeswarappa, B., & Deshpande, A. S. (2009). Investigations into the effect of tool shapes with size factor consideration in sink electrical discharge machining (EDM) process. *The International Journal of Advanced Manufacturing Technology*, *45*(11-12), 1131.